POLITECNICO DI TORINO

Master Degree in Biomedical Engineering
Master Thesis

Molecular modelling to tailor glicodendrimers as drug delivery systems for anticancer nucleoside analogues targeting haematological malignancies

Thesis Advisor:
Prof. M. A. Deriu

Candidate:
Alessia Chiaro

ACADEMIC YEAR 2018-2019

Solo coloro che osano sfidarsi nella vita,

ne usciranno vincenti.

Alessia

Contents

Abstract

Worldwide the overall incidence of hematological diseases appears to increase yearly, especially in Western countries. This family of malignancies includes various malignant neoplasms that affect blood such as leukemia, which often occurs in adults older than 55, but it is also the most common childhood cancer. To fight leukemia, many types of treatment are suggested, and the most used technique is chemotherapy. Among the various drugs, the nucleotide analogues (NAs) are one of the most efficient antimetabolites used to treat leukemia. The NAs, as their name suggests, are able to mime physiological nucleosides in terms of uptake and metabolism. These therapeutic compounds are able to decrease the activity of enzymes involved in metabolism of natural nucleoside and nucleotides, and to inhibit the DNA and RNA synthesis. Fludarabine and clofarabine are the two NAs considered in our study, and their cytotoxic effect strongly depends on the entrance and on their activation inside the cell. Due to their hydrophilic nature, NAs cannot passively cross the cellular membrane and they must be phosphorylated to their active triphosphate form once inside the cell. To overcome the various NAs problems, the use of dendrimers as drug delivery system has been suggested. The poly(propyleneimine) dendrimers of fourth generation (PPI G4) provide high loading capacity, improved solubility and biodistribution of the drug. Moreover, PPI dendrimers with the surface partially modified with maltose moieties (PPI-Mal OS G4) have been suggested to be superior among the other NAs carriers. Indeed, the use of glycodendrimers to treat leukemia is especially justified by the overexpression of surface lectin receptors on leukemic cells, which bind carbohydrate ligands with high affinity. Furthermore, drug-dendrimer complexation is based on non-covalent physical incorporation of the drug molecules into the dendrimer structure. In this study we present computational approaches, based on Molecular Dynamics simulations, by representing a powerful tool for exploring molecular features of clofarabine and fludarabine. The main goal is to provide quantitative and dynamic information on the molecular reasons responsible of different interaction mechanism with the dendrimers. The compound-dendrimer complexes were protonated to simulate their behavior at neutral or acid environment condition. Our results confirmed what seen with *in vivo* experiments. Interestingly, both of the drug nucleoside forms did not interact with the PPI G4 dendrimer, neither with PPI-Mal OS G4. Furthermore, in compound-dendrimer complexes, it was evident that the dendrimer protonation affects the interaction mode in terms of drug orientation. Indeed, clofarabine triphosphate completelly changes its orientation in presence of PPI-Mal OS G4 dendrimer in acid environment and the electrostatic potential of this dendrimer surface was completely neutralized by the

clofarabines. On the other hand, the fludarabine nucleotide was able to interact with the dendrimer surface and to settle in different positions and it did not alter the positive charge of the dendrimer surface. Most likely, the PPI-Mal OS G4 dendrimer can efficiently deliver the fludarabine nucleotide inside the cell and the compound can easily detach from the dendrimer surface. Surprisingly, the clofarabine behavior may limit the ability of compound-dendrimer complex to enter the cell, since positively charged nanoparticles have much greater tendency to penetrate cell membranes than neutral or negatively charged ones. The computational approaches applied in this study can be used as basis for future experimental and computational design of strategies aimed to predict the interaction mode of drug-carrier systems.

Estratto

In tutto il mondo l'incidenza complessiva delle malattie ematologiche sembra aumentare annualmente, soprattutto nei paesi Occidentali. Questa famiglia di tumori comprende varie neoplasie maligne che colpiscono il sangue come la leucemia, che si verifica spesso negli adulti di età superiore ai 55 anni, ma è anche il tumore infantile più comune. Per trattare la leucemia, sono suggeriti molti tipi di trattamento e la tecnica più utilizzata è la chemioterapia. Tra i vari farmaci, gli analoghi nucleotidici (AN) sono uno degli antimetaboliti più efficaci usati per trattare la leucemia. Gli AN, come suggerisce il loro nome, sono in grado di mimetizzare i nucleosidi fisiologici in termini di assorbimento e metabolismo. Questi composti terapeutici sono in grado di ridurre l'attività degli enzimi coinvolti nel metabolismo del nucleoside e dei nucleotidi naturali e di inibire la sintesi del DNA e dell'RNA. La fludarabina e la clofarabina sono le due AN considerate nel nostro studio e il loro effetto citotossico dipende fortemente dal loro ingresso e dalla loro attivazione all'interno della cellula. A causa della loro natura idrofila, le AN non possono attraversare passivamente la membrana cellulare e devono essere fosforilate alla loro forma trifosfato attiva una volta all'interno della cellula. Per superare i vari problemi dei AN, è stato suggerito l'uso di dendrimeri come sistema di somministrazione di farmaci. I dendrimeri poli(propilenimmine) di quarta generazione (PPI G4) forniscono un'elevata capacità di carico, una migliore solubilità e una biodistribuzione del farmaco. Inoltre, i dendrimeri PPI con la superficie parzialmente modificata con frazioni maltose (PPI-Mal OS G4) sono stati suggeriti come superiori tra gli altri portatori di AN. In effetti, l'uso di glicodendrimeri per il trattamento della leucemia è particolarmente giustificato dalla sovra espressione dei recettori della lectina di superficie sulle cellule leucemiche, che legano i ligandi di carboidrati con alta affinità. Inoltre, la complessazione del farmaco-dendrimero si basa sull'incorporazione fisica non covalente delle molecole del farmaco nella struttura del dendrimero. In questo studio presentiamo approcci computazionali, basati su simulazioni di dinamica molecolare, che rappresentano un potente strumento per esplorare le caratteristiche molecolari della clofarabina e della fludarabina. L'obiettivo principale è quello di fornire informazioni quantitative e dinamiche sui motivi molecolari responsabili dei diversi meccanismi di interazione con i dendrimeri. I complessi composti da dendrimeri sono stati protonati per simulare il loro comportamento in condizioni di ambiente neutro o acido. I nostri risultati hanno confermato quanto visto con esperimenti in vivo. È interessante notare che entrambe le forme dei farmaci nucleosidici non interagiscono con il dendrimero PPI G4, né con PPI-Mal OS G4. Inoltre, nei complessi farmaco-dendrimero, era evidente come la protonazione del dendrimero influenzasse la

modalità di interazione in termini di orientamento del farmaco. Infatti, la clofarabina trifosfato modifica completamente il suo orientamento in presenza di dendrimero P4-Mal OS G4 in ambiente acido e il potenziale elettrostatico di questa superficie di dendrimero veniva completamente neutralizzata dalle clofarabine. D'altra parte, il nucleotide fludarabina era in grado di interagire con la superficie del dendrimero e di stabilirsi in posizioni diverse, non alterando la carica positiva della superficie del dendrimero. Molto probabilmente, il dendrimero PPI-Mal OS G4 può veicolare efficientemente il nucleotide fludarabina all'interno della cellula e il composto può facilmente staccarsi dalla sua superficie. Sorprendentemente, il comportamento della clofarabina può limitare la capacità del complesso farmaco-dendrimero di entrare nella cellula, poiché le nanoparticelle caricate positivamente hanno una tendenza molto maggiore a penetrare nelle membrane cellulari rispetto a quelle neutre o cariche negativamente. Gli approcci computazionali qui applicati possono essere usati come base per la futura progettazione sperimentale e computazionale di strategie volte a prevedere la modalità di interazione di sistemi di portatori di farmaco.

1. Introduction

In this chapter we are going to introduce the present master thesis work, together with its aims and objectives. At the end there is a summary about all the chapter treated in this composition.

The World Health Organizations reports that the overall incidence of hematological malignancies appears to rapidly rise, with 250,000 new cases diagnosed every year in Western countries. Despite the huge progress in the detection and treatment of these malignant neoplasms, tailored and effective therapy remains indispensable. Mostly due to the fact that this is the first common childhood cancer.

Nanotechnology offers an unprecedented opportunity in rational and target delivery of drugs, and poly(propyleneimine) dendrimers of fourth generation have been studied as efficient carriers for nucleotide anticancer drugs.

Indeed, the nucleotide analogues are antimetabolites able to decrease the activity of enzymes involved in metabolism of natural nucleoside and nucleotide, but their direct use is widely limited.

The present master thesis work is focused on Poly(propyleneimine) dendrimers of fourth generation partially modified with maltose moieties used as drug delivery system.

The aim of the work is to investigate the interactions between two nucleoside analogues, the clofarabine and the fludarabine with the studied dendrimer. This is a challenging task for computational and theoretical approach to explain biological *in vivo* results.

In this connection, computational molecular methods represent a powerful tool to provide quantitative and dynamic information on the molecular reasons, responsible of the different conformation of the complexes.

The present manuscript is divided in sections briefly described in the following.

Chapter 1 is the present introductory part.

Chapter 2 introduces the hematological malignancy milestone of our study, the leukemia. The chapter starts with a quick introduction to leukemia disease, followed by an overview on leukemia treatments (section 2.2). In this section, particular attention is given on the Nucleotide Analogues, due to their leading role in this case of study. Finally the last part analyzes the Drug Delivery Systems used to treat leukemia, and it is mainly focused on Poly(propyleneimine) dendrimers and on their interaction with nucleotide analogues.

Chapter 3 provides a general description of the Materials and Methods employed in the presented work. The chapter begins with an introduction about computational molecular modelling, used as virtual microscope for investigating biological phenomena. Section 3.2 introduces the so called "Molecular Mechanics" approach, to provide a background on physical basis behind molecular modelling. The following section is devoted to the Classical Molecular Dynamics method, describing the theoretical method together with algorithm implementation details. Finally the last section introduces an overview of the analysis methods used in this case of study.

Chapter 4 presents an investigation focused on clofarabine and fludarabine interactions with PPI G4 and its maltose modified version PPI-Mal OS G4, by means of MD simulations. To better understand the complexes with real pH conditions, these dendrimers have been analyzed in their standard and protonated form. The results provide an atomistic investigation of the compound-dendrimer complex, focusing the attention on: the dendrimer protonation, the complexation modes, the orientation and the penetration of the compound over the dendrimer surface and the interactions between compound parts and dendrimer layers.

Chapter 5 is focused on the clofarabine and the fludarabine interactions with the PPI G4 and PPI-Mal OS G4 full protonated dendrimers, by means of MD simulations. The results provide an atomistic investigation of the compound-dendrimer complex, focusing the attention on: the complexation modes, the orientation and the penetration of the compound over the dendrimer surface and the interactions between compounds and dendrimer at ratio 10:1.

Chapter 6 is devoted to general conclusions and future developments of this work.

2. Scientific background

This section introduces the hematological malignancy milestone of our study, the leukemia. The chapter is organized in three main parts: a quick introduction to Leukemia disease (section 2.1), an overview on Leukemia treatments (section 1.2) and the Drug Delivery Systems used to treat leukemia (section 1.3). In section 1.2 particular attention is given on the Nucleotide Analogues, due to their leading role in this case of study. Finally in section 1.3, our interest is mainly focused on Poly(Propyleneimine) dendrimers and on their interaction with nucleotide analogues.

Worldwide the overall incidence of hematological malignancies appears to rise every year, especially in Western countries were 250,000 new cases are diagnosed every year.[1,2] Hematological malignancies are malignant neoplasms that affect blood or lymph systems. The cancer may begin in blood-forming tissue (e.g., bone marrow) or in immune system cells.[3] The major groups of hematological malignance are: leukemia, Non-Hodgkin lymphoma, Hodgkin lymphoma and Multiple myeloma. In this case of study, our interest is focalized on leukemia treatments. Leukemia is an acute or chronic disease characterized by an abnormal increase in the number of white blood cells in the tissues and also often in the blood. The type of leukemia depends on the kind of blood cell that becomes cancer and on its proliferation rate. This malignancy often occurs in adults older than 55, but it is also the most common childhood cancer.[4] To treat leukemia, many types of treatments are suggested. The most used technique is the chemotherapy, where chemical substances are injected to directly treat the cancer. Among the various chemotherapeutic drugs, the nucleotide analogues (NAs) are one of the most efficient antimetabolites used to treat leukemia. The NAs, as their name suggests, are able to mime physiological nucleosides in terms of uptake and metabolism.[5] These therapeutic compounds are antimetabolites able to decrease the activity of enzymes involved in metabolism of natural nucleoside and nucleotides, and are able to inhibit the DNA and RNA synthesis. Indeed, NAs are able to be incorporated into newly synthesized chains of DNA or RNA, causing synthesis inhibition and chain termination, and leading to the induction of apoptosis. The cytotoxic effect of the NAs strongly depends on the entrance and activation of the drug inside the cell. Due to their hydrophilic nature, these drugs cannot passively cross the cellular membrane and they require specialized nucleoside transporters to overcome the membrane barrier.[6] Moreover, NAs must be phosphorylated to their active triphosphate form, once inside the cell. Among the various NAs approved by FDA to treat leukemia, we have analyzed the fludarabine and the clofarabine drugs, which will be deeply

investigated below.[7] A promising approach suggested to overcome the various problems connected to the direct use of NAs, is using drug delivery systems. The drug delivery systems are useful cargo that can passively cross the cellular membrane and protect the drugs from degradation or catabolism. These nanoparticles should be characterized by low toxicity, low immunogenicity and target delivery, which diminish undesirable interactions of the drugs with healthy cells.[8] Recent studies have demonstrated that Poly(propyleneimine) dendrimers (PPI), also with partially modified surfaces, are superior nanoparticles for drug delivery.[9,10] PPI dendrimers provide high loading capacity, improved solubility and biodistribution of the drug. Their strength is the nanometric size and their globular shape, which enable cellular entry and extend blood circulation time.[11] Moreover, PPI dendrimers with the surface partially modified with maltose moieties proved promising.[12] Indeed the presence of sugar modifications, reduces PPI cytotoxic activity and maintains surface positive charge, allowing for electrostatic interactions with negatively charged phosphate groups.[6,8] The use of glycodendrimers to treat leukemia is especially justified by the overexpression of surface lectin receptors on leukemic cells, which bind carbohydrate ligands with high affinity. Furthermore, drug-dendrimer complexation is based on non-covalent physical incorporation of the drug molecules into the dendrimer structure. This non-covalent incorporation enables easy carrier system preparation, without causing changes in pharmacological activity of the drug. Therefore non-covalent complexes may transport active drug forms directly inside the cancer cells, overcoming chemotherapeutics limitations such as multidrug resistance, rapid drug metabolism and unfavorable biodistribution. In this case of study, our interest is focused on the interaction between the clofarabine and the fludarabine compounds and the Poly(propyleneimine) of fourth generation dendrimers, in their normal and maltose-modified forms.

2.1 Leukemia

Leukemia is a term used to describe a group of malignant blood diseases that originates from tumor proliferation of hematopoietic cells.[4] Hematopoietic cells are stored in bone marrow and their function is to produce normal blood cells: red blood cells (RBCs), white blood cells (WBCs) and platelets. In leukemic patient, the bone marrow loses the ability to generate normal cells by acquiring the pathological one of producing cancer cells. Cancer cells, escaping the physiological control mechanisms, tend to accumulate in bone marrow and to invade it, causing the alteration of its functions. The accumulation of tumor cells in the marrow can also extends to the blood, leading to an abnormal increase in the number of leukemic WBCs. WBCs are a vital part of human immune system, they protect human body from invasion by bacteria, viruses and fungi, as well as from abnormal cells and other foreign substances. In leukemia patients, the WBCs don't work like normal WBCs. They are also able to divide too quickly and eventually crowd out normal cells.[13,14] Based on the hematopoietic cells involved, leukemias can be of lymphoid origin (T and B cells) or of myeloid origin (neutrophils, basophils, eosinophils and monocytes).[15] Furthermore, leukemias are divided in two main types: acute and chronic. Acute leukemia appears when immature WBCs or blast have rapidly evolved in an uncontrollable proliferation, on the other hand leukemia is chronic when it derives from mature cells slow-growing. The four main types of leukemia (Figure 1) are: chronic lymphocytic leukemia (CLL), chronic myeloid leukemia (CML), acute lymphoblastic leukemia (ALL) and acute myeloid leukemia (AML).[16]

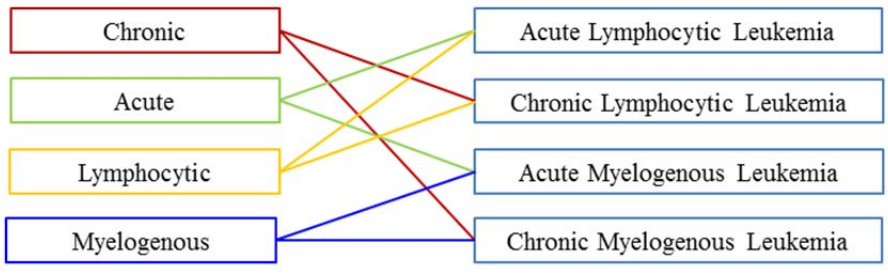

Figure 1. Leukemia types. Based on the time-develop of malignant cells, leukemias can be defined acute or chronic. Beside, based on the hematopoietic cells involved, leukemias can be of lymphoid origin (T and B cells) or of myeloid origin.

The overall annual incidence of leukemia is of about 4 cases per 100,000 people, with approximately 70% of cases of the "acute" type and "myeloid" phenotype. In 2018 were estimated 60,300 new cases of leukemia and 24,370 deaths due to this malignancies in USA.[17] The incidence of leukemia is age-dependent, indeed leukemia is highly present in pediatric subjects and in people with over 60 years of age. In general, the adult-elderly patients present chronic and myeloid leukemias, while pediatric patients are affected by acute forms, where lymphoid type prevails. CLL is a common adults leukemia, with an incidence of 4.2 cases per 100,000 population of median age of 71 years at diagnosis. It can also occur in young adults, rarely affects children, and it is more popular in men than in women.[15] Instead CML is rare. The ALL is the most common type of leukemia among young children, with global incidence of 3 per 100,000 population, with around three of four cases occurring in children under six years. Patients with acute leukemia typically have quickly deterioration. In USA, the incidence of AML ranges from 3 to 5 cases per 100,000 and it is the most common acute leukemia in adults.[18] Recent study shows that a relatively higher proportion of CLL is present in most European and North American countries, whereas rates of ALL remained relatively high among adults in selected South American, Caribbean, Asian and African populations. Notable is the fact that highest leukemia incidence rates for both sexes were estimated in Australia and New Zealand (11.3 in males and 7.2 in females over 100,000), followed by Northern America and Western Europe, and the lowest was in in Western Africa (1.4 in males and 1.2 in females). Rates were generally higher in males than females and in children, ALL was the main subtype in all studied countries for both sexes, and characterized by a bimodal age-specific pattern.[19]

2.2 Leukemia treatments

Medicine progress allow to develop treatment options that aim complete leukemia remission, in which the cancer disappears completely for at least 5 years after treatment. Indeed the chance of patient survival, after receiving leukemia diagnosis, has significantly increase from 33.1% in 1975 to 61.4% in 2014.[20] Treatment choice is patient-dependent, and must take into account various factors such as leukemia type, patient age and the overall state health. Based on these factors, the doctor can follow different treatment protocols choosing among chemotherapy, radiotherapy, stem cell transplantation and targeted therapy. The major worldwide leukemia treatment used is the chemotherapy, where drugs are chemically used to kill malignant cells.[21] The mechanism of action of chemotherapy is cell division interruption and/or promotion of tumor cells apoptosis. The big challenge that an anticancer drug must overcome is the cell-specific interaction.[22] Indeed the drug must be able to identify the subtle changes that distinguish a tumor cell from the other two hundred different types of healthy cells found in the body, therefore recognize them and being able to provide a sufficiently high dose of toxic agent to kill them. Depending on the type of leukemia, the chemotherapeutic may be injected directly in vein or provided in pill form, as single drug or as a combination of drugs. Usually patients are subjected to a cycle of chemotherapy, based on the alternation of the rest and treatment periods. Chemotherapy drug types that act directly to impair DNA include: DNA-damaging agents, antitumor antibiotics, antimetabolites and DNA-repair enzyme inhibitors. DNA-damaging agents, referred to as alkylating agents, damage the DNA so severely that the cancer cell is killed (e.g., Leukeran® and Cytoxan®). Antitumor antibiotics are able to insert into a cancer cell DNA, prevent the DNA normal functions and often kill cancer cells. DNA-repair enzyme inhibitors attack the cancer cell proteins used to repair DNA, preventing DNA damage reconstruction. Finally, antimetabolites mimic the substances that the cancer cell needs to build DNA and RNA. When the cancer cell uses the antimetabolite instead of natural substance, it is unable to produce normal DNA and RNA, and it is destined to die. Antimetabolites disrupt nucleic acid synthesis by interfering with production of a major nucleotide metabolite or by substituting for the natural metabolite.[23,24] They can be classified in folic acid antagonists and nucleobase/nucleoside analogues, which include purine and pyrimidine antimetabolites.[25]

2.2.1 Nucleoside Analogues

Nucleotide Analogues (NAs) were one of the first chemotherapeutics developed for the cancer treatment.[26] These therapeutic compounds, as their name suggests, are able to mimic physiological nucleosides in terms of uptake and metabolism.[5] The NAs are antimetabolites able to decrease the activity of enzymes involved in metabolism of natural nucleoside and nucleotides, or able to inhibit the DNA and RNA synthesis. Indeed, NAs are able to be incorporated into newly synthesized chains of DNA or RNA, causing synthesis inhibition and chain termination, and leading to the induction of apoptosis. All anticancer NAs share common intracellular transport and metabolic pathways, which include active transfer through the cell membrane and activation by intracellular kinases leading the formation of activate triphosphate forms. NAs are hydrophilic molecules, therefore these compounds cannot penetrate the cell membrane by passive diffusion and require nucleoside-specific membrane transport carrier (NTs) to facilitate the cell entry. The NTs are proteins generally divided into two subclasses: equilibrative (ENTs) and concentrative (CNTs) nucleoside transporters. Moreover both nucleobase and nucleoside chemotherapeutics are pro-drugs, they require chemical modification, such as sequential phosphorylation, to generate their active metabolites. Once inside the cell, NAs are phosphorylated, to mono-, di- and triphosphates by kinases (e.g., deoxycytidine or thymidine kinases) to activate the 5'-triphosphate derivative form, which is essential for cytotoxic activity of this class of therapeutics (Figure 2).[27] Indeed the cytotoxic mechanism of NAs strongly depends on their structure, stability, specificity and affinity for intracellular enzymes and molecular targets.[28]

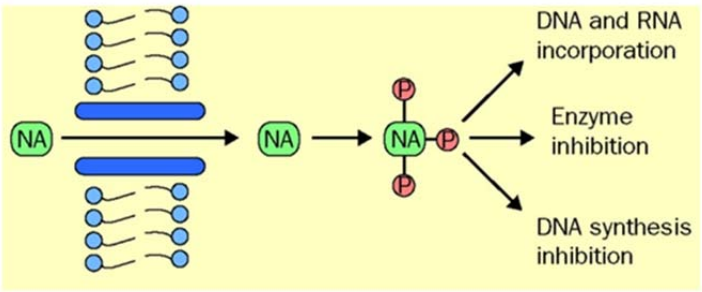

Figure 2. Nucleoside analogue metabolism. NAs are hydrophilic molecules and therefore require specialized transporter proteins to enter cells. Once inside, they are activated by kinases to triphosphate derivatives. Active derivatives of nucleoside analogues can exert cytotoxic activity by being incorporated inside and altering the DNA and RNA macromolecules or by interfering with various enzymes involved in synthesis of nucleic acids, such as DNA polymerases and ribonucleotide reductase. These actions result in inhibition of DNA synthesis and apoptotic cell death.[5]

Noteworthy is that human NTs can only transport dephosphorylated compounds [29,30], therefore this limit the administration of NAs to prodrug forms instead of active triphosphates. The NAs complex metabolism generates several resistance mechanisms, which significantly limit the therapeutic potential of this drug. Decreased expression of NTs and reduced activity of intracellular kinases are examples of the induced resistance, leading to poor cellular uptake and inadequate phosphorylation of NAs. The application of NAs in anticancer therapy may additional encumber by their uncontrolled bio-distribution, low solubility, fast degradation and systemic toxicity. [28,31] Therefore a promising approach that bears to circumvent the above-mentioned resistance mechanism, due by the direct use of NAs, is the application of drug delivery systems (DDSs) (see Drug Delivery Systems). The primary NAs pharmacological effect is identical, as they function as classic chain- terminators of DNA synthesis. However, these NAs are often subdivided into two distinct classes: purine and pyrimidine analogues. The distinction is based on differences in pharmacokinetic behavior rather than pharmacodynamic properties. Indeed the cytarabine, a pyrimidine NA, is highly toxic against actively replicating cells as it is primarily utilized during the S phase of the cell cycle.[32] On the other hand, purine NAs, such as cladribine and fludarabine, are more cytotoxic against slowly replicating cells, for example they can be utilized to inhibit the repair of double strand bonds in indolent lymphoma. Currently the FDA has approved fourteen NAs (Table 1) that account for about 20% of all drugs used in chemotherapy. [33] In this case of study were analyzed two purine analogues: fludarabine and clofarabine. These compounds have different treatment protocols but both are inhibitors of the ribonucleotide reductase enzyme (RR), which is critically involved into the process of de novo synthesis of deoxynucleoside diphosphates (dNDPs).[34] The inhibition of RR leads to imbalance the pool of dNDPs, and let the possibility to the nucleoside analogues to be incorporated into newly synthesized DNA strand, and it may cause the inhibition of chain elongation.

Table 1. Purine and Pyrimidine Nucleoside Analogs Used in Chemotherapy in Chronological Order of Approval by the FDA

Purine and Pyrimidine NAs Used in Chemotherapy in Chronological Order of Approval by the FDA
6-mercaptopurine (6-MP)
5-fluorouracil (5-FU)
6-thioguanine (6-TG)
Arabinofuranosylcytosine (cytarabine, Ara-C)
5-fluoro-29-deoxyuridine (floxuridine)
29-deoxycoformycin (pentostatin)
Arabinofuranosyl-2-fluoroadenine (fludarabine, F-ara-A)
2-chloro-29-deoxyadenosine (cladribine)
2,2-difluoro-29-deoxycytidine (gemcitabine)
N4-pentyloxocarbonyl-59-deoxy-5-fluorocytidine (capecitabine)
5-aza-cytidine (vidaza)
2-fluoro-29-deoxyarabinofuranosyl-2-chloroadenine (clofarabine)
O6-methylarabinofuranosyl guanine (nelarabine)
5-aza-29-deoxycytidine (decitabine)

2.2.2 Fludarabine

Fludarabine is a synthetic halogen-substituted analogue of deoxyadenosine, and it is the prodrug of 9-β-D-arabinosyl-2-fluoroadenine (F-ara-A). Its development arises from the success of the cytosine analogue Cytarabine (ara-C), used in the AML treatments, and of the adenosine analogue Vidarabine (ara-A), which is a successful anti-viral agent with limited anti-cancer activity.[35] Then, to overcome these limitations, the scientists Montgomery and Hewson conducted structural modification of the vidarabine, leading to synthesize the fludarabine (F-ara-A).[36] Nowadays fludarabine is the most extensively studied purine analogue, widely used in many leukemia treatments and the most effective in indolent CLL treatments. Indeed it is used for first- and second-line treatments of B-cell chronic lymphocytic leukemia.[37] Fludarabine can be administrated as a powder or solution for injection, under the trade name Fludara®, or as an oral formulation available in tablets of 10 mg generically, under the trade name Oforta®.[38] This drug has been approved by FDA in December 2008.[39]

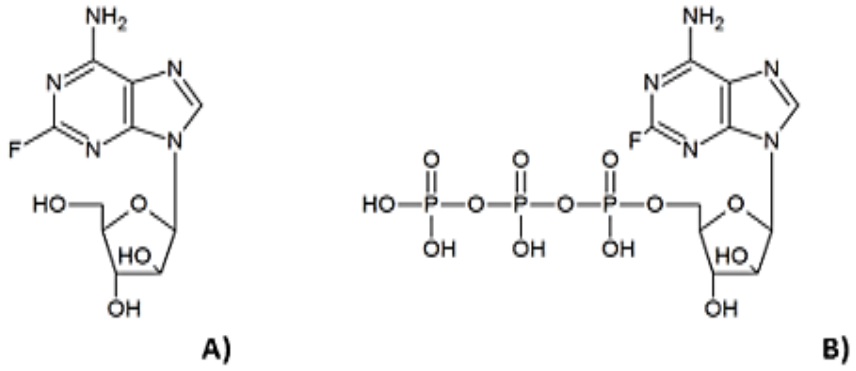

Figure 3. Fludarabine nucleoside analogue. A) Nucleoside fludarabine. B) Fludarabine triphosphate, which is the terminal stage of the activation process inside the cell.

Fludarabine phosphate is a water-soluble prodrug that is rapidly dephosphorylated to 2-fluoro-vidarabine (2F-ara-A), and it is actively transported into cells (Figure 3-A). As previously said, all NA needs to be intracellularly phosphorylated to generate their active metabolites, therefore 2F-ara-A is re-phosphorylated via deoxycytidine kinase to its active triphosphate derivative (2F-ara-ATP) (Figure 3-B).

2.2.3 Clofarabine

The clofarabine is a second generation purine analogue and it was design to overcome the problems of the vidarabine and of the fludarabine. The presence of a fluorine in 2'-clofarabine (Figure 4-A), significantly increase the stability of the glycosidic bond in acidic solution and toward phosphorolytic cleavage, as compared to fludarabine.[36] Compared to vidarabine, the chlorine substitution at the 2-position of the adenine base avoids production of a 2-fluoroadenine analogue, a precursor to the toxic 2-fluoro-adenosine-5′-triphosphate, and prevents deamination of the base.[40] Clofarabine is the prodrug of 2-chloro-2′-arabino-fluoro-2′-deoxyadenosine (CAFdA). This drug is used in treatments of both acute lymphoblastic leukemia and acute myelogenous leukemia. Clofarabine is used in pediatrics to treat a type of leukaemia called relapsed or refractory acute lymphoblastic leukaemia (ALL), only after the failure of at least other two types of treatment.[41] This drug can be administrated in vein by injection and it is marketed as Clolar®, in USA and Canada, and as Evoltra®, in Europe and Australia/New Zealand.[42]

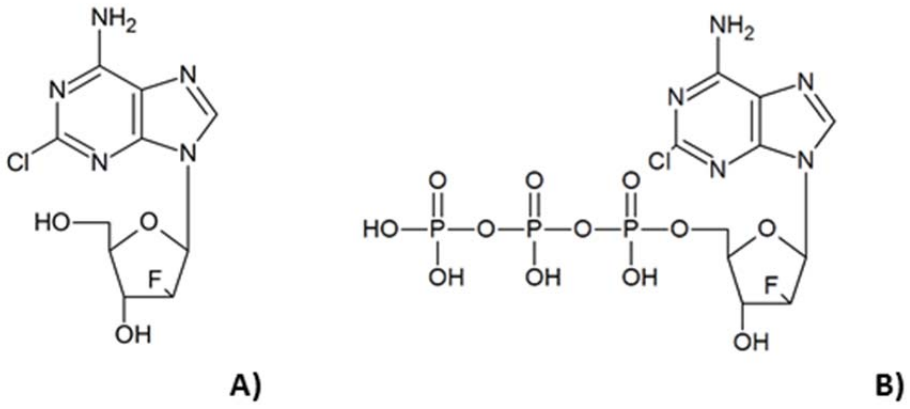

Figure 4. Clofarabine nucleoside analogue. A) Nucleoside clofarabine. B) Clofarabine triphosphate, which is the terminal stage of the activation process inside the cell.

Like fludarabine, clofarabine needs to be dephosphorylated to enter inside the cell. Afterwards it is metabolized intracellularly to the active 5'-monophosphate metabolite by deoxycytidine kinase and 5'-triphosphate metabolite by mono- and di-phospho-kinases (Figure 4-B). Clofarabine has high affinity with the activing phosphorylating enzyme, deoxycytidine kinase, equal to or greater than that of the natural substrate, deoxycytidine.

2.3 Drug Delivery Systems

Drug Delivery Systems (DDSs) are engineered technologies for the targeted delivery and/or controlled release of therapeutic agents. DDSs are capable to allow targeted transport of the drug directly to the cancer cells and to eliminate adverse side effects.[43] Using nanocarriers with autonomous modes of cellular entry, enable the possibility to deliver the NAs in their triphosphate form inside the cell. DDS should be characterize by prolonged blood half-life, specific tumor accumulation, efficient intracellular transport, low toxicity and controlled drug release.[44] Various nanoparticles present these requirements, and it is important to underline that perfectly branched dendrimers have been recently defined superior to other nanoparticles for drug delivery.[10]

2.3.1 Dendrimers

Dendrimers were introduced in the early 1980's and since then worldwide scientists have studied their properties and potential applications.[45] Vogtle in 1978 was the pioneer in making first attempt to design and synthesize dendritic structure, originally known as "cascade molecule".[46] After several years, a new category of cascade molecules containing amides was established and it was named "dendrimer". [47] The name dendrimer comes from the combination of the Greek words 'dendron' and 'meros', which respectively means 'tree' and 'part'. Indeed dendrimers are highly branched polymers of nanoscale size with well-defined three-dimensional structure. They are formed by three distinguishing architectural components: the core moiety, the interior layer, and the exterior layer (Figure 5).[48]

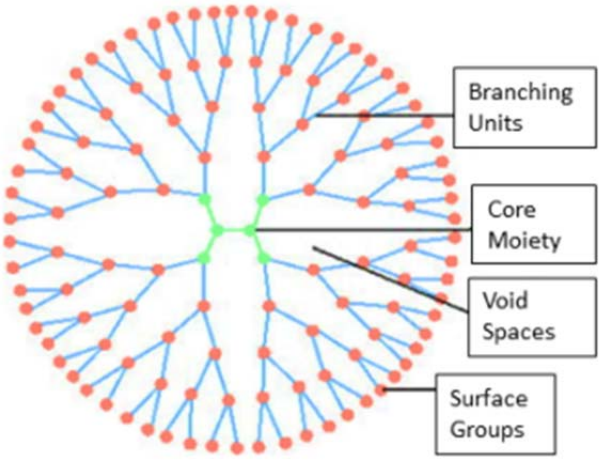

Figure 5. Dendrimer structure. Dendrimers are highly branched polymers of nanoscale size with well-defined three-dimensional structure. They are composed by three architectural components: the core moiety, the interior layer (composed by branching units and void spaces) and the surface groups.[49]

The central core of the dendrimer is composed by an atom or a group of structures, where carbon branches or other elements are added through sequence of chemical reactions to produce a spherical dendritic structure. Dendrimers are produced in an iterative step reaction sequence, using the divergent or convergent growth method.[49] The number of branching points, from the central core to the external layer, determines the generation number of the dendrimer. Indeed a dendrimer holding three branching points is called of third generation, and it is denoted as G3-dendrimer. The outermost part of the dendrimer is the surface, which contains many functional groups that can interact with the external groups or molecules. Dendrimers possess the ability to bind drugs inside their structure, as well as the numerous functional peripheral groups present on their surface and offer areas where drug molecules can dynamically stay attached.[50,51] The guest molecule-dendrimer interaction is mainly with the exterior surface of the dendrimer. Noteworthy, dendrimer structure determines the type and number of incorporated molecules and its loading potential can be considerably enhanced by modulating the association of guest with its external terminal groups.

The different ways of drug-dendrimer interaction are shown in Figure 6. Due to the dendrimer open nature architecture, encapsulation of drugs within dendrimer branches is possible (Figure 6-A). Physical entrapment or non-bonding interactions with specific structures of the dendrimer can be used as encapsulation methods for drugs. When the molecular groups present on dendrimer surface are charged, the surface may electrostatically attract oppositely charged molecules, determining drug-dendrimer electrostatic interaction (Figure 6-B). As well as drug can stay attached to the dendrimer with covalently or non-covalently interactions (Figure 6-C).

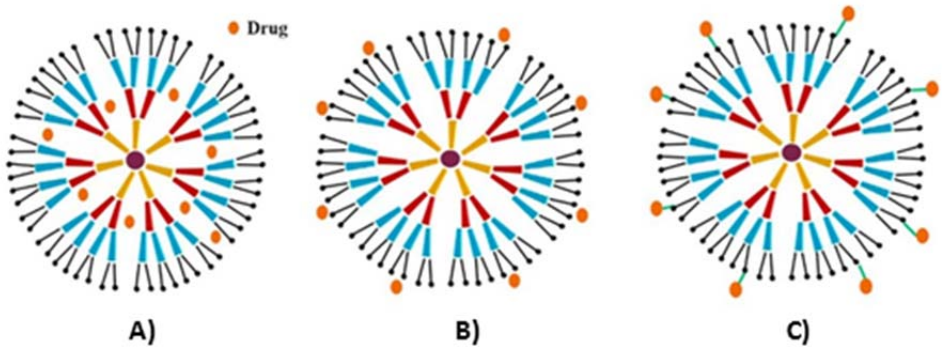

Figure 6. Various drug-dendrimer interactions. A) Drugs physical entrapment drugs inside dendrimer structure. B) Drug adsorption on dendrimer surface via intramolecular interaction. C) Conjugation of drug molecules to the surface groups of dendrimer.[52]

Furthermore dendrimers are charactherized by narrow polydispersity, nanometer size range and globular shape, and to allow easier passage across the biological barriers. Dendrimers provide improved solubility of the drug, controllable distribution patterns and enhance blood circulation time.[53] In order to utilize dendrimer as biological agents is necessary to fulfill certain biological demands. These branched polymers should be non-toxic, non-immunogenic, able to cross biobarriers, able to target specific structures and able to stay in circulation for the needed time of clinical effect. In recent years, many different designed functional dendrimers have been investigated such as: polypropylene imine dendrimer, polyamidoamine dendrimer (PAMAM), frechet-type dendrimer, core-shell tecto dendrimer, chiral dendrimer, liquid crystalline dendrimer, peptide dendrimer, hybrid dendrimer and glycodendrimer. In this case of study were studied polypropylene imine dendrimers.

2.3.2 PPI dendrimers

Over the last couple of years, many different dendrimers were considered as potential carriers for chemotherapeutic drugs, and one of the most promising scaffolds is poly(propileneimine) (PPI). PPI dendrimers core is composed by a central 1,4-diaminobutane molecule, from which poly(propyleneimine) chains are radially branched.[54] The presence of external and internal amino groups is responsible of their overall strong positive charge at physiological pH, which led to form long-lasting electrostatics interaction with different types of anionic drug molecules. Among others, PPI dendrimers form stable non-covalent complexes with NAs, which are the anionic drug molecules treated in our case of study.[9,55,56] On the other hand, the presence of positive charges on the PPI surface, determines highly cytotoxicity of the dendrimer and precludes their clinical application. Therefore it is necessary to weaken the charge of PPI dendrimer surface with neutral molecules, in order to obtain a more biocompatible nanocarrier.[57,58] Multiple surface modification have been studied to achieve this problem, and surface glycosylation seems to diminish its positive charge. PPI dendrimers, with the addition of sugar moieties, have lower innate cytotoxic properties, as well as they have improved their interaction with selected cell types.[10,59,60,61] Hence, glycosylation of the PPI dendrimer surface enable to create a stable and biocompatible DDS, based on non-covalent interactions between the PPI dendrimer and the NA. Furthermore the use of glycodendrimers as antileukaemics is justified due to the fact that leukaemic cells usually overexpress surface lectin receptors, which have high affinity to bind carbohydrate ligands, enabling receptor-mediated endocytosis. This highlights that cancer cells have active interactions with sugar-modified PPI dendrimers, bearing to decrease harmful effects on healthy tissues.[62]

The main goal is to develop an efficient dendrimer-based nanocarrier for NAs, with the right balance between the density of surface modification and the ability of macromolecules to interact with negative charged molecules. In this case of study, open shell poly(propyleneimine) dendrimers of 4th generation (PPI OS G4) were evaluated in their standard and glycosylated forms, where 43 maltose units were added (PPI-Mal OS G4). PPI OS G4 dendrimer possesses 64 terminal amino groups and the 4th generation is characterized by the semi-open structure, which facilitate ligand bonding (Figure 7). This dendrimer has a moderately rigid structure with internal cavities and charged terminal groups available for the guest molecules. Furthermore the 4th generation dendrimers adopt globular structure, in which the density increase regularly from the core to the surface region.[63]

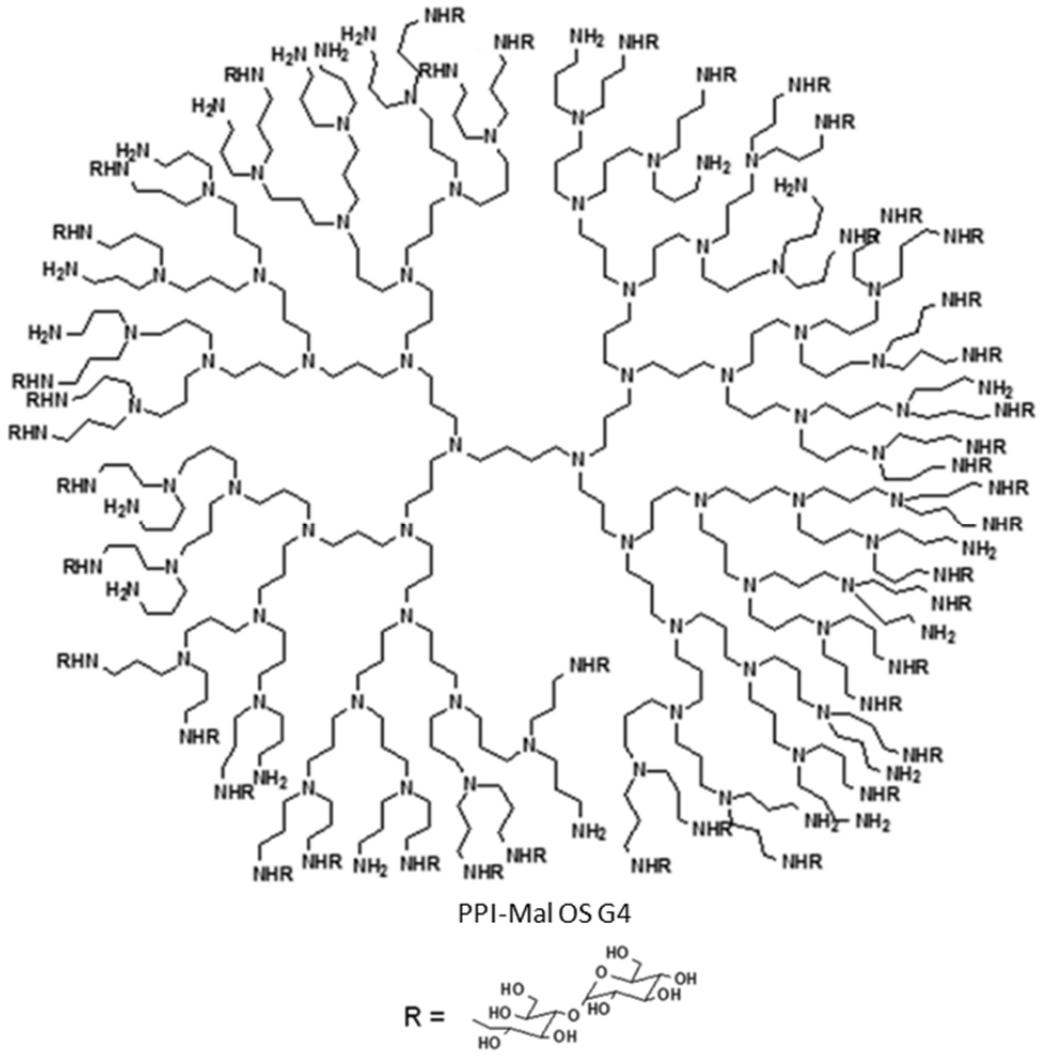

Figure 7. Chemical structure of the open-shell poly(propyleneimine) dendrimer of 4th generation, partially modified with 43 maltose units (PPI-Mal OS G4). The dendrimer has 43 maltose moieties coupler to the PPI scaffold in R positions.

PPI OS G4 dendrimers were investigated in their standard and glycosylate form to analyze their toxicity and pro-apoptotic activity in vivo. These dendrimers were tested on the MEC1 cell lines, which are the ones derived from B-CLL. It was confirmed that the PPI OS G4 dendrimers not only decrease MEC1 cells viability by inducing apoptosis, but they were also able to inhibit cancer cells proliferation. These two actions are equally important, indeed proliferation inhibition is a necessary condition as well as the cytotoxic effect in cancer and leukemia treatments.[8] Besides the PPI OS G4 dendrimer partially modified with the maltose units appears to be a solution to reduce dendrimer toxicity and its activity retention, and it enables more suitable for biomedical applications. Internalization mechanisms and intracellular trafficking of PPI OS glycosylate dendrimers were studied in melanoma cells, and provide valuable guidance in dendrimer coupling strategies with antitumor or diagnostic agents.[64] Studies were conducted on PPI-Mal OS G4 conjugated with fluorescein molecule, to analyze basic interactions between the PPI dendrimer and two distinct types of leukemia cell models: CCRF-1301 lymphoid cell line and HL-60 myeloid cell line. It has been recognized that cells from myeloid and lymphoid lineage strongly differ in many cellular features. Dendrimer internalization method is cell-related, and the shown differences have important repercussions on the potential applications of this glycodendrimers as drug delivery agents. In myeloid cells (HL-60), PPI internalization is very fast and freelance of binding to the cell surface. The dendrimer proceeds from the fluid phase via classical clathrin-dependent mechanism and stops its flows in the endolysosomal compartment from which is no further released. Instead, in lymphoid cells (CCRF-1301), the PPI internalization process is relatively slow and based on endocytosis process, leads by cholesterol mechanism and clathirin- and caveolin- indipendent, and this induces cell polarity changes.[65,66] Therefore, on both types of leukemia cells, glycodendrimer internalization is provided. PPI OS G4 glycosylate dendrimers can be used as high-volume carrier for drug molecules with myeloid cells, on the other hand, in case of lymphoid cells, the glycodendrimers can be potentially applied as highly specific carrier of nucleotide anticancer/antiviral drugs, delivering the sensitive cargo directly to the cytoplasm without exposure to harsh lysosomal conditions.

2.3.3 PPI dendrimer interactions with NAs

Poly(propyleneimine) dendrimers seem to be highly promising as drug delivery carriers in cancer treatments. Among the various drugs used to treat leukemia, PPI dendrimers are good nanocarriers of NAs groups. Indeed the use of PPI dendrimers let the possibility to overcome the problem of the triphosphate active-drug entrance inside the cell (Figure 8). As previously said (2.2.1 Nucleoside Analogues) all NAs need to be intracellularly phosphorylated to generate their active metabolites, but in presence of PPI dendrimer is possible to vehicular intracellularly directly the active drug. Inside PPI dendrimer the drug is encapsulated with hydrogen bonds, electrostatic or hydrophobic interactions, and drug binding on the surface of the dendrimer is due to electrostatic interaction or covalent bonds. Use of dendrimer-drug complexes increases drug targeted activity, thanks to a more stable, soluble and biocompatible anticancer treatment.[67] It is necessary to take into account that interactions between PPI dendrimers and NAs strongly depend on the chemical structure of both components, and can be crucial to understand complex behavior in presence of cancer cells.

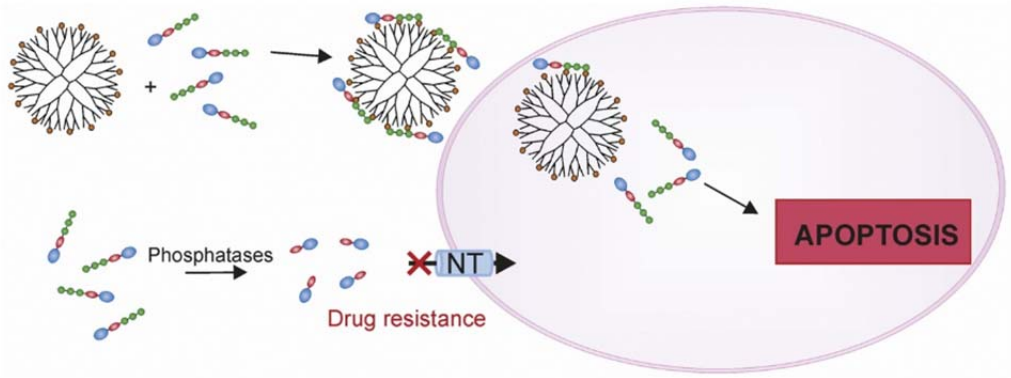

Figure 8. Schematic presentation of intracellular activity of NAs as free drug and complexed with PPI-Mal OS G4 dendrimer. Free drug needs to be dephosphorylated before entering inside the cell. It is intracellularly transported as a nucleoside form via transmembrane protein nucleoside transporter (NT). Instead, with the use of PPI-Mal OS G4 dendrimer, it is possible to directly transport the NA in its active form. Indeed the dendrimer enters inside the cell independently by the NTs and it can deliver the active triphosphate NA form inside the cell, causing its apoptosis.[65]

Recent studies have confirmed that PPI OS G4 dendrimer can form stable electrostatic complexes with active 5'-triphosphate NA forms. The interactions between the PPI OS G4 dendrimer, in its standard and glycosylate forms, and the cytidine-5'-triphosphate (Ara-CPT) were investigated by Isothermal Titration Calorimetry method. The Ara-CPT is a model of pyrimidine NA commonly used in leukemia treatments, and it has been studied its behavior with 1301 leukemic cells. Comparing the Ara-CPT alone with the Ara-CPT binds to PPI OS G4 dendrimer, it was evident that the second compound increase the cytotoxicity and the apoptosis of the leukemic cells. Moreover PPI-Mal OS G4 shows higher efficiency to create clever complexes with nucleotide triphosphates.[68] Furthermore, isothermal titration calorimetry and zeta potential titration were applied to determine the stoichiometry and thermodynamic parameters of interaction between PPI OS G4 (modified with maltose and unmodified forms) and adenosine-5'-triphosphate (ATP), in a pH- and salt-dependent manner. The ATP-dendrimer complexes make ionic pairs between the negatively charged phosphate residues and the positive terminal amino moieties on the glycodendrimers. These complexes are relatively stable, and the process of complexation is spontaneous, associated with advantageous exothermic changes in enthalpy and depends on buffer composition and pH. Indeed environmental parameters significantly affect nucleoside-dendrimer interactions, with strongest binding in organic buffer, as well as higher binding capacity at lower pH. These experiments confirmed previous reports that complexation of PPI dendrimers with nucleotides is pH-dependent.[69] Acidic environment enhances electrostatic interactions and triggers changes in the conformation of dendrimer, thus facilitating dendrimer-ATP binding. At lower pH values can be observed an increased number of active sites in PPI dendrimers, which is most likely associated to the repulsion between the positively charged surface moieties and inner amino groups of the macromolecule. As a consequence, PPI dendrimers adopt more open structure and expose multiple surface amino groups to ATP molecules. This behavior can be explained by the dendrimer conformation change, known as the "backfolding effect".[70,71] Recently, theoretical calculations, has suggested that the backfolding process may also occur for the maltose unit of PPI-Mal OS G4 dendrimer.[71] At neutral pH, may occur the hydrogen bonds between positively charged surface amino groups and uncharged amino groups inside the dendrimer. Consequently, terminal residues turn to the interior of the dendrimer, causing further reduction of cationic surface charge and limiting the ATP binding capacity. Remarkable is the fact that the number of nucleotide binding sites is decreased in sugar- modified PPI dendrimers, but the resulting binding is sufficient for potential drug delivery purposes.[56] These properties allow to consider maltose-modified dendrimers as especially promising carriers for adenosine analogues, and this efficiency was also confirmed

during recent studies on the interaction between fludarabine and PPI OS G4 dendrimers. The dendrimers were analyzed in their standard and maltose forms, and the complexes where tested on different leukemia cells: CCRF (acute lymphoblastic T cell leukemia), THP-1 (acute monocytic leukemia) and U937 (histiocytic lymphoma). The results demonstrate that U937 cells were the most vulnerable to fludarabine toxicity and these were the ones with the highest basal overall transcription rate. Moreover PPI-Mal OS G4 dendrimer was able to improve intracellular cytotoxicity of the fludarabine and to bypass the resistance associated with the presence of hENT1 nucleoside transporter. It was evident that glycosylate PPI dendrimer does not alter specific activity of the fludarabine, contrariwise it enhances its cellular entry and enables directly and phosphorylation-independent toxicity, most probably due to the autonomous mode of cell entry.[53]

3. Materials and Methods

This chapter describes the theory underlying the present master thesis work, with the aim of explaining the physical background behind the computational approach. In detail, section 2.1 presents a quick introduction to computational molecular modelling, while sections 2.2 and 2.3 describe the Molecular Mechanics and Molecular Dynamics approaches respectively. Finally section 2.4 is an overview of the analysis methods conducted to investigate this case of study.

3.1 Introduction to computational molecular modelling

Molecular modelling encompasses all theoretical methods and computational techniques used to model and mimic the complex behavior of chemical systems (e.g., molecules, proteins) in term of atomistic description, aimed to predict and to understand macroscopic properties of these systems. Molecular systems are composed by a huge number of molecules and this strongly determine the impossibility to analytically evaluate the properties of the system. To overcome the analytical intractability, these systems can be studied using numerical methods. Molecular Dynamics (MD) is a powerful tool to understand molecular processes, due to its capacity to make a connection between theory and laboratory experiments. MD is a multidisciplinary method based on physic, information theory, chemistry, statistical and molecular mechanics. This technique uses Newton equations of motion to computationally simulate the time evolution of a set of interacting atoms.[72] Nowadays, MD is mostly applied in biomolecules modelling and in materials science. The following list shows some MD applications: protein structure and dynamic, protein folding/unfolding, molecules docking, polymers chains analysis, transport and diffusion properties, multiscale modelling and there is much more. These applications are possible thanks to the improvement of computer power, which enable to simulate biological systems of millions of atoms in a relative reduced simulation time.

3.2 Molecular mechanics

Molecular dynamics technique is based on solving Newton equation of motion, therefore it is necessary to define a potential energy function that can describe the simulated system. The molecular mechanics (MM) method uses Newtonian mechanics to model molecular system, without considering the electronic motions and analyzing the system as a set of atoms interacting through a potential energy function.[73] MM is based on rather simple model, due to the Born-Oppenheimer approximation [74], atoms (ensemble nucleus and electrons) are represented by spherical particles with their own radius. Based on the idea of '30s works of Andrew[75], atoms and their bonds are modeled such as balls joined by springs, where classical mechanical spring theory is applied to describe bond stretching, twisting and bending. Moreover, non-bonded interactions as electrostatic and Van der Waals are also taken into account and exhaustively explained in the following sections. Therefore, the core of the MM approach is the set of equations and parameters used to describe the potential energy function V of a molecular system, also named force field (FF).

3.2.1 The potential energy function

The FF allows to compute the potential energy of the molecular system in a given conformation, as a sum of individual energy contribution:

Eq. 1

$$V = V_{covalent} - V_{non-covalent}$$

Where the components of the covalent and non-covalent terms are given by the following equations:

Eq. 2

$$V_{covalent} = V_{bond} + V_{angles} + V_{dihedrals} + V_{improper\ dihedrals}$$

Eq. 3

$$V_{non-covalent} = V_{electrostatic} + V_{Van\ der\ Waals}$$

Each of the term mentioned above, can be modelled in different way, depending on the particular simulation settings being used.[76]

3.2.2 Treatment of the bond and non-bond interactions

The potential energy function implementation plays a central role in the MM approach. The potential energy as a function of the position *r* of N atoms can be described as follow:

Eq.4

$$V(r^N) = \sum_{bond} \frac{k_{il}}{2} * \left(l_i - l_{i,0}\right)^2 + \sum_{angles} \frac{k_{i\theta}}{2} * \left(\theta_i - \theta_{i,0}\right)^2 + \sum_{dihedrals} \frac{V_n}{2} * \left(1 + cos(n\omega - \eta)\right)$$
$$+ \sum_{\substack{improprer \\ dihedrals}} k_{i\Phi} * \left(\Phi_i - \Phi_{i,0}\right)^2 + \sum_{i=1}^{N} \sum_{j=i+1}^{N} \left(4\varepsilon_{ij} \left[\left(\frac{\sigma_{ij}}{r_{ij}}\right)^{12} - \left(\frac{\sigma_{ij}}{r_{ij}}\right)^{6} \right] + \frac{q_i * q_j}{4\Pi\varepsilon_0 * r_{ij}} \right)$$

The first term in *Eq.4* represents the interaction between bonded atoms, which is describe with a harmonic potential inducing potential energy increase when the bond length *l* departs from the reference value l_0. The second term describes the angle among three atoms, modelled using a harmonic potential. The third term is a torsional potential which describes bond rotation and the fourth term, represented by improper dihedrals, models the deformations outside the plane. The bond term is composed by all previous mentioned contributions, considered together. Instead the non-bond interactions are represented by fifth term. The FF equation previously shown (*Eq.4*) consists of two distinct components: the set of equations used to generate the potential energies and the parameters used in this set of equations. The FF parameters are usually derived empirically or through a quantistic approach. The non-bond interactions represent an important component of the MD force field, due to their dominant role in the interaction between molecules, which is necessary to maintain the three-dimensional structure of the system. Usually, non-bond terms are modelled as functions inversely proportional to the distance between two atoms. As shown in the last term of *Eq.4*, the non-bond interactions are usually determined by the sum of two components: Van Der Waals forces and electrostatic interactions. The electrostatic interaction can be described by using the Coulomb's law:

Eq. 5

$$V = \frac{Q_i Q_j}{4\pi\varepsilon_0\varepsilon_r r_{i,j}}$$

The denominator $4\pi\varepsilon_0\varepsilon_r r_{i,j}$ is the electric conversion factor, where the term ε_0 is the free space permittivity and ε_r is the relative permittivity. This type of interaction is defined as long-range interaction, due to the fact that the energy decreases with the distance between two atoms as $1/r$.

The interaction between two atoms is also characterized by the Van Der Waals forces, represented by the sum of the attractive/repulsive forces between molecules (or between parts of the same molecule), caused by correlations in the fluctuating polarizations of nearby particles. Van Der Waals interactions are relatively weak compared to covalent bonds, nevertheless they play a fundamental role in defining many organic compound properties, including their solubility in polar and non-polar media. Van Der Waals potential is often represented with the Lennard-Jones equation,[77] which is an approximate model for the isotropic part of a total Van der Waals force (repulsion plus attraction) as a function of distance :

Eq. 6

$$V_{Lennard-Jones} = 4\,\varepsilon_{i,j}\left[\left(\frac{\sigma_{i,j}}{r_{i,j}}\right)^{12} - \left(\frac{\sigma_{i,j}}{r_{i,j}}\right)^{6}\right]$$

Lennard-Jones (LJ) potential (Eq. 6) contains two parameters: the well depth $\varepsilon_{i,j}$ and the collision diameters $\sigma_{i,j,}$ that is the distance after which the Van der Walls interactions produce a zero contribution (Figure 9). This potential is characterized by a repulsive component (the first term in Eq. 6) due to the overlapping between electron orbitals and an attractive component (the second term in Eq. 6). Both the parameters are dependent on the types of atoms involved in the interaction. Therefore, the calculation of non-bond forces is really expensive in terms of computational effort, due to the increased number of the non-bond interaction as the square of the number of atoms in the system. To properly reduce the computational expense, the non-bond interactions are computed by applying the cutoff distance. With the application of the cutoff distance, every interaction between two atoms is computed only if their distance is smaller than the cutoff.

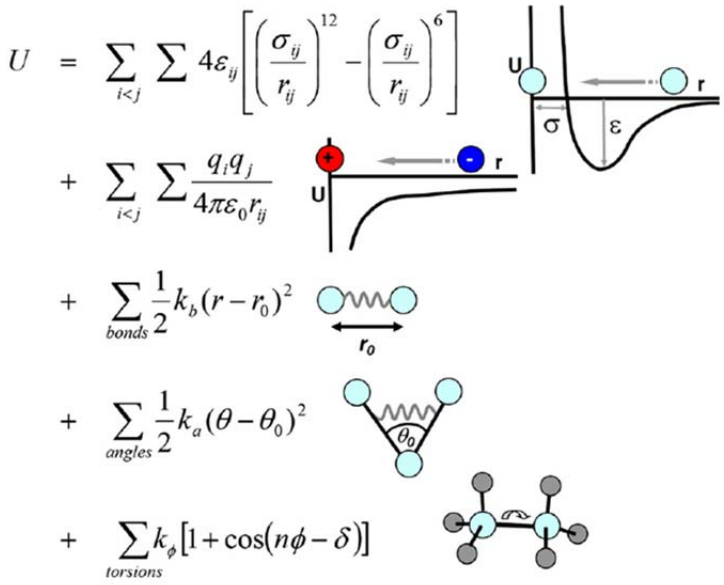

Figure 9. Potential energy function for molecular interactions in the molecular mechanic approximation. The first and the second term describe the non-bond terms, which are respectively Van der Waals and Coulomb forces. The following terms represent the bond terms (bond, angles and torsions).[78]

3.2.3 Periodic Boundary Conditions

In order to minimize the edge effects in a finite system, the computational model of a molecular system is characterized by Periodic Boundary Conditions (PBC). All the system atoms are contained in a three-dimensional box, usually filled with water, implicitly or explicitly modelled. This box is encircled by translated copies of itself (Figure 10), with the purpose of eliminating boundaries of the system. The presence of PBC causes imprecisions that are considered less heavy than the errors deriving from an artificial boundary with vacuum. In the minimum image convention, the particles near the boundary of the main box can feel the interactions with the particles in the nearest periodic box, and if a molecule leaves the box during the simulation, it is replaced by its own periodic image that comes into the box from a neighbor. Therefore the number of particles in the main box remains constant. Applying a cutoff distance, for short range interactions as the LJ potential, it is not a trouble, since LJ decreases very rapidly. In case of long-range interaction model, it is necessary to use more accurate methods (e.g., shift functions and switch functions) with the purpose of preventing discontinuities in the potential energy calculation. Other approaches, in addition to the cutoff method, are employed to overcome these problems and to properly evaluate the electrostatic interaction: Particle Mesh Ewalds [79], Reaction Field [80] and Multipole Cells [80].

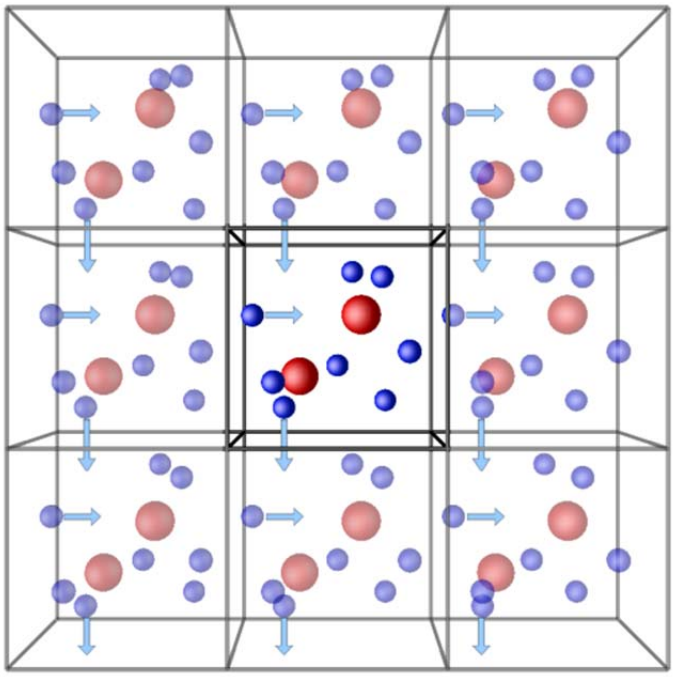

Figure 10. Periodic boundary conditions. The first box is in center and then it is replicated all around it, to eliminate the system boundaries. It contains atoms (red balls) and water molecules (blue balls).

3.2.4 Potential Energy Minimization

The Potential Energy function is a complex multidimensional function of the molecular system coordinates. The minimum point of the Potential Energy Surface (PES) correspond to stable states of the system: any movement away from this configuration is characterized by higher energy level. However, there are also a lot of local minimums in the PES and the one with the lowest energy is called global minimum. Starting from the MM description of the molecular system, in term of FF, the energy minimization is able to reduce the potential energy of the system. Notable is the fact that there are two different approaches to identify the minimum point of the PES: the derivative and the non-derivative method. The set of derivative minimization methods is built up from first order methods (e.g., Steepest Descent [81], Conjugate Gradient [82]) and second order methods (e.g., Newton-Raphson, L-BFGS). In the first order methods, the direction of the first derivative of the energy (the gradient) indicates where the minimum lies. Second derivatives indicates the curvature of the function, showing where the energy function changes direction. Energy minimization is widely performed before a molecular dynamic simulation, especially to simulate complex systems, such as macromolecules.

3.3 Molecular Dynamic: theoretical method

3.3.1 Statistical ensemble

There are two categories of macroscopic properties in a complex chemical system: static equilibrium properties (e.g., average potential energy, radial distribution function) and dynamic or non-equilibrium properties (e.g., the dynamics of phase changes, diffusion processes). A representative statistical ensemble defines all the accessible physical states of a molecular system. It is generated at a given temperature to calculate the macroscopic system properties. The space in which all possible physical states of a system are represented is known as phase space, which often consists of all the possible values of position and momentum variables. In general, every degree of freedom of the system is represented as an axis of multidimensional space. In a system containing N atoms, 6N values are required to define the state of the system (three coordinates of position and three components of momentum) and each possible state corresponds to one unique point in the phase space. The state of the system is described by a single point in the phase space, and the succession of these plotted points represent all that the system can be. There are different points in the phase space characterized by the same thermodynamic state. The collection of all possible system configurations which has different microscopic states but an identical thermodynamic state is known as statistical ensemble (Table 2). There are different ensembles and each of them represents a different thermodynamic state:

The *Micro-Canonical ensemble (NVE)* in which the thermodynamic state is characterized by a fixed number of atoms *N*, a fixed volume *V* and a fixed energy *E*. This corresponds to an isolated system.

The *Canonical Ensemble (NVT)* in which thermodynamic state is characterized by a fixed number of atoms *N*, a fixed volume *V* and a fixed temperature *T*. This corresponds to a closed system.

The *Grand canonical Ensemble (mVT)*: the thermodynamic state for this ensemble is characterized by a fixed chemical potential *m*, a fixed volume *V* and a fixed temperature *T*. This corresponds to an open system.

The *Isobaric-Isothermal Ensemble (NPT)*: this ensemble is characterized by a fixed number of atoms *N*, a fixed pressure *P* and a fixed temperature *T*.

Table 2. Statical ensembles. The thermally isolated equilibrium ensemble, also known as microcanonical or NVE ensemble, number of particles N, volume V and total energy E are constant. The statistic ensemble in thermal equilibrium with a heat reservoir, also known as canonical or NVT ensemble, is characterized by fixed number of particles N, volume V and temperature T. The Isobaric-isothermal ensemble is characterized by fixed number of particles N, pressure p and temperature T. In the Grand canonical ensemble, there are variable number of particles, but fixed volume, temperature and chemical potential.

ENSEMBLE	FIXED VARIABLES
Thermally isolated equilibrium	N, V, E
Thermal equilibrium with heat reservoir	N, V, T
Isobaric-isothermal	N, p, T
Grand canonical or Gibbs	μ, V, T

There are different approaches for the generation of a representative statistical ensemble: the most widely used are Molecular Dynamics and Monte Carlo simulations. The right technique is chosen based on the type of problem to examine. The MD method samples the phase space in a way that is representatives of the equilibrium state and is able to calculate the ensemble average of the macroscopic property. The ensemble average of property A is determined by integrating over all possible configurations of the system by:

Eq. 7

$$< A > = \iint A\,(p^N, r^N)\,\rho(p^N, r^N)\,dp^N\,dr^N$$

$A(p^N, r^N)$ is the element of interest, where p is the momenta and r is the atomic positions. The probability density function $\rho(p^N, r^N)$ of the ensemble is given by:

Eq. 8

$$\rho(p^N, r^N) = \exp\frac{(-E(p^N, r^N)/K_B T)}{Q}$$

where K_B is the Boltzmann factor, T is the temperature and $E(p^N, r^N)$ is the Hamiltonian. The denominator Q is called the partition function, and that is a dimensionless normalizing sum of Boltzmann factors over all microstates of the system:

Eq. 9

$$Q = \iint \exp\left[\frac{-H(p^N, r^N)}{K_b T}\right] dp^N dr^N$$

The partition function (*Eq. 9*) is extremely important because a lot of thermodynamics properties can be calculated with the previous equation. The partition function relates microscopic thermodynamic variables to macroscopic properties, but the analytical solution of the previous equation is really impossible to calculate due to the fact that it is extended to all possible states of the system. However, in order to overcome this problem, it can be used the ergodic hypothesis. This hypothesis states that, over long periods of time, the time-average of a certain physical property represents the
ensemble-average of the same property:

Eq. 10

$$< A >_{time} = < A >_{ensemble}$$

The time-average $<A>_{time}$ can be computed by:

Eq. 11

$$< A >_{time} = \lim_{\tau \to \infty} \frac{1}{\tau} \int_{t=0}^{\tau} A(p^N(t), r^N(t)) dt \simeq \frac{1}{M} \sum_{t=1}^{M} A\,(p^N, r^N)$$

where t is the simulation time, $A(p^N, r^N)$ is the instantaneous value of the calculated property and M is the number of time steps in the simulation . Therefore, from an efficient sampling of microstates in a specific ensemble sequentially in time, can be computed an ensemble-average property of the system under investigation.[76]

3.3.2 Molecular Dynamics implementation schedule

Molecular Dynamics allows to investigate and to study molecular motion through computer power and theoretical biophysics principles. The basic idea of the MD method is to solve Newton's equations of motion for a system of N interacting atoms or particles. For each atom, the acceleration a_i is given as the derivative of the potential energy with respect to the position, r:

Eq. 12

$$a = -\frac{1}{m}\frac{dV}{dr}$$

The potential energy is a function of the atomic position. There is not an analytical solution of the previous equation (*Eq. 12*), due to the complex nature of this function. The solution of this equation can be obtained by using some numerical integration schemes. To integrate the equation two important choices must be taken: the integration time-step (usually fs) in order to avoid instability and the sampling time to correctly sample the phase space. The possible MD integration methods are various, such as the variation of the Verlet algorithm, called the Leap Frog Algorithm.[83] The following figure describes the MD flowchart (Figure 11), starting from the molecular system input data. The initial atoms velocities v_i are chosen randomly from a Maxwell-Boltzmann distribution at a given temperature and the initial atomic positions r_i are known (e.g., from Protein Data Bank). Following the MD flowchart represented in Figure 11, the set of atoms coordinates and velocities is generated step by step, giving the trajectory that describes positions, velocities and accelerations of the particles as functions of time. The MD method is deterministic: once the positions and velocities of each atom are known, the state of the system can be predicted at any time in the future or in the past. After initial changes, the molecular system reaches an equilibrium state. The equilibrium state can be interpreted as a statistical ensemble that will provide a macroscopic description of the behavior of the system. Using the output trajectory of the MD, the macroscopic thermodynamic properties (e.g., temperature, energy, pressure) can be calculated as time averages.

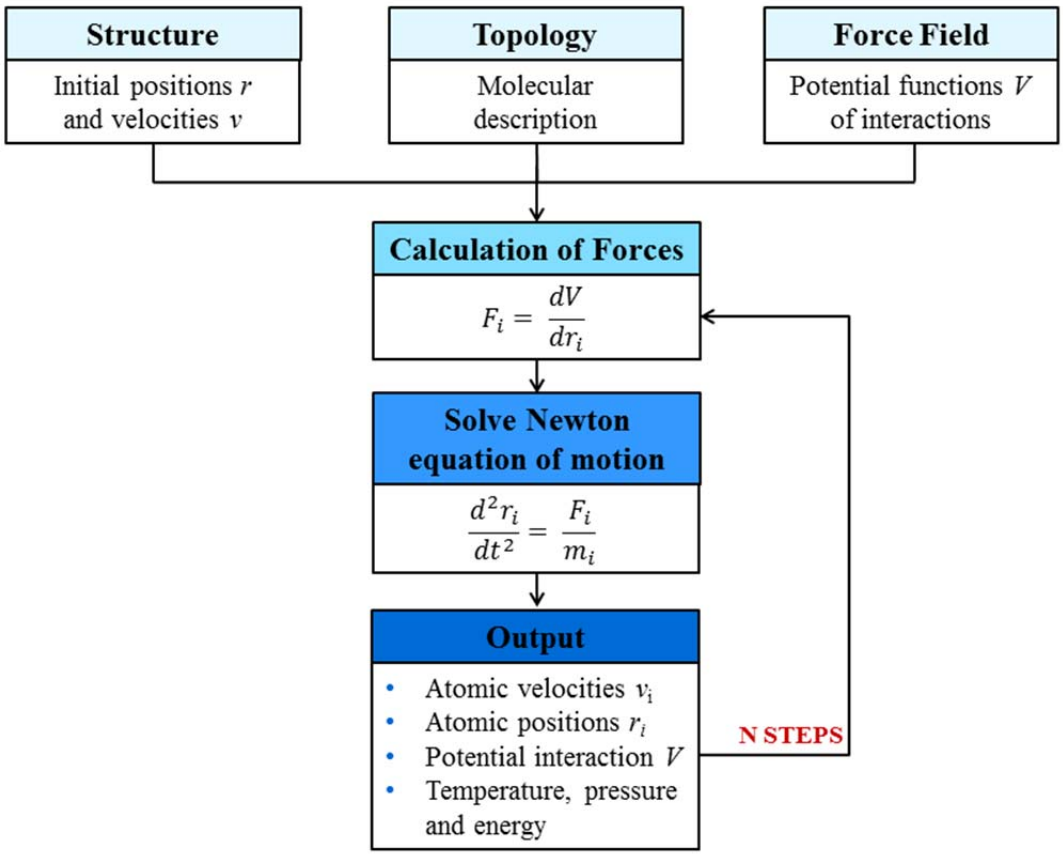

Figure 11. MD flow chart. In the MD algorithm scheme the input datas are the structure (initial positions *r* and velocities v), the topology (information about the molecular description) and the Force Field (potential functions *V* of interactions). The scheme continues with the calculation of the forces Fi acting on each atom, by deriving the potential energy function. Then the integration of the Newton equation of motion leads to the calculation of new position r_i and velocities v_i. The cycle goes on for a number of N steps until the equilibrium is reached (convergence of the computed equilibrium property).

3.3.3 Software packages

There is a wide variety of MD codes for biomolecular simulation, such as: AMBER[84], CHARMM[85], GROMACS[86] and NAMD[87]. GROMACS (GROningen MAchine for Chemical Simulations) is a molecular dynamics simulation package originally developed in the University of Groningen, now maintained and extended to different places and universities. GROMACS is written for Unix-like operating systems and the entire package is available under the GNU General Public License. GROMACS is a versatile tool to perform MD simulations and energy minimization. It is primarily designed for biochemical molecules like proteins, lipids and nucleic acids that have a lot of bonded interactions, but it is very fast in the calculation of non-bonded interactions. For this reason many research groups are also using it for non-biological systems, e.g. polymers.[88]

3.4 Analysis methods

After having run a MD simulation, it can be widely analyzed using GROMACS tools. Many are the possible analysis that can be conducted on the trajectory file, to investigate the various behavior of the system.[89] Here below will be discussed the analysis methods used in this thesis work.

3.4.1 Cluster analysis

The MD trajectory usually contains a wide number of snapshots. Therefore data-mining such as clustering methods can be helpful to gather together similar representative conformations. A clustering approach divides, according to the method used, the data or conformations into different groups called clusters. Each point inside the cluster is ideally more similar to the points of the same cluster, while is far from the data of the other clusters.[90] This method shows how a given molecule is sampling the phase space and allows a more simple characterization of the system. The reversible formation of clusters from monomers (such as molecule, macromolecule or colloidal particle) is important for many condensed-phase problems.[91] An useful GROMACS command is *gmx clustsize*, which computes the size distributions of molecular/atomic clusters in gas phase. The output consists in a .xpm file extension and the total number of clusters is written to an .xvg file.

3.4.2 Distance

To monitor specific bonds in the system conformation, or more generally to monitor distances between points, is possible to calculate the distance values between atoms, molecules or groups of them. It is necessary to create a traditional index file, where there are defined the groups such as pair of atom numbers. This index file is the input file of the command *gmx distance*.[89] The GROMACS command *gmx distance* can calculate distances as a function of time, as well as the distribution of the distance. Each selection specifies an independent set of distances to calculate, and it should consists in pairs of positions, where the distances are computed between positions 1-2, 3-4, etc.

3.4.3 Radius of Gyration

To have a rough measure of the compactness of the structure, it is possible to calculate the radius of gyration with the GROMACS program *gmx gyrate*, as follows:

Eq. 13

$$R_g = \left(\frac{\sum_i \|r_i\|^2 \, m_i}{\sum_i m_i} \right)^{\frac{1}{2}}$$

where m_i is the mass of atom i and r_i the position of atom i with respect to the center of mass of the molecule.[89] This function is especially useful to characterize polymer solutions and proteins. The GROMACS program will also provide the radius of gyration around the coordinate axis (or, optionally, principal axes) by only summing the radii components orthogonal to each axis, for instance:

Eq. 14

$$R_{g,x} = \left(\frac{\sum_i \left(r_{i,y}^2 + r_{i,z}^2 \right) m_i}{\sum_i m_i} \right)^{\frac{1}{2}}$$

3.4.4 Radial Distribution Function

To analyze how the density of a system of particles (e.g., atoms or molecules) varies as a function of distance from a reference particle (Figure 12), it is possible to calculate the radial distribution function (RDF).

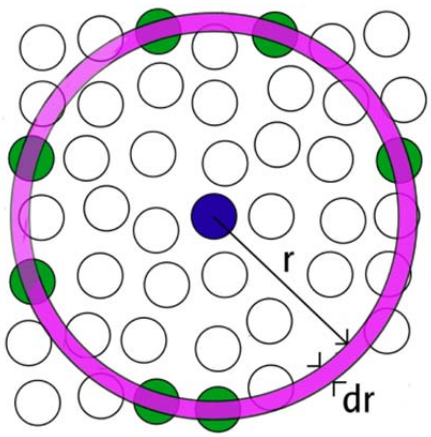

Figure 12. Space discretization for the evaluation of the radial distribution function.

To proceed with the RDF calculation, the $g_{AB}(r)$ of A with respect to B is calculated as:

Eq. 15

$$4\pi r^2 g_{AB}(r) = V \sum_{i \in A}^{N_A} \sum_{j \in B}^{N_B} P(r)$$

where V is the volume and P(r) is the probability of finding a B atom at distance r from an A atom. By having the user define the atom numbers for groups A and B in a simple file, g_{AB} can calculate this in the most general way, without having to make any assumptions in the RDF program about the type of particles. Groups can therefore consist of a series of atom numbers, but in some cases also of molecule numbers. The radial distribution function (RDF) or pair correlation function $g_{AB}(r)$ between particles of type A and B is defined in the following way:

Eq. 16

$$g_{AB}(r) = \frac{\langle \rho_B(r) \rangle}{\langle \rho_B \rangle_{local}} = \frac{1}{\langle \rho_B \rangle_{local}} \frac{1}{N_A} \sum_{i \epsilon A}^{N_A} \sum_{j \in B}^{N_B} \frac{\sigma(r_{ij} - r)}{4\pi r^2}$$

with $\langle \boldsymbol{\rho_B}(\boldsymbol{r}) \rangle$ the particle density of type B at a distance r around particles A, and $\langle \boldsymbol{\rho_B} \rangle_{\boldsymbol{local}}$ the particle density of type B averaged over all spheres around particles A with radius r_{max}. Generally the value of r_{max} is half of the box length. The averaging is also performed in time, indeed in practice the analysis program gmx rdf divides the system into spherical slices from r to r+dr (Figure 12) and makes a histogram instead of the function.

3.4.5 Molecular Mechanics Poisson-Boltzmann Surface Area

The Molecular Mechanics Poisson-Boltzmann Surface Area (MM-PBSA) method has been applied to predict binding free energies and to evaluate the relative stabilities of different biomolecular structures.[92] Combined with MD simulations, MM-PBSA can incorporate conformational fluctuations and entropic contribution of binding energy.[93] The MM-PBSA method expresses the free energy of binding as the difference between the free energy of the complex and the free energy of the receptor plus the ligand (*Eq. 17*), and this difference is averaged over a number of trajectory snapshots.

Eq. 17

$$\Delta G_{binding} = G_{complex} - \left(G_{protein} + G_{ligand}\right)$$

The free energy of each individual entity of the system can be given the combination of three energetic terms (*Eq. 18*). The first term is the potential energy in vacuum and the second accounts for the desolvation of the different species. The third term accounts for the configurational entropy associated with the complex formation in gas phase.[94]

Eq. 18

$$G_x = \langle E_{MM} \rangle - TS + \langle G_{solvation} \rangle$$

Where TS, the second term, refers to the entropic contribution to the free energy in a vacuum where T and S denote respectively the temperature and the entropy. As previously said the first term, $\langle E_{MM} \rangle$ represent the vacuum potential energy, which include the energy of both the bonded and non-bonded interactions:

Eq.19

$$E_{MM} = E_{bonded} + E_{non-bonded} = E_{bonded} + (E_{VdW} + E_{elec})$$

Where E_{bonded} indicates bond, angle, dihedral and improper interactions. The non-bonded interactions include both electrostatic and Van der Waals interactions (*Eq.19*) and are modelled using a Coulomb and Lennard-Jones (LJ) potential function respectively. Finally, the last term presents in *Eq. 18* ($\langle G_{solvation} \rangle$) is the free energy of solvation. This value is the energy required to transfer a solute from vacuum into the solvent. Using MM-PBSA approach, $G_{solvation}$ is calculated using an implicit solvent and it is expressed as the sum of two terms:[95]

Eq. 20

$$G_{solvation} = G_{polar} + G_{nonpolar}$$

Where G_{polar} and $G_{nonpolar}$ are the electrostatic and non-electrostatic contributions to the solvation energy. GMXPBSA 2.0 calculates this two values using Adaptative Poisson-Boltzmann Solver (APBS) program.[95] The polar solvation energy G_{polar} is calculated by solving the Poisson-Boltzmann (PB) equation[96], which is given by:

Eq.21

$$\nabla.[\varepsilon(r).\varphi(r)] - \varepsilon(r)k(r)^2 sinh[\varphi(r)] + \frac{4\pi\rho^f(r)}{kT} = 0$$

Where ε(r) is the dielectric constant, φ(r) is the electrostatic potential and $\rho^f(r)$ is the fixed charge density. As shown in *Eq.21*, the PB is a second-order nonlinear elliptic partial differential equation, and it can become linear only when φ(r)<< kT and sinh[φ(r)] ≈ φ(r). Furthermore, the non-electrostatic term of solvation free energy $G_{nonpolar}$, presents in *Eq. 20*, includes attractive and repulsive forces between solute and solvent, that are generated by Van der Waals interactions and cavity formation respectively.

Eq. 22

$$G_{nonpolar} = G_{cavity} + G_{VdW}$$

Where G_{cavity} corresponds to the work done by the solute, to create a cavity in the solvent and it is geometry and shape solute dependent. Instead, G_{VdW} is the attractive Van der Wals energy between the solute and the solvent. The terms present in *Eq. 22* can be estimated using different models.[94]

4. Comparison between clofarabine and fludarabine interaction with poly(propyleneimine) dendrimers PPI G4 and PPI-Mal OS G4 and their protonated forms

This chapter presents an investigation focused on clofarabine and fludarabine interactions with PPI G4 and its maltose modified version PPI-Mal OS G4, by means of MD simulations. To better understand the complexes with real pH conditions, these dendrimers have been analyzed in their standard and protonated form. The results provide an atomistic investigation of the compound-dendrimer complex, focusing the attention on: i) dendrimer protonation, ii) the complexation modes, iii) the orientation and the penetration of the compound over the dendrimer surface and iiii) the interactions between compound parts and dendrimer layers.

4.1 Abstract

Fludarabine and clofarabine are nucleoside analogue antimetabolites widely used in modern chemotherapy to treat hematological malignancies. Their complex pharmacokinetic, which requires active transmembrane transport and intracellular phosphorylation to triphosphate nucleotide forms, limits the therapeutic potential of these drugs. We investigate poly(propyleneimine) dendrimers of fourth generation (PPI G4) partially modified with maltose (PPI-Mal OS G4) as efficient nucleotide carriers. In this study we present computational approaches, based on Molecular Dynamics simulations, to elucidate the molecular reasons behind clofarabine and fludarabine different displacement/interaction with the dendrimers. The compound-dendrimer complexes were protonated to simulate their behavior at neutral or acid environment condition. Our results confirmed what seen with *in vivo* experiments. Interestingly, both the drug nucleoside forms do not interact with the PPI G4 dendrimer, neither with PPI-Mal OS G4 one. Furthermore, in compound-dendrimer complexes, it was evident that the dendrimer protonation affects the interaction mode in term of drug orientation. Indeed clofarabine triphosphate completelly change its orientation in presence of PPI-Mal OS G4 dendrimer in acid environment. It was characterize by the phosphate part turned to the center of the dendrimer, which interacted with the inner parts of the dendrimer, and its acid nucleic base stay exposed to the solvent. On the other hand, the fludarabine nucleotide was able to interact with the dendrimer surface and to settled in different positions. Therefore these compound displacements suggest that the fludarabine triphosphate had a more flexible structure compared to the clofarabine triphosphate. Most likely, the PPI-Mal OS G4 dendrimer can efficiently deliver the fludarabine nucleotide inside

the cell and the compound can easily detach from the dendrimer surface. Contrariwise, the clofarabine nucleotide orientation do not allow an easy released of the drug inside the cell, and the use of PPI G4 dendrimer as carrier do not extol its cytotoxicity.

4.2 Introduction

Nucleotide analogues are a versatile class of antimetabolite drugs with numerous applications in chemotherapy, such as treatments of hematological malignancies (e.g., leukemia and lymphoma). [26] The naturally occurring nucleosides represent a unique starting point for drug design owing to their involvements in several critical biological processes and being central components for both DNA and RNA synthesis.[97] These purine and pyrimidine derivatives exhibit mechanisms that decrease the activity of enzymes, which are involved in the metabolism of natural nucleosides and nucleotides. Additionally, these can be directly incorporated into the newly synthesized nucleic acid chains. These action results in the inhibition of DNA and RNA synthesis, which lead to the induction of cellular apoptosis. The cytotoxic mechanisms of NAs strongly depend upon their chemical structures and affinity with the intracellular targets.[28,5] Noteworthy, all anticancer NAs share common metabolic pathways and cellular uptake. Due to their hydrophilic nature, NAs cannot enter passively into the cell because they need specialized nucleoside transporters (NTs) to cross cell membrane. Once inside the cell, nucleosides are progressively phosphorylated by the intracellular kinases to their triphosphate forms, which are crucial for their cytotoxic effect.[98,99] Intriguingly, NTs can transport only dephosphorylated substrates and this limits the administration of prodrug forms instead of active metabolite forms. This complex metabolism enables a number of possible resistance mechanisms; it may also result in poor cellular uptake and insufficient intracellular phosphorylation of NAs. Furthermore, NAs activity is unspecific for cancer cells and thus there is a high risk of their toxicity.[28,100] To overcome the mentioned resistance mechanisms, it is possible to introduce the application of drug delivery systems (DDS). A DDS should be able to hold an adequate amount of therapeutic agent and to overcome obstacles such as drug resistance, rapid clearance from the bloodstream and disadvantageous biodistribution. Other required characteristics include prolonged blood half-life, efficient intracellular transport, specific cancer accumulation and controlled drug release.[101] Many DDS are able to satisfy these requirements and can be used to directly deliver NAs triphosphate active forms into the cells. Recent studies have demonstrated that poly(propyleneimine) dendrimers (PPI), with partially modified surfaces, are superior nanoparticles for drug delivery.[9,10] PPI dendrimers, as previously explained (Section 1.3.2), provide high loading capacity, improved solubility and biodistribution of drugs. Their strength is the nanometric size and their globular shape, which enable cellular entry and extended blood circulation time.[11] Moreover, PPI dendrimers with the surface partially modified with maltose has been moieties proved promising.[12] Indeed the presence of sugar modifications reduces PPI cytotoxic activity and maintains the surface positive charge,

allowing for electrostatic interactions with negatively charged phosphate groups.[6,8] The use of glycol-dendrimers to treat leukemia is especially justified by the overexpression of surface lectin receptors on leukemic cells, which bind carbohydrate ligands with high affinity. Furthermore, drug-dendrimer complexation is based on non-covalent physical incorporation of the drug molecules into the dendrimer structure. This non-covalent incorporation enables preparation of easy carrier system, without causing changes in the pharmacological activity of the drug. Therefore non-covalent complexes may transport active drugs directly into the cancer cells, overcoming chemotherapeutics limitations such as multidrug resistance, rapid drug metabolism and unfavorable biodistribution. Recent studies have demonstrated that "open-shell" maltose-modified dendrimers (PPI-Mal OS) form stable complexes with nucleoside triphosphates and shield them from enzymatic degradation.[67] The main goal of studies conducted *in vivo* was to investigate and compare the behavior of drug-dendrimer complex in the presence of two different drugs: fludarabine and clofarabine. To better understand the differences, both ligands were studied in nucleoside and nucleotide forms, and free and in drug-dendrimer complexes (see Supporting Informations).[53,7] In the present work, PPI G4 and its maltose functionalized version (PPI-Mal OS G4) were studied in their standard and protonated forms as they appear in human metabolism. Indeed, one of the major feature of cancer is altered metabolism, associated with acidification of the extracellular milieu.[102] Uncontrolled proliferation of cancer cell prefers the glucose metabolism, which is independent from the oxygen levels. This phenomenon is known as "aerobic glycolysis" or "Warburg effect". As a consequence of this metabolic phenotype, where cells exhibit high rates of glycolysis, there is an increase in the production of high amounts of lactic acid, which lead to acidification of the microenvironment.[103,104] Different protonation states were considered aimed at emulating neutral (pH 7.0) and acid (pH 5.0) conditions. At neutral pH, both dendrimers remain neutrals, whereas under acid environment the amine are protonated.[105,106]

.

4.3 Materials and Methods

4.3.1 Molecular systems

Clofarabine and fludarabine compounds in their triphosphate and nucleoside forms were considered in this work (Table 3).

Table 3. Formula and molecular weight information of considered compounds.

Name	**Drug**	**Formula**	**MW (Da)**
CL0	Clofarabine	$C_{10}H_{11}ClFN_5O_3$	303,677
CL	Clofarabine Triphosphate	$C_{10}H_{14}ClFN_5O_{12}P_3$	543,615
FL0	Fludarabine	$C_{10}H_{12}FN_5O_4$	285,235
FL	Fludarabine Triphosphate	$C_{10}H_{15}FN_5O_{13}P_3$	525,17

Poly(PropylenImmine) dendrimer generation 4 (PPI G4) was considered with and without a MALtose functionalization as reported in a recent literature[12,53,55,68,65] These dendrimers have been protonated as follow:

Table 4. Dendrimers PPI G4 and PPI-Mal OS G4 Type, Generation, Protonated atoms and charge.

Dendrimer	Type	Gen.	Protonated Atoms	Charge
PPI G4	***PolyPropilenImmine***	**4**	**None**	**0**
PPI G4 p	***PolyPropilenImmine protonated***	**4**	**Primary Amines**	**+64**
PPI-Mal OS G4	***PolyPropilenImmine modified with 43 Open Shell Maltose groups***	**4**	**None**	**0**
PPI-Mal OS G4 p	***PolyPropilenImmine protonated and modified with 43 Open Shell Maltose groups***	**4**	**Primary Amines**	**+21**
PPI-Mal OS G4 pp	***PolyPropilenImmine protonated and modified with 43 Open Shell Maltose groups***	**4**	**Primary and Secondary amines**	**+64**

4.3.2 Simulation Protocol

System Set Up

Avogadro chemical editor [107] and Linux bash scripts made in house were used to develop 3D models of dendrimers (PPI G4 and PPI-Mal OS G4) and nucleosides (CL0, CL, FL0 and FL). Different protonation states of the dendrimers surface were considered aimed at emulating neutral (pH 7.0) and acid (pH 5.0). Each PPI G4 dendrimer was considered as made of three main hyperbranched residue types: AAA (dendrimer core), BBB (dendrimer branch) and CCC (dendrimer terminal). In case of PPI-Mal OS G4 dendrimers the most external residue type was CMC (dendrimer maltose terminal). The General Amber Force Field (GAFF)[108] was considered to describe the molecule topologies. Partial charges were calculated considering separate residues by the Restrained Electrostatic Potential (RESP) fitting method, at the HF/6-31G level of theory using AM1-BCC charges as in a number of previous works [109–114]. A proper distribution of the partial charges was provided, which correctly takes into account the conformation of dendrimer and related bonds. Then, the topology and the parametrization were developed using antechamber and GROMACS associated tools [115–119] and a in house code[114].

Molecular Dynamics

Five molecular systems were created by a single dendrimer (Table 3) in a dodecahedron box filled with explicit water molecules (TIP3P)[120] and ions (NA+ and CL-) at a physiological concentration (0.15 M), to neutralize the system charge. The resulting molecular systems (e.g. PPI-Mal OS G4) were composed by roughly 25000 interacting particles. Each system was energy minimized by 1000 steps of steepest descent energy minimization algorithm, followed by preliminary NVT (N=number, V=Volume, and T=temperature) of 50 ps. V-rescale thermostat was applied to keep temperature at 300 K with a time constant of 0.1 ps.[121] A 100 ps position restrained MD was performed at 300 K[121] and 1 atm[122]. V-rescale thermostat[121] and Berendsen[122] methods were used as temperature and pressure coupling. Finally a 100ns long MD was performed in the NVT ensemble at 300K, using V-rescale thermostat[121]. Atom velocities were randomly initialized following a Maxwell Boltzmann distribution.

Furthermore, twenty molecular systems were created by combining each nucleoside/nucleotide in Table 3 with dendrimers in Table 4. Each system consisted in a single compound and a single dendrimer (ratio 1:1). The compound and the dendrimer were positioned at a starting distance of 1.5 nm and a random orientation in a dodecahedron box filled with explicit water molecules (TIP3P)[120] and ions (NA+ and CL-) at a physiological concentration (0.15 M), to neutralize the system charge. The resulting molecular systems (e.g. CL-PPI G4) were composed by roughly 50000 interacting particles. Each system was energy minimized by 1000 steps of steepest descent energy minimization algorithm, followed by preliminary NVT (N=number, V=Volume, and T=temperature) of 40 ps. V-rescale thermostat was applied to keep temperature at 300 K with a time constant of 0.1 ps.[121] A 100 ps position restrained MD was performed at 300 K[121] and 1 atm[122]. V-rescale thermostat[121] and Berendsen[122] methods were used as temperature and pressure coupling. Finally a 100ns long MD was performed in the NVT ensemble at 300K, using V-rescale thermostat[121]. Atom velocities were randomly initialized following a Maxwell Boltzmann distribution. For each compound-dendrimer system, a combination of 3 independent repetition of the above-explained procedure was carried out. In total, 300 ns of MD was performed to sample the conformational space of each considered system combination. The last 50 ns of 3 MD replicas were used as a single ensemble trajectory. Therefore, the total ensemble trajectory considered for statistical analysis was 150 ns long and made of 75 million molecular configurations.

GROMACS 5 package was used for all MD simulations and data analysis.[119] Long-ranged electrostatic interactions were calculated for each step with the Particle-Mesh Ewald method with a cut-off of 1 nm. The same cut-off was also applied to Lennard-Jones interactions. LINCS algorithm[123] approach allowed an integration time step of 2 fs. Visual Inspection of the Simulations was performed by The Visual Molecular Dynamics (VMD)[124] package and used for the visual inspection of the simulated systems.

4.4 Results

4.4.1 Dendrimer analysis

Stand-alone dendrimer analysis were conducted to analyze the results of the dendrimer protonation. Results of the dendrimer protonation reflects on radius of gyration (Figure 13). As expected the radius of gyration increased with the protonation of both the PPI G4 and PPI-Mal OS G4 dendrimers.

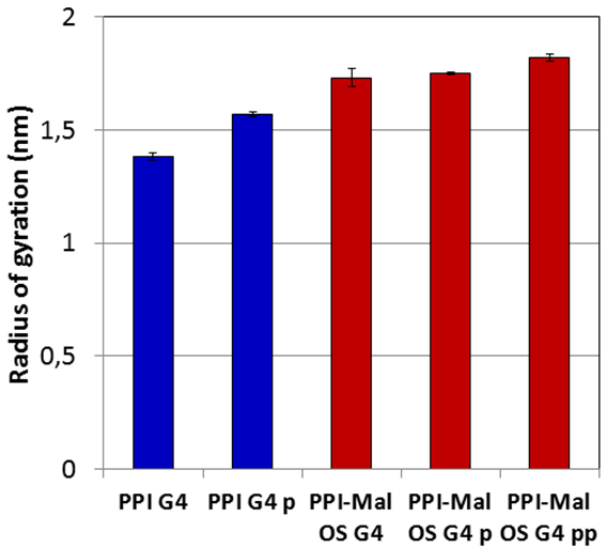

Figure 13. Dendrimer radius of gyration calculated as average ± standard deviation. Maltose modified dendrimers are shown with red bar, whereas non-modified dendrimers are shown in blue.

Solvent-Accessible Surface Area (SASA) was calculated for the five studied dendrimers. Analyzing Figure 14, the first histogram shows the total SASA of the dendrimer and the second and the third one shows respectively the hydrophobic and the hydrophilic surfaces. The maltose modification of the PPI G4 dendrimer surface determined an increase of the 60% of the total SASA of the dendrimer, in accordance with the radius of gyration values. Notable is the fact that the protonation of the dendrimer caused an increase of the hydrophilic SASA. Indeed in case of the PPI-Mal OS G4 double protonated dendrimer, the hydrophilic SASA was the 58% of the total SASA

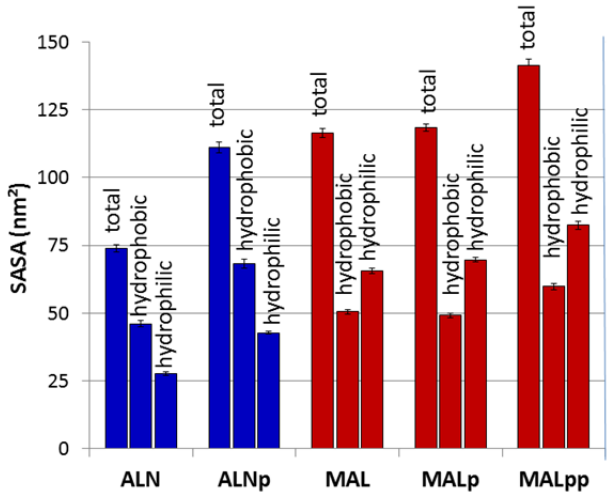

Figure 14. Dendrimer Solvent-Accessible Surface Area calculated as average ± standard deviation. Maltose modified dendrimers are shown with red bar, whereas non-modified dendrimers are shown in blue. The first histogram shows the total SASA of the dendrimer. The second and the third one shows respectively the hydrophobic and the hydrophilic parts. Notable is the fact that the protonation of the dendrimer caused an increase of the hydrophilic SASA.

Figure 15 shows representative trajectory snapshots providing a clear picture of the PPI G4 and PPI-Mal OS G4 dendrimers. In the first line there are PPI G4 dendrimer and its protonated version with +64 added hydrogens. Moreover in the second line, there are PPI-Mal OS G4 dendrimer and its protonated versions, +43 added hydrogen version and +64 added hydrogens.

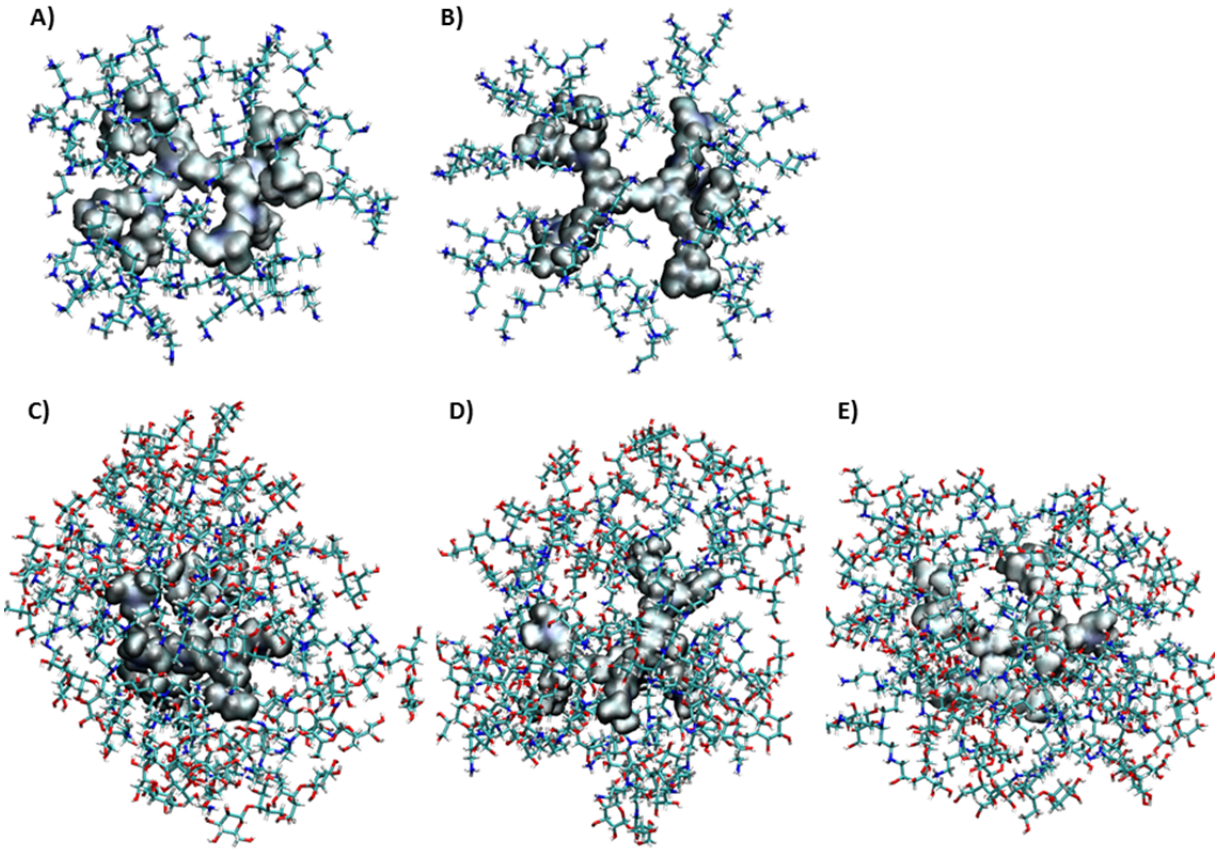

Figure 15. Representative snapshots of the dendrimer. Figures A and B show the PPI G4 dendrimer, respectively in its regular and protonated form. Figures C, D and E show the PPI-Mal OS G4 dendrimer, in its regular, protonated and double protonated forms.

4.4.2 Compound-dendrimer analysis

Complexation analysis was applied to identify compound-dendrimer complexes throughout the overall MD simulation ensemble, following a previously described method.[125] A cutoff distance between dendrimer and compound was chosen (0.2 nm) and applied to discriminate between bound and unbound compound-dendrimer systems. As showed in Figure 16, the complexation probability was evaluated as the percentage of simulation frames in which the system appeared a complex (compound bound to the dendrimer) over the total simulation frames (ensemble trajectory). Cluster percentage values below 70% indicated that the compound was able to attach and to detach from the dendrimer several times during the simulation, suggesting a low binding energy (i.e. close to the thermal energy, kT).

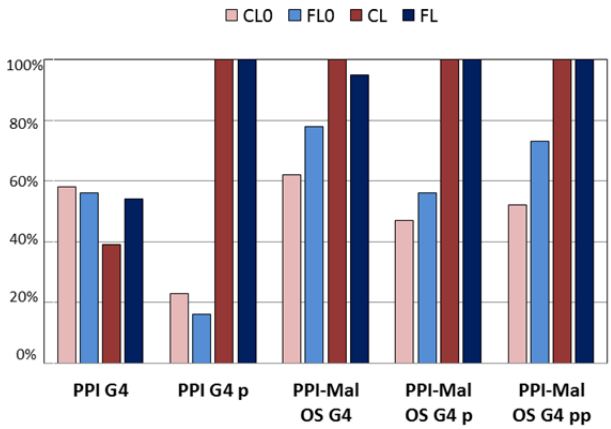

Figure 16. Probability to create a ligand-dendrimer complex. The complex ligand triphosphate–dendrimer showed value close to 100% in case of protonated PPI G4 dendrimer and of maltose decorated dendrimers. Nucleoside compounds (indicated by CL0 and FL0) showed comparable in case of PPI G4 or lower ability to complex with the dendrimer with respect to the triphosphate form. Interestingly, the maltose functionalization of the PPI G4 dendrimer influence clofarabine and fludarabine triphosphate complexation ability.

In case of protonated and maltose functionalized dendrimers, the probability of create nucleotide–dendrimer complex showed values of about 100%. Nucleoside compounds consistently showed comparable (in case of PPI G4, with primary amines not protonated) or much lower ability to complex the dendrimer with respect to the triphosphate forms. In nucleoside compound-dendrimer systems, an alternation of attached and detached configurations was noticed throughout the simulation, which highlight a binding energy of nucleoside compounds for the dendrimer of about kT.

Noteworthy, is the case of maltose functionalization where the amine protonation failed to influence the ability of clofarabine and fludarabine triphosphate to complex the dendrimer.

4.4.3 Interaction Energy

The result of complexation analysis reflects on binding enthalpy (Figure 17). To calculate the binding enthalpy the well-known "Molecular Mechanics/Generalized Born model augmented with the solvent accessible surface area term (GBSA)" approach was considered. This approach facilitates the estimation and comparison of binding energies calculated from MD simulations, as has been practiced in earlier literature.[126–132] It is worth mentioning that the calculated binding enthalpy cannot provide any indication on the absolute value of affinity given that the binding entropy has not been calculated. However, the data can be used to rank similar systems. As an example, the plot may provide an indication of affinity rank for different compounds bound to the same dendrimer.

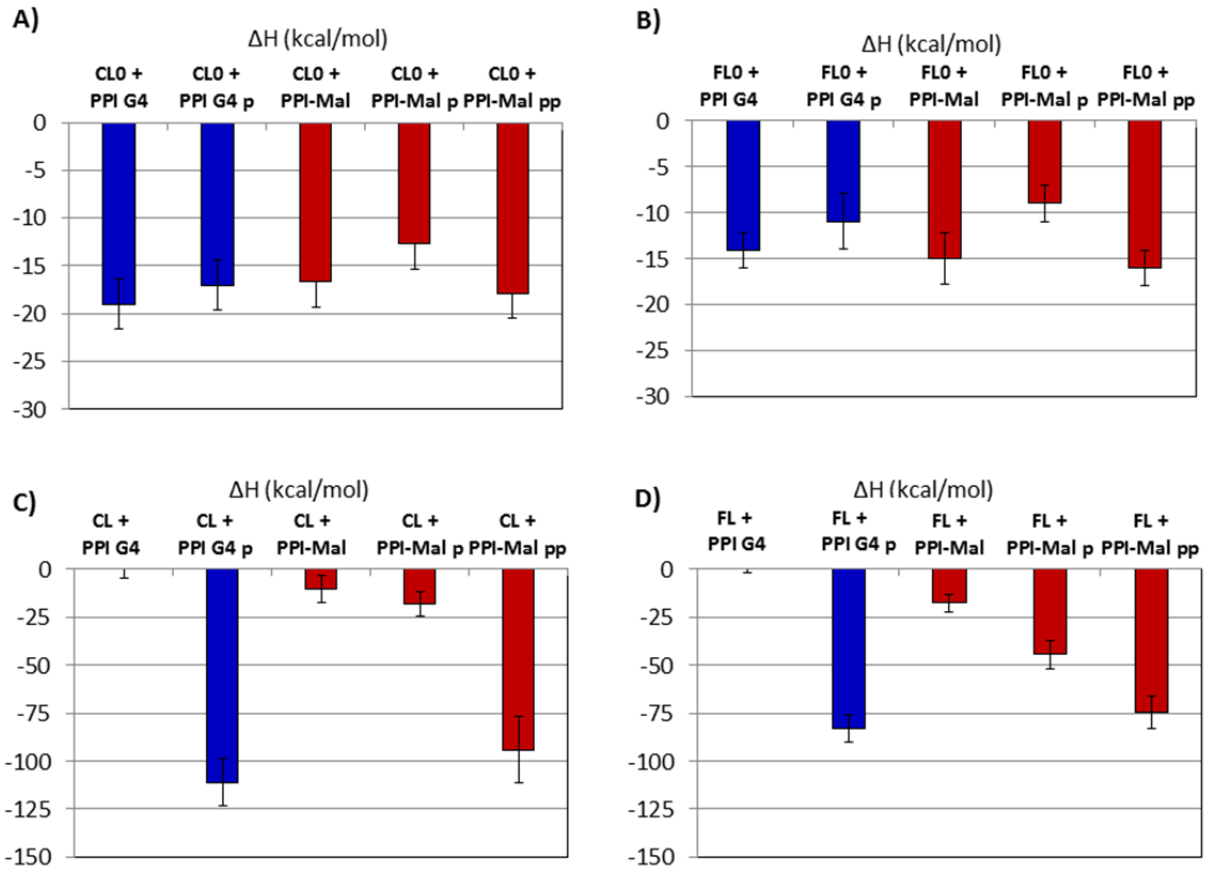

Figure 17. Binding enthalpy calculated by sampling all frames in which the compound and dendrimer are complexed. Maltose modified dendrimers are shown with red bar, whereas non-modified dendrimers are shown in blue. Standard errors are reported for each value.

In line with the complexation analysis, triphosphate forms propose much lower binding enthalpy for unmodified dendrimer with respect to nucleosides forms. Instead, binding enthalpy values were insufficiently different to identify an affinity discrepancy between clofarabine and fludarabine for both non decorated and decorated dendrimers. In other words, both compounds bind the dendrimer with similar affinity in not functionalized dendrimers.

4.4.4 Interaction Modes: Binding Orientation and Distance

The interaction mode has been investigated by determining compound orientation and distance with respect to the dendrimer, and overall conformational states of the complex system (75 million of configuration states were considered for each system). The calculation of the orientation of the compound over the surface of the dendrimer, was conducted by analyzing the variation of the amplitude of a specific angle (ϑ) during the simulation. The angle was defined by 3 identified regions (Figure 18-A) as follows: the dendrimer center of mass, the center of mass of the tail phosphate atoms (P, P1 and P2) and the nitrogen atoms compound head (N, N1, N2 and N4). In case of nucleosides, there is no phosphate tail; hence the orientation analysis remained poorly descriptive . The dendrimer compound distance was calculated as the distance between the center of mass of the compound and the dendrimer center of mass (Figure 18-B).

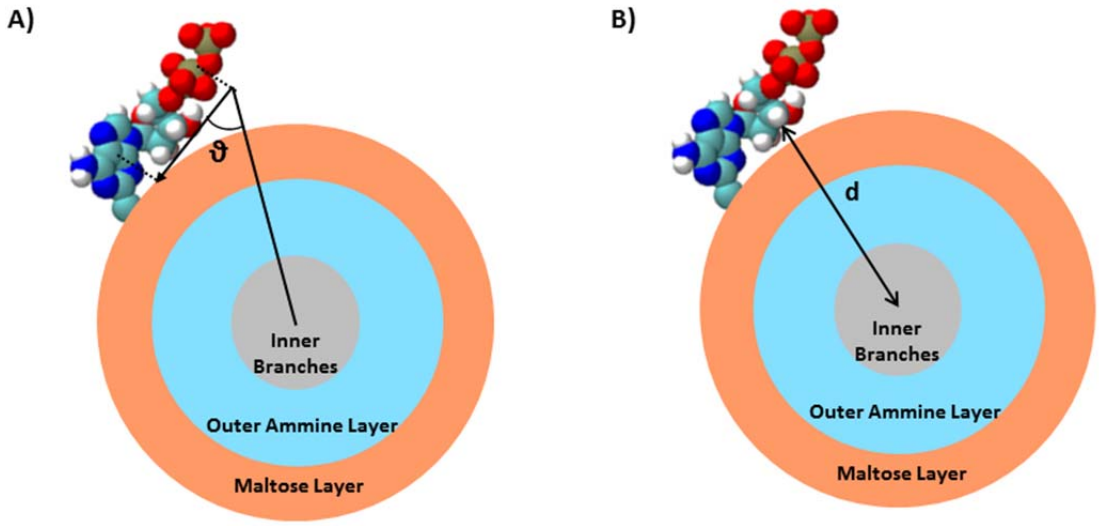

Figure 18. The dendrimer structure is simplified in inner branches (grey area), outer ammine layer (blue areas) and maltose layer (orange area). A) To calculate the orientation of the ligand over the dendrimer has been defined an angle (ϑ) connecting 3 regions: the dendrimer center of mass, the center of mass of the tail phosphate atoms (P, P1 and P2) and the nitrogen atoms present on the head of all the compounds (N, N1, N2 and N4). B) The distance is calculated between the center of mass of the compound and the dendrimer center of mass (black line).

The calculated angle was directly correlated with the compound orientation, with respect to the dendrimer surface as shown in Figure 19. Comprehensively, an angle value equivalent to 0° indicated the compound oriented with the head toward the dendrimer center (Figure 19-A), and an angle value of 180° indicated the compound oriented with the tail toward the dendrimer center (Figure 19-C). Finally, an angle value = 90° indicated the compound flat over the dendrimer surface (Figure 19-B).

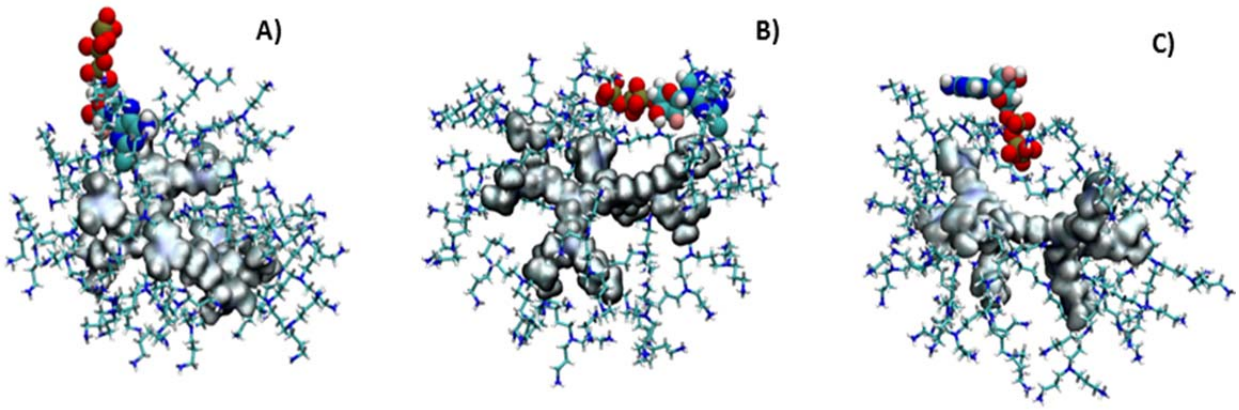

Figure 19. Compound orientation over dendrimer surface. This case shows the clofarabine triphosphate orientation over the PPI G4 dendrimer. A) The compound oriented with the head toward the dendrimer center. B) The compound lies flat over the dendrimer surface. C) The compound oriented with the tail toward the dendrimer center.

The probability of each of three compound orientations was calculated throughout the ensemble trajectory considering only frames with complexed compound-dendrimer. For the sake of simplification, angle values were discretized in 3 outcomes: 0°-75° (head oriented toward the dendrimer center), 75°-105° (flat), 105°-180° (tail oriented toward the dendrimer center). The angle probability along the ensemble trajectory of the ligand triphosphate-dendrimer complex is shown in Figure 20.

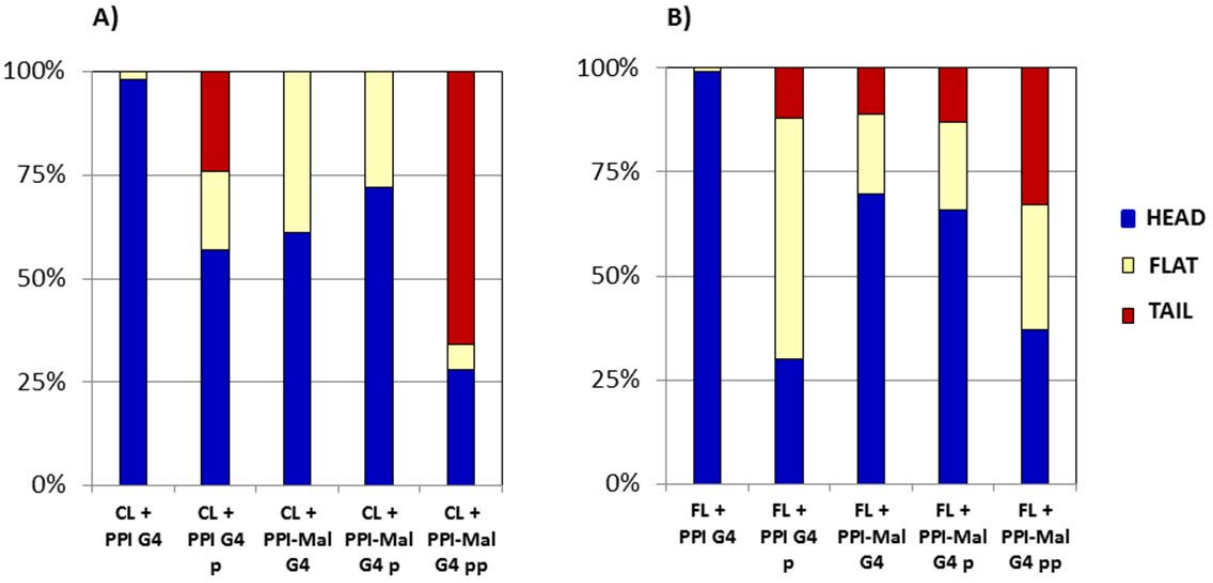

Figure 20. Probability of the triphosphate compound orientation when complexed with the dendrimer. The blue histograms represent the probability of the compound oriented with the head turned to the center of the dendrimer (angle in a range 0°-75°). The yellow histograms show the probability of the ligand to have a flat placement over the dendrimer surface (angle in a range 75°-105°). The red histograms represent the probability of the ligand placed with the tail turned to the center of the dendrimer (angle in a range 105°-180°).

It is interesting to notice how the dendrimer protonation affects the interaction mode in term of orientation. In particular, the probability of finding the compound oriented with the tail toward the dendrimer center increased with the dendrimer protonation. This was an expected effect due to the negative charge of the compound (-4) and the positive charge of protonated dendrimers.

The angle probability along the ensemble trajectory of the nucleoside-dendrimer complex is illustrated in Figure 21.

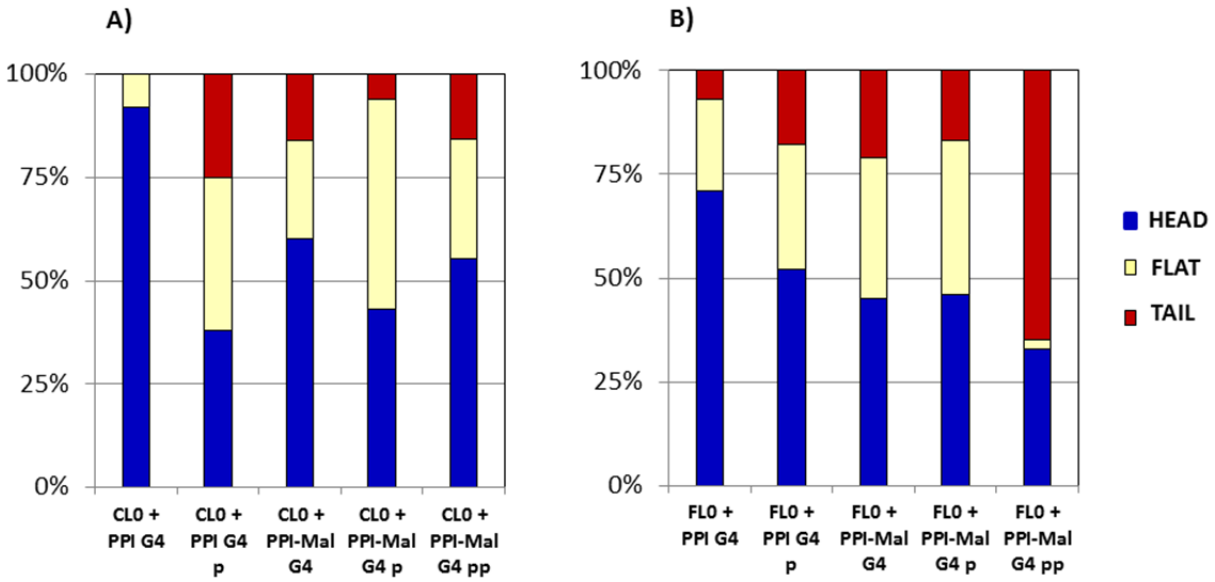

Figure 21. Probability of the nucleoside compound orientation when complexed with the dendrimer. The blue histograms represent the probability of the compound oriented with the head turned to the center of the dendrimer (angle in a range 0°-75°). The yellow histograms show the probability of the ligand to have a flat placement over the dendrimer surface (angle in a range 75°-105°). The red histograms represent the probability of the ligand placed with the tail turned to the center of the dendrimer (angle in a range 105°-180°).

The results of the nucleoside- dendrimer complex confirmed the finding of triphosphate ligand-dendrimer complex. Also in this case, how the dendrimer protonation affects the interaction mode in term of orientation was obvious. Particularly, fludarabine nucleoside highlights how the probability of finding the compound oriented with the tail toward the dendrimer center increases with the dendrimer protonation.

The calculation of the compound penetration into the dendrimer layers was conducted by analyzing the variation of the distance between the compound and the dendrimer and by comparing it with the dendrimer radius of gyration layer-by-layer (Figure 22Figure 23 and Figure 23). The histograms show the radius of gyration of the dendrimer layers, starting from the inner branches (grey histogram), the outer amine layer (blue) and the maltose layer (orange). The black dot with error bars represents the mean value of the distance between the compound and the dendrimer center of mass. The plot highlights when the compound lies inside a specific layer of the dendrimer as for the case of CL-PPI G4, in which the compound penetrated until the dendrimer inner layers.

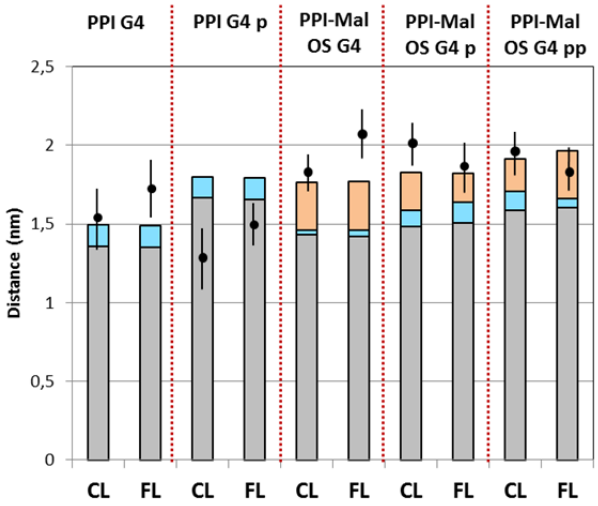

Figure 22. Graphics of the penetration data of the triphosphate compound-dendrimer systems. The histograms shows the radius of gyration of the dendrimer layers, starting from the inner branches (grey), to the outer amine layer (blue) and the maltose layer (orange). The black point represents the mean value and the standard deviation of the distance between the compound and the dendrimer.

Both clofarabine and fludarabine triphosphate compounds were continuously positioned on the outside layers in non-protonated PPI G4 and maltose decorated dendrimers. In line with binding enthalpy data (see Figure 17), the compounds were completely embedded in PPI G4 p dendrimers. Besides, it was necessary to underline that the thickness of PPI-Mal OS G4 layers is different in case of interaction with fludarabine or clofarabine. The differences were always in the same order of the standard deviation of the layer size (around 0.05 nm). Therefore, these could be considered negligible and mostly correlated with structure fluctuations and dendrimer orientation in the sampled ensemble.

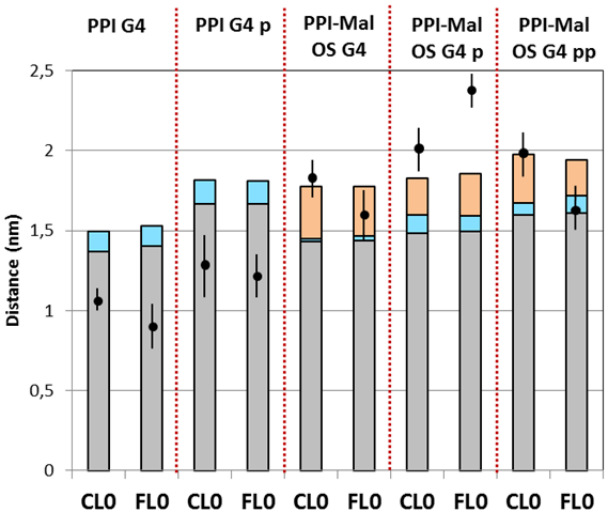

Figure 23. Graphics of the penetration data of nucleoside compound-dendrimer systems. The histograms shows the radius of gyration of the dendrimer layers, starting from the inner branches (grey), to the outer amine layer (blue) and the maltose layer (orange). The black point represents the mean value and the standard deviation of the distance between the compound and the dendrimer.

Using the same approach nucleoside compound-dendrimer systems (Figure 23) were analyzed. A significant difference was observed in case of the fludarabine nucleoside, due to the fact that the compounds were able to penetrate also inside not protonated dendrimers (PPI G4 and PPI-Mal OS G4). In line with binding enthalpy data (Figure 17), the nucleoside compounds showcased higher binding enthalpy for unmodified dendrimer with respect to PPI-Mal OS G4.

4.4.5 Interaction Mode: Associated Molecular Interactions

The Radial Distribution Function (RDF) was calculated to reveal precise information on the molecular phenomena driving the compound-dendrimer system complexation, as function of the compound-dendrimer distance. RDFs were calculated for two well defined atom groups (Figure 24) of the compound (Head and Tail) in respect to the outer dendrimer layer. The Head group (blue atoms presented in Figure 24) was composed of the nitrogen atoms and by the chlorine and fluorine atoms for the clofarabine compound. Instead, the Head group was composed of the nitrogen atoms and by the fluorine and the oxygen of the 2' end of the ribose for the fludarabine compound. In contrast, the Tail (red atoms present in Figure 24) was composed of seven oxygen atoms, which were connected to the triphosphate group, in the triphosphate compounds.

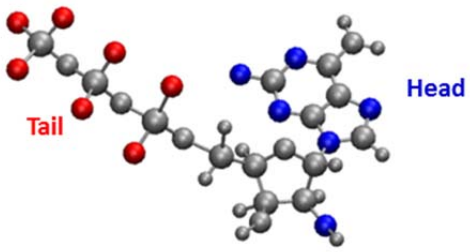

Figure 24. The Head group is composed by the blue atoms, and the tail group is composed by the red atoms. The Head group was composed by the nitrogen atoms and by the chlorine and fluorine atoms for the clofarabine compound. Instead, the Head group was composed by the nitrogen atoms and by the fluorine and the oxygen of the 2' end of the ribose for the fludarabine compound. The Tail was composed by the seven oxygen atoms which are connected to the triphosphate group, in the triphosphate compounds.

Showed in Figure 25 and Figure 26 indicate, the radial distribution function of the Head group (on left side) and of the Tail group (on right side). The black line shows the RDF of the clofarabine nucleotide and the red line shows the fludarabine nucleotide. Both compounds had primary interaction with the outer dendrimer layer. Analyzing RDFs of PPI G4 dendrimer (Figure 25), was possible to note that both the Head groups of the nucleotide compounds had the main peak higher than the Tail group. Interestingly, RDFs of the compound-dendrimer in case of the protonated dendrimer were at least one order of magnitude greater than the not protonated PPI G4 dendrimer. This confirmed what expected by the insertion of 64 positive charge protons. Plots were in agreement with orientation (Figure 19) and penetration data (Figure 22) which indicate compounds oriented with the head toward the dendrimer center and embedded into the PPI G4 dendrimer whereas the tail was coordinated by the outer layer

of the dendrimer. The compound was oriented in flat position in the case of fludarabine-PPI G4 protonated dendrimer interaction.

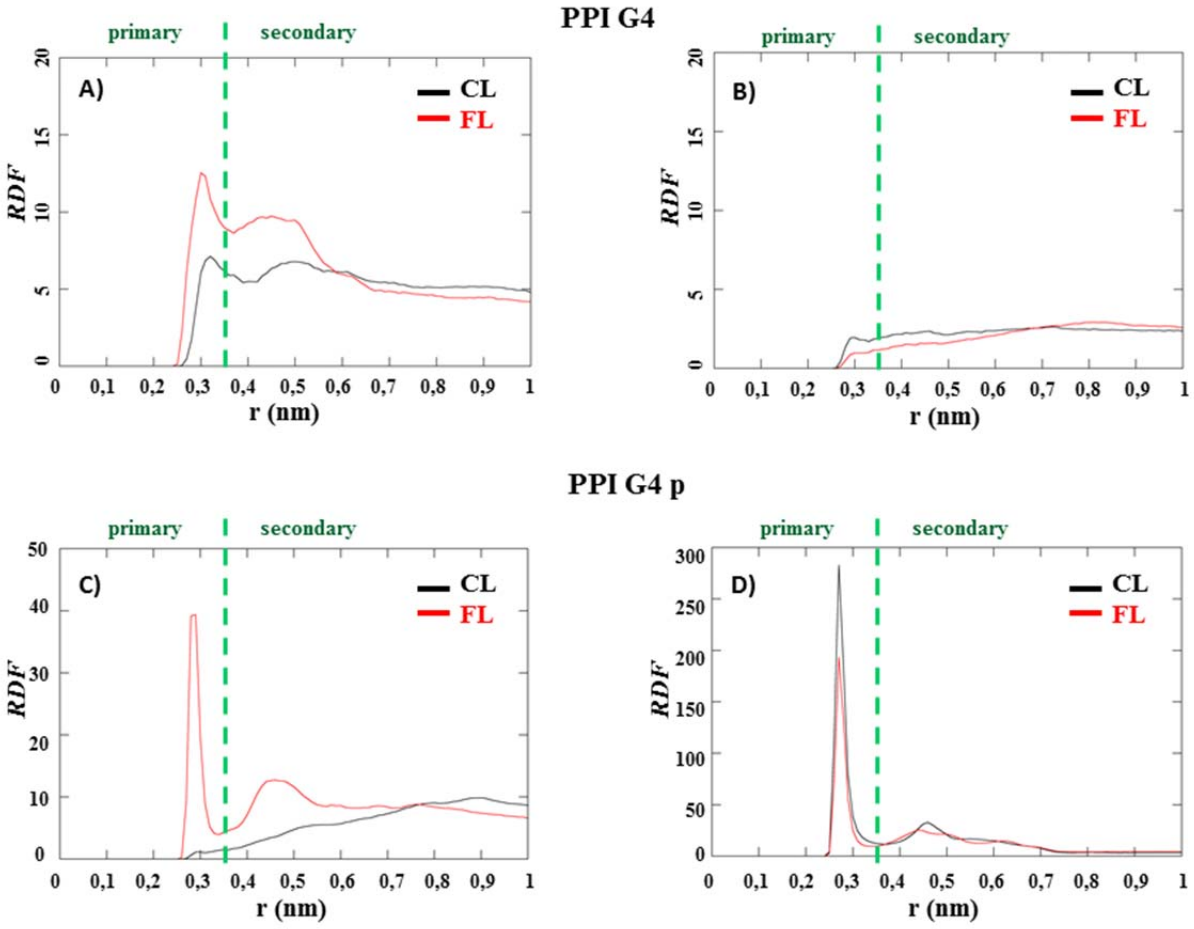

Figure 25. Radial Distribution Functions of the triphosphate compounds respect to the PPI G4 and PPI G4 protonated dendrimers. Figures A) and C) represent the Head group RDFs for respectively the clofarabine triphosphate-dendrimer complex (black curve) and the fludarabine triphosphate-dendrimer complex (red curve). Figures B) and D) represent the Tail group RDFs for respectively the clofarabine triphosphate-dendrimer complex (black curve) and the fludarabine-triphosphate dendrimer complex (red curve).

Using the same approach RDF of compound-PPI-Mal OS G4 dendrimer systems (Figure 26) were calculated. Noteworthy, RDFs in case of protonated dendrimers were at least one order of magnitude greater than the not protonated one. Analyzing RDFs of PPI-Mal OS G4 is possible to note that both the Head groups of the nucleotide compounds had the main peak higher than the Tail group. Notable is the variation of the clofarabine RDF, when it interacted with the double protonated PPI-Mal OS G4 dendrimer. In these case (Figure 26 E and F) the Tail group had the main peak one order higher than the Head group, and this confirm what predicted by the penetration and orientation studies.

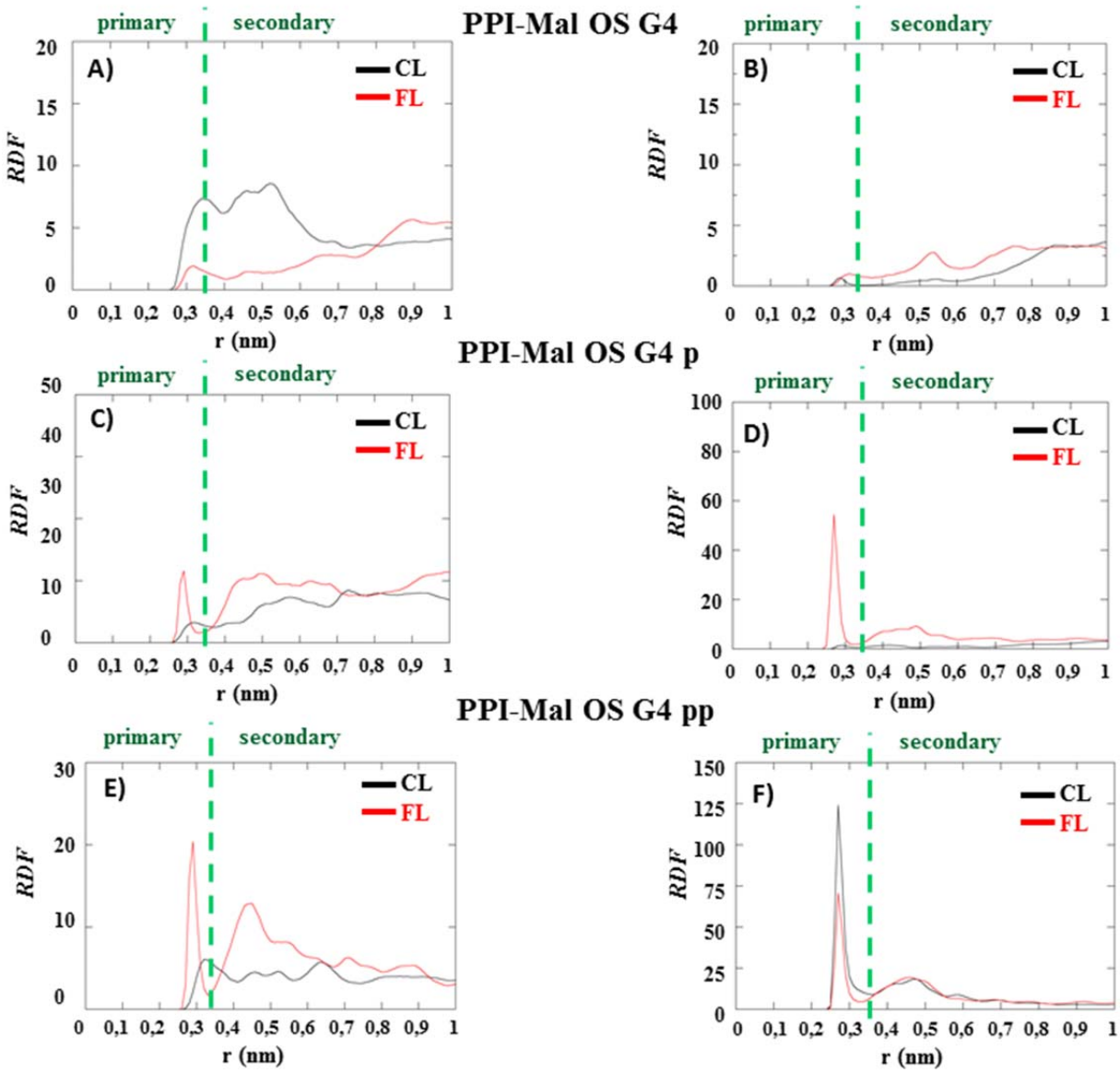

Figure 26. Radial Distribution Functions of the triphosphate compounds respect to the PPI-Mal OS G4 and its protonated forms. Figures A) and C) represent the Head group RDFs for respectively the clofarabine triphosphate-dendrimer complex (black curve) and the fludarabine triphosphate-dendrimer complex (red curve). Figures B) and D) represent the Tail group RDFs for respectively the clofarabine triphosphate-dendrimer complex (black curve) and the fludarabine-triphosphate dendrimer complex (red curve).

Data from orientation, penetration and RDF analysis highlighted the interaction mode of both compounds when they bound to PPI G4 and PPI-Mal OS G4 dendrimers. Figure 27 shows representative trajectory snapshots providing a clear picture of the interaction mode between nucleotide and PPI G4 dendrimers. As previously said, the clofarabine triphosphate was characterized by the nucleotide head oriented toward the dendrimer center and interacting with the more deep layers. On the other hand, fludarabine triphosphate interaction mode with the PPI G4 dendrimer was similar to the clofarabine ones. Otherwise in fludarabine-PPI-G4

protonated complex, was possible to underline that the compound could change its orientation over the dendrimer surface, and it interacted only with the outer layer with a flat orientation.

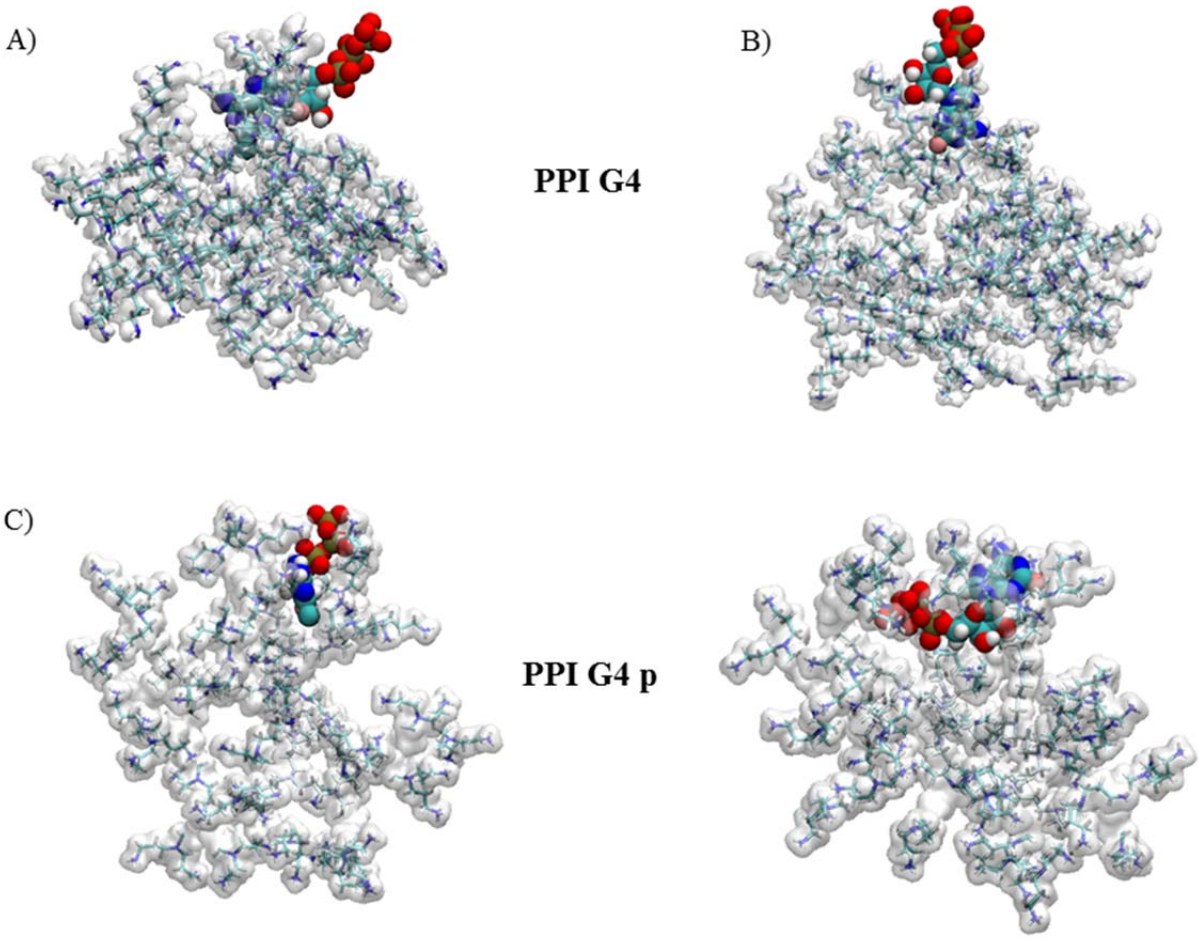

Figure 27. Representative snapshots of the nucleotide-dendrimer configuration for each investigated system. Figures A and C show the clofarabine triphosphate and the figures B and D show the fludarabine triphosphate. Both the nucleotide- PPI G4 complexes highlight that the head of the compounds is oriented to the center of the dendrimer. Only in Figure D is notable that the fludarabine is able to have a flat position over the dendrimer PPI G4 protonated surface.

Using the same approach nucleoside compound- PPI-Mal OS G4 dendrimer systems representative trajectory snapshots were analyzed (Figure 28). As previously said, the clofarabine triphosphate was characterized by the nucleotide head oriented toward the dendrimer center. Noteworthy was the complete change that the clofarabine triphosphate had when it interacted with the PPI-Mal OS G4 double protonated dendrimer. Indeed this drug had the tail oriented toward the dendrimer center, and its head was exposed to the solvent. On the other hand, fludarabine triphosphate interaction mode with the PPI-Mal OS G4 dendrimer did not show significant differences in the interaction mode. In all cases, the fludarabine head was oriented toward the dendrimer center.

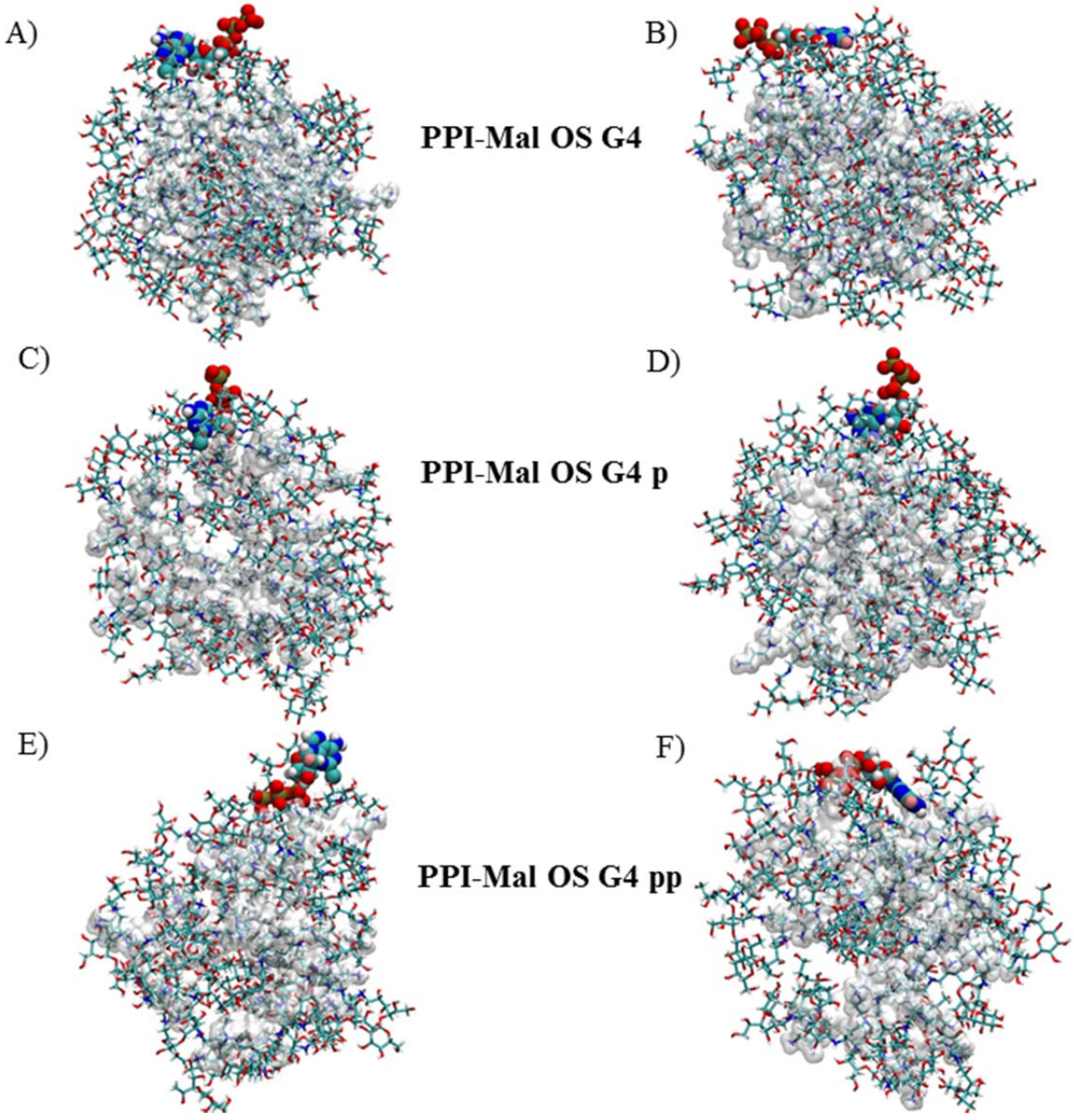

Figure 28. Representative snapshots of the nucleotide-dendrimer configuration for each investigated system. Figures A, C and E show the clofarabine triphosphate and the figures B, D and F show the fludarabine triphosphate. Both the nucleotide- PPI-Mal OS G4 complexes highlight that the head of the compounds is oriented to the center of the dendrimer.

4.5 Discussion

Nucleoside analogues are being investigated for clinical use for almost 50 years, and these were one of the first chemotherapeutic agents introduced for the medical treatment of cancer. Nowadays, these antimetabolites are commonly used against hematological malignancies, including leukemia and lymphomas, as well as against solid tumors.[9] NAs includes a variety of purine and pyrimidine nucleoside derivatives with numerous cytotoxic activities. Indeed their toxic mechanisms are various. These compounds can be directly incorporated into newly synthesized nucleic acid chain and causing DNA and RNA synthesis inhibition. Additionally, NAs can decrease the activity of the enzymes involved in metabolism of natural nucleosides and nucleotides. The main NAs goal is to induce cell apoptosis. This is achieved through different modes of action which depend on NAs structure, specificity, stability and interaction with cell components and protein involved in cellular metabolic processes.[133] All NAs share common intracellular transport and metabolic pathways. These compounds are hydrophilic molecules; hence they cannot penetrate the cell membrane by passive diffusion. It is necessary the presence of a nucleoside transporter, which mediates the cellular entry and enable active transfer through the cell membrane. The limit of using NTs is that these proteins are able to delivery only dephosphorylated forms, therefore NA entries inside the cell in a deactivated form. Once inside, it needs to be progressively phosphorylated to its triphosphate form, which is critical for its cytotoxic activity.[134] The use of NT leads to delayed NA therapeutic effects and emergence of drug resistance due to downregulation of transporter expression or decreased activity of intracellular kinases.[98] Moreover the effectiveness of clinically used anticancer drug is limited by various undesirable factors such as unfavorable bio-distribution, fast metabolism, low specificity of interaction and nonspecific toxicity.[68] The not cancer specificity of the NAs is a crucial point that can endanger all the type of cells, and it can determine the emergence of various side effects.[28,98] In order to overcome all the mentioned resistance mechanisms may involve the application of drug carrier systems, which provide enhanced cellular uptake of active triphosphate forms independently of NTs. Numerous studies have been conducted on the use of dendrimers as DDS and it has been highlighted that PPI dendrimers, with their surface partially modified with maltose moieties, can be a very promising vehicle for nucleotides.[68] Indeed, dendrimers provide high loading capacity, improved solubility and bio-distribution of the drug. Cellular entry and blood circulation are facilitated by their nanometric size and globular shape. Furthermore, the presence of sugar moieties on the dendrimer surface, improves its biocompatibility and bioavailability. The use of glycosylate dendrimers helps also to overcome the not cancer specificity of the drug, due to the fact that leukemic cells usually overexpressed lectin

receptors which bind carbohydrate ligands with high affinity.[135,59] Sugar modified PPI dendrimers have the potential of active interaction with cancer cells and they allow to decrease the detrimental effects on healthy tissues. Moreover, drug-dendrimer complexation is based on non-covalent physical incorporation of drug molecules into PPI dendrimer structure, and this conjugation enhances relative easy preparation of carrier system and lead the possibility to not modify the pharmacological activity of the therapeutic. Non-covalent complexes may transport active triphosphate compound forms directly inside the cells, potentially overcoming the limits of standard chemotherapy.[136] Our studies were concentrated on the use on PPI G4 and PPI-Mal OS G4 dendrimers for the delivery of clofarabine and fludarabine, in their nucleoside and activate triphosphate forms. Firstly, the dendrimer structures were investigated at different protonation states, aimed at emulating neutral (pH 7.0) and acid (pH 5.0) conditions. At neutral pH, both dendrimers remain neutrals, whereas under acid environment the amine are protonated. Notable was that the maltose modification of the PPI G4 dendrimer surface determined an increase of the 60% of the total SASA of the dendrimer, in accordance with the radius of gyration values. Moreover, the protonation of the dendrimer caused an increase of the hydrophilic SASA. Indeed in case of the PPI-Mal OS G4 double protonated dendrimer, the hydrophilic SASA was the 58% of the total SASA. Subsequently, the ensemble trajectory frames of the compound-dendrimer complexes were analyzed. It was evident that both the nucleoside compounds (CL0 and FL0) and the nucleotide ones (CL and FL) show a very low complexation probability value with the PPI G4 dendrimer, with a cluster percentage value below 70%. This low value indicated that during the simulation the compound was able to attach and to detach from the not modified dendrimer several times, suggesting a low binding energy (i.e. close to the thermal energy, kT). Supporting these results, also the enthalpy analysis highlighted that CL and FL had a very low value of affinity. Therefore our investigation was mainly directed to the interaction with the protonated and maltose modified PPI dendrimer. Noteworthy was notice how the dendrimer protonation affects the interaction mode in term of drug orientation. In particular, the probability of finding the compound oriented with the tail toward the dendrimer center increased with the dendrimer protonation. This was an expected effect due to the negative charge of the compound (-4) and the positive charge of protonated dendrimers. In order to further characterize the interaction patterns, the RDFs of compound-dendrimer complexes were calculated. Interestingly, both the Tail groups (nucletide's phosphate residues) of the drugs were responsible for primary interactions with the amino surface group of PPI-Mal OS G4 dendrimers. Furthermore, the clofarabine orientation completely change with the increase of protonation. Indeed, it was oriented with its Tail group turned to the center of the

dendrimer, where it could interact with amino groups of the PPI-Mal OS G4 pp dendrimer. Moreover, its Head group did not penetrate into PPI-Mal OS G4 pp dendrimer layer probably due to the steric hindrance, and stay exposed to the solvent. The clofarabine position might further stabilize the interaction by trapping the nucleotide within the dendrimer structure, and make it difficult to self-release the drug once inside the cell. On the other hand, the fludarabine showed a similar orientation in presence of PPI G4 dendrimer, but its behavior changed for PPI-Mal OS G4 dendrimer. Fludarabine triphosphate had the 20% of probability to stay flat over the maltose modified PPI G4 dendrimer, as well as it had the 12% of probability to have its Tail group oriented to the center of the dendrimer. The possibility of this compound displacements suggests that the fludarabine triphosphate had a more flexible structure respect to the clofarabine triphosphate. Most likely, the PPI-Mal OS G4 dendrimer can deliver the fludarabine nucleotide inside the cell and the compound can easily detach from the dendrimer surface. This behavior was also noticed *in vivo* studies, where the fludarabine active form alone and complexed with the maltose modified PPI G4 dendrimer were tested on U937 cells (histiocytic lymphoma cells).[53] Using radiolabeled compounds it was demonstrate that PPI-Mal OS G4 dendrimer significantly enhance cellular uptake of fludarabine triphosphate, even in presence of hENT1 inhibitor. In line with the *in vivo* experiments, we can postulate that PPI-Mal OS G4 dendrimer significantly enhance cellular uptake of fludarabine triphosphate without causing any change to its pharmacological activity.[53,67]

4.6 Conclusions

In this chapter, twenty different compound-dendrimer complexes (CL0, FL0, CL and FL with the PPI G4 dendrimer standard, protonated and maltose modified forms) were analyzed. The aim of this study was to compare different dynamic behaviors and their interactions to understand more stable and effective structures. *In vivo* studies were conducted to investigate the actual differences of these drugs and drug-dendrimer complexes in U937 cancer cells. Our intent was to further verify *in vivo* experiments, using MD simulations by showing conformational changes of compound-dendrimer complexes. Different protonation states were considered aimed at emulating neutral (pH 7.0) and acid (pH 5.0) conditions. At neutral pH, both dendrimers remain neutrals, whereas under acid environment the amine are protonated. Analyzing the chemical differences between two studied drugs, it was evident that the clofarabine differed from the fludarabine only for the presence of a chlorine and a fluorine atom on its nucleoside part. This atomic difference determined that the clofarabine carried a more rigid structure and influenced its orientation and interaction over the dendrimer surface. Thus, we have decided to investigate these complexes analyzing the interactions between 10 drugs in presence of protonated forms of PPI G4 and PPI-Mal OS G4 dendrimers.

5. Comparison between fludarabine and clofarabine interaction with full protonated poly(propyleneimine) dendrimers PPI G4 and PPI-Mal OS G4

This chapter presents an investigation focused on clofarabine and fludarabine interactions with the PPI G4 and PPI-Mal OS G4 protonated dendrimers, by means of MD simulations. The results provide an atomistic investigation of the compound-dendrimer complex, focusing the attention on: i) the complexation modes, ii) the orientation and the penetration of the compound over the dendrimer surface and iii) the interactions between compounds and dendrimer at ratio 10:1.

5.1 Abstract

Nowadays, nanotechnology-based chemotherapy is widely applied to treat many types of cancer, such as hematological malignancies. The aim of this work was to provide computational investigations of two approved nucleoside analogues (NAs) drugs used to treat leukemia: the clofarabine and the fludarabine. These antimetabolites have a complex pharmacokinetic, which requires active transmembrane transport and intracellular phosphorylation to triphosphate nucleotide forms, which limits their therapeutic potential. To overcome the various problems connected to the direct use of NAs, we investigate poly(propyleneimine) dendrimers of fourth generation (PPI G4) partially modified with maltose (PPI-Mal OS G4) as efficient nucleotide carriers. In this study we present computational approaches, based on Molecular Dynamics simulations, to elucidate the molecular reasons behind clofarabine and fludarabine different displacement/interaction with the dendrimers. The compound-dendrimer complexes were protonated to simulate their behavior at acid environment condition and our results confirmed what seen with *in vivo* experiments. Interestingly, both the drug nucleoside forms did not interact with the PPI G4 dendrimer, neither with PPI-Mal OS G4 one. Furthermore, in compound-dendrimer complexes, it was evident that these two drugs had completelly different interaction with the dendrimer surface. Noteworthy were the interactions with the maltose modified PPI G4 dendrimer, where the clofarabine was characterized by the phosphate part turned to the center of the dendrimer, interacting with the inner layers, and its acid nucleic base stayed exposed to the solvent. Contrariwise, the fludarabine nucleotide was able to settle in a flat position over the dendrimer surface, suggesting that the fludarabine triphosphate had a more flexible structure compared to the clofarabine triphosphate. Moreover, the electrostatic potential investigation of complex formulations showed that the clofarabine was able to neutralize the

dendrimer surface charge, and this feature may limit the ability of compound-dendrimer complex to enter the cell and the drug delivery potential of PPI macromolecules may be significantly decreased. Most likely, the PPI-Mal OS G4 dendrimer can efficiently deliver the fludarabine nucleotide inside the cell and the compound can easily detach from the dendrimer surface, but it did not allow an easy released of the clofarabine inside the cell.

5.2 Introduction

Nucleoside analogues (NAs) are a versatile family of drugs used to treat several diseases, due to their multiple mechanisms of action and potential indications.[137] The naturally occurring nucleosides represents a unique starting point for drug design owing to their involvements in numerous critical biological processes and being essential building blocks for both DNA and RNA synthesis.[97] The NAs were among the first chemotherapeutics developed for cancer treatment and are widely applied to treat hematological malignancies.[138] These compounds are antimetabolites and their primary cytotoxic activity involves disruption of metabolism of natural nucleotides. This action applies an impact on the enzymes involved in the synthesis of nucleic acid, as well as to direct incorporation of the drug into newly synthesized DNA or RNA chain.[5] Noteworthy, the main goal of NAs is inducing cellular apoptosis. The cytotoxic mechanisms of NAs are strongly depend upon their chemical structure and on their affinity with the intracellular targets. [5,28] All anticancer NAs share common intracellular transport and metabolic pathways, such as the active transfer across the cell membrane and the activation by intracellular kinases to form their active triphosphate forms. Indeed, NAs are hydrophilic molecules, and this determines that they cannot enter passively inside the cell but they need specialized nucleoside transporters (NTs) to do so. Once inside the cell, nucleosides are progressively phosphorylated by the intracellular kinases to their triphosphate forms, which are crucial for their cytotoxic effect.[98,99] However, the use of NTs determine some limitation to NAs; since they can transport only dephosphorylated substrates and this limits the administration of prodrug forms instead of active metabolite forms. This complex metabolism enables a number of possible resistance mechanisms, it may also results in poor cellular uptake and insufficient intracellular phosphorylation of NAs. Moreover, NAs activity is not cancer cell specific therefore there is high risk to have emergence of side effects due to their toxicity.[28,100] To overcome the mentioned resistance mechanisms, it was tested to introduce the application of drug delivery systems (DDS). A DDS should be able to hold an adequate amount of therapeutic agent and to overcome obstacles such as drug resistance, rapid clearance from the bloodstream and disadvantageous biodistribution. Other required characteristics are prolonged blood half-life, efficient intracellular transport, specific cancer accumulation and controlled drug release.[101] During the years, many are the DDS found able to satisfy these requirements and they can be used to directly deliver the NAs triphosphate active forms inside the cells. Recent studies have demonstrated that Poly(propyleneimine) dendrimers (PPI), also with partially modified surfaces, are superior nanoparticles for drug delivery.[139,9,10] PPI dendrimers, as previously explained (Section 1.3.1.1), provide high loading capacity, improved solubility and biodistribution of the drug. In particular their

strength are their nanometric size and globular shape, which enable cellular entry and extend blood circulation time.[11] Notable is that PPI dendrimers with the surface partially modified with maltose moieties proved promising transport of NAs.[12] Indeed the presence of sugar moieties reduces PPI cytotoxic activity and maintains surface positive charge, allowing for electrostatic interactions with negatively charged phosphate groups.[6,8] The use of glycol-dendrimers to treat leukemia is especially justified by the overexpression of surface lectin receptors on leukemic cells. The lectin receptors tends to bind carbohydrate ligands with higher affinity, therefore they can interact better with maltose modified dendrimers. Furthermore, drug-dendrimer complexation is based on non-covalent physical incorporation of the drug molecules into the dendrimer structure. This non-covalent incorporation enables easy carrier system preparation, without causing changes in pharmacological activity of the drug. Therefore non-covalent complexes may transport active drug forms directly inside the cancer cells, overcoming chemotherapeutics limitations such as multidrug resistance, unfavorable biodistribution and rapid drug metabolism. Recent studies have demonstrated that "open-shell" maltose-modified dendrimers (PPI-Mal OS) can form stable complexes with nucleoside triphosphates as well as they can shield the drug from enzymatic degradation.[67] To mimic the experimental conditions, it was used protonated PPI OS G4 dendrimers as host molecules for NAs. PPI OS G4 dendrimer has the external amine groups that can be protonated in water solution and this protonation is strongly influenced by pH and other environmental conditions. Indeed all amine groups are expected to be fully protonated at low pH, as well as they should remain neutral in high pH solutions.[140,106] The main goal of the *in vivo* studies (see Supporting Information), was to investigate and compare the behavior of drug-dendrimer complex in presence of two different NA drugs: fludarabine and clofarabine. In the present work, molecular dynamic simulations were conducted to study PPI G4 and its maltose functionalized version (PPI-Mal OS G4) in their protonated forms as they appear in human sick metabolism. Indeed, one of the major feature of cancer is altered metabolism, associated with acidification of the extracellular milieu.[102] Uncontrolled proliferation of cancer cell prefers the glucose metabolism, which is independent from the oxygen levels. This phenomenon is known as "aerobic glycolysis" or "Warburg effect". As a consequence of this metabolic phenotype, where cells exhibit high rates of glycolysis, there is an increase in the production of high amounts of lactic acid, which lead to acidification of the microenvironment.[103,104] Different protonation states were considered aimed at emulating neutral (pH 7.0) and acid (pH 5.0) conditions. In this case of study acid environment was investigated, where the amine are fully protonated.[105,106]

5.3 Materials and Methods

5.3.1 Molecular systems

Clofarabine and fludarabine compounds in their triphosphate and nucleoside forms were considered in this work (Table 5).

Table 5. Formula and molecular weight information of considered compounds.

Name	**Drug**	**Formula**	**MW (Da)**
CL0	Clofarabine	$C_{10}H_{11}ClFN_5O_3$	303,677
CL	Clofarabine Triphosphate	$C_{10}H_{14}ClFN_5O_{12}P_3$	543,615
FL0	Fludarabine	$C_{10}H_{12}FN_5O_4$	285,235
FL	Fludarabine Triphosphate	$C_{10}H_{15}FN_5O_{13}P_3$	525,17

Poly(PropylenImmine) dendrimer generation 4 (PPI G4) was considered with and without a MALtose functionalization as reported in a recent literature.[55,68,65,53,12] These dendrimers have been protonated as follow:

Table 6. Protonated dendrimers PPI G4 and PPI-Mal OS G4 Type, Generation, Protonated Atoms and Charge.

Dendrimer	**Type**	**Gen.**	**Protonated Atoms**	**Charge**
PPI G4 p	***PolyPropilenImmine***	**4**	**Primary Amines**	**+64**
PPI-Mal OS G4 pp	***PolyPropilenImmine protonated and modified with 43 Open Shell groups***	**4**	**Primary and Secondary Amines**	**+64**

5.3.2 Simulation Protocol

System Set Up

Avogadro chemical editor [107] and Linux bash scripts made in house were used to develop 3D models of dendrimers (PPI G4 and PPI-Mal OS G4) and nucleosides (CL0, CL, FL0 and FL). The General Amber Force Field (GAFF)[108] was considered to describe the molecule topologies. Partial charges were calculated considering separate residues by the Restrained Electrostatic Potential (RESP) fitting method, at the HF/6-31G level of theory using AM1-BCC charges as in a number of previous works [109–114]. A proper distribution of the partial charges was provided, which correctly takes into account the conformation of dendrimer and related bonds. Then, the topology and the parametrization were developed using antechamber and GROMACS associated tools [115–119] and a in house code[114].

Molecular Dynamics

Eight molecular systems were created by combining each compound in Table 5 with protonated dendrimers in Table 6. Each system consisted of a single compound and a single dendrimer (ratio 1:1). The compound and the dendrimer were positioned at a starting distance of 1.5 nm and a random orientation in a dodecahedron box filled with explicit water molecules (TIP3P)[120] and ions (NA+ and CL-) at a physiological concentration (0.15 M), to neutralize the system charge. The resulting molecular systems (e.g. CL-PPI G4) were composed by roughly 50000 interacting particles. Each system was energy minimized by 1000 steps of steepest descent energy minimization algorithm, followed by preliminary NVT (N=number, V=Volume, and T=temperature) of 40 ps. V-rescale thermostat was applied to keep temperature at 300 K with a time constant of 0.1 ps.[121] A 100 ps position restrained MD was performed at 300 K[121] and 1 atm[122]. V-rescale thermostat[121] and Berendsen[122] methods were used as temperature and pressure coupling. Finally a 100ns long MD was performed in the NVT ensemble at 300K, using V-rescale thermostat[121]. Atom velocities were randomly initialized following a Maxwell Boltzmann distribution. For each compound-dendrimer system, a combination of 3 independent repetition of the above-explained procedure was carried out. In total, 300 ns of MD was performed to sample the conformational space of each considered system combination. The last 50 ns of 3 MD replicas were used as a single ensemble trajectory. Therefore, the total ensemble trajectory considered for statistical analysis was 150 ns long and made of 75 million molecular configurations.

Four system combinations (CL-PPI G4 p, CL-PPI-Mal OS G4 pp, FL-PPI G4 p, and FL-PPI-Mal OS G4 pp) were also investigated simulate a compound-dendrimer ratio 1:10. In this case, 10 compounds of the same type were randomly positioned around the dendrimer at a starting distance of about 1.5 nm, in a dodecahedron box filled with explicit water molecules (TIP3P)[120] and ions (NA+ and CL-) at a physiological concentration (0.15 M). The resulting molecular system (e.g. CL-PPI G4 p) was composed by roughly 80000 interacting particles. Each system was energy minimized by 1000 steps of steepest descent energy minimization algorithm. A 100 ps position restrained MD was performed at 300 K [121] and 1 atm [122]. Finally, 5 repetitions of 100ns long MD were performed in the NVT ensemble. Atom velocities were randomly initialized following a Maxwell Boltzmann distribution. In total, 500 ns of MD was performed to sample the conformational space of each considered system. The last 50 ns of each replica were used as a single trajectory for data analysis.

GROMACS 5 package was used for all MD simulations and data analysis.[119] Long-ranged electrostatic interactions were calculated at every step with the Particle-Mesh Ewald method with a cut-off of 1 nm. The same cut-off was also applied to Lennard-Jones interactions. LINCS algorithm[123] approach allowed an integration time step of 2 fs. Visual Inspection of the Simulations was performed by The Visual Molecular Dynamics (VMD)[124] package and used for the visual inspection of the simulated systems.

5.4 Results (Compound-Dendrimer ratio 1:1)

Complexation analysis was employed to identify compound-dendrimer complexes throughout the overall MD simulation ensemble, following a method described earlier.[125] A cutoff distance between dendrimer and compound was chosen (0.2 nm) and applied to discriminate between bound and unbound compound-dendrimer systems. As shown in Figure 29, the complexation probability was evaluated as the percentage of simulation frames in which the system is found as a complex (compound bound to the dendrimer) over the total simulation frames (ensemble trajectory). Cluster percentage values below 70% indicated that the compound was able to attach and to detach from the dendrimer several times during the simulation, suggesting a low binding energy (i.e. close to the thermal energy, kT).

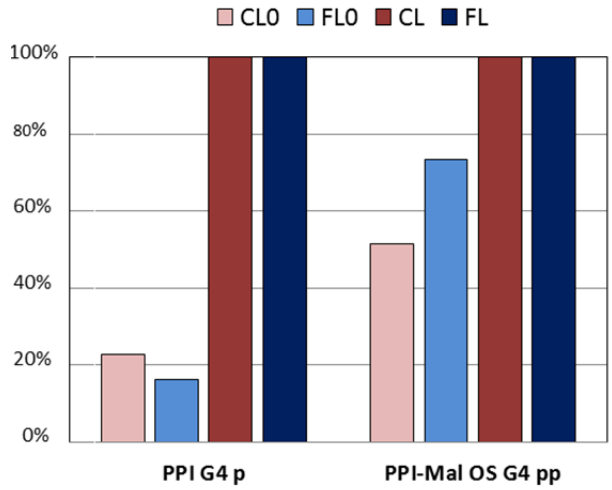

Figure 29. Probability to create a ligand-dendrimer complex. The complex ligand triphosphate–dendrimer showed value close to 100% in case of protonated dendrimers. Nucleoside compounds (indicated by CL0 and FL0) showed always lower ability to complex with the dendrimer with respect to the triphosphate form. Interestingly, the protonation of both the dendrimers influence clofarabine and fludarabine triphosphate complexation ability.

Nucleoside compounds showed always comparable much lower ability (less than 70% of probability) to complex the dendrimer with respect to their triphosphate forms. Indeed in nucleoside compound-dendrimer systems, an alternation of attached and detached configurations was noticed throughout the simulation, suggesting a binding energy of nucleoside compounds for the dendrimer of about kT. The complex nucleotide–dendrimer showed probability values of about 100% to create the complex, for both PPI G4 p and maltose functionalized PPI G4 pp dendrimers.

5.4.1 Interaction Energy

The result of complexation analysis reflects on binding enthalpy (Figure 30). To calculate the binding enthalpy the well-known "Molecular Mechanics/Generalized Born model augmented with the solvent accessible surface area term (GBSA)" approach was considered. This approach facilitated the estimation and comparison of binding energies calculated from MD simulations, as has been practiced in earlier literature.[126–132] It is worth mentioning that the calculated binding enthalpy cannot provide any indication on the absolute value of affinity given that the binding entropy has not been calculated. However, the data can be used to rank similar systems. As an example, the plot may provide an indication of affinity rank for different compounds bound to the same dendrimer.

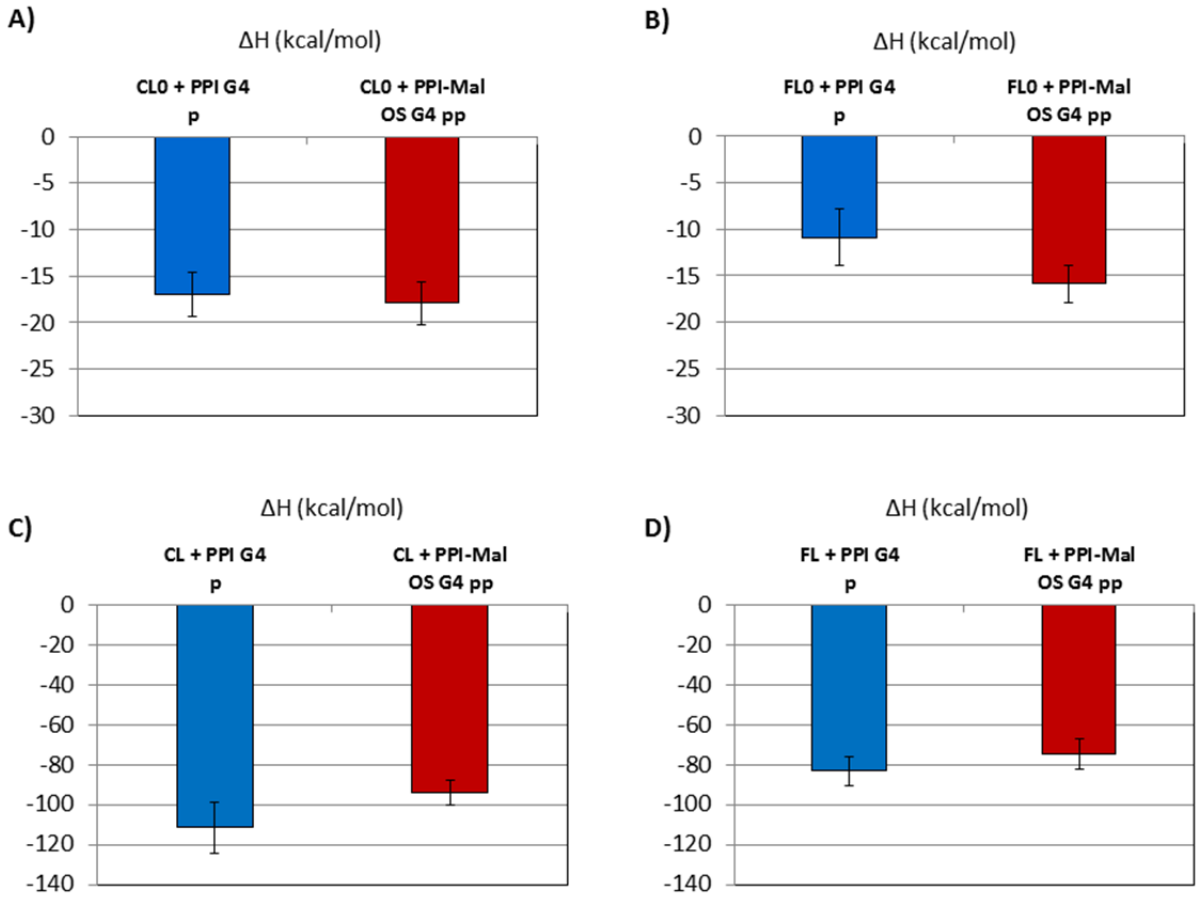

Figure 30. Binding enthalpy calculated by sampling all frames in which the compound and dendrimer are complexed. Maltose modified dendrimers are shown with red bar, whereas non-modified dendrimers are shown in blue. Standard errors are reported for each value.

In line with the complexation analysis, triphosphate forms present much higher binding enthalpy for protonated dendrimer and maltose decorated dendrimers with respect to nucleosides forms. Instead, binding enthalpy values were not sufficiently different to identify

an affinity discrepancy between clofarabine and fludarabine for both non decorated and decorated dendrimers. In other words, both compounds bind the dendrimer with similar affinity in both non functionalized and functionalized dendrimers.

5.4.2 Interaction Modes: Binding Orientation and Distance

The interaction mode has been investigated by determining compound orientation and distance with respect to the dendrimer, and overall conformational states of the complex system (75 million of configuration states were considered for each system). The calculation of the orientation of the compound over the surface of the dendrimer, was conducted by analyzing the variation of the amplitude of a specific angle (ϑ) during the simulation. The angle was defined by 3 identified regions (Figure 31-A) as follows: the dendrimer center of mass, the center of mass of the tail phosphate atoms (P, P1 and P2) and the nitrogen atoms compound head (N, N1, N2 and N4). In case of nucleosides, there is no phosphate tail; hence the orientation analysis remained poorly descriptive . The dendrimer compound distance was calculated as the distance between the center of mass of the compound and the dendrimer center of mass (Figure 31-B).

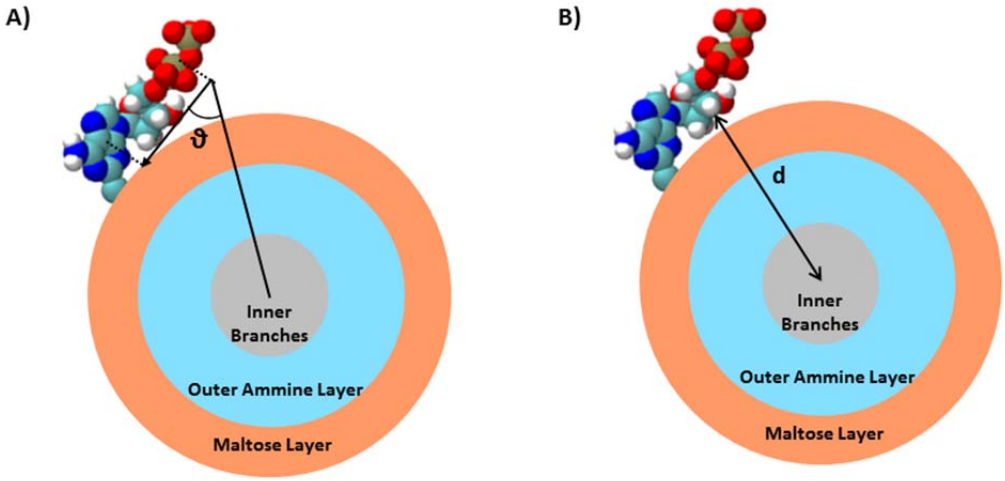

Figure 31. The protonated dendrimer structure is simplified in inner branches (grey area), outer ammine layer (blue areas) and maltose layer (orange area). A) To calculate the orientation of the ligand over the dendrimer has been defined an angle (ϑ) connecting 3 regions: the dendrimer center of mass, the center of mass of the tail phosphate atoms (P, P1 and P2) and the nitrogen atoms present on the head of all the compounds (N, N1, N2 and N4). B) The distance is calculated between the center of mass of the compound and the dendrimer center of mass (black line).

The calculated angle was directly correlated with the compound orientation, with respect to the dendrimer surface as shown in Figure 32. Comprehensively, an angle value equivalent to 0° indicated the compound oriented with the head toward the dendrimer center (Figure 32-A), and an angle value of 180° indicated the compound oriented with the tail toward the dendrimer center (Figure 32- C). Finally, an angle value = 90° indicated the compound flat over the dendrimer surface (Figure 32-B).

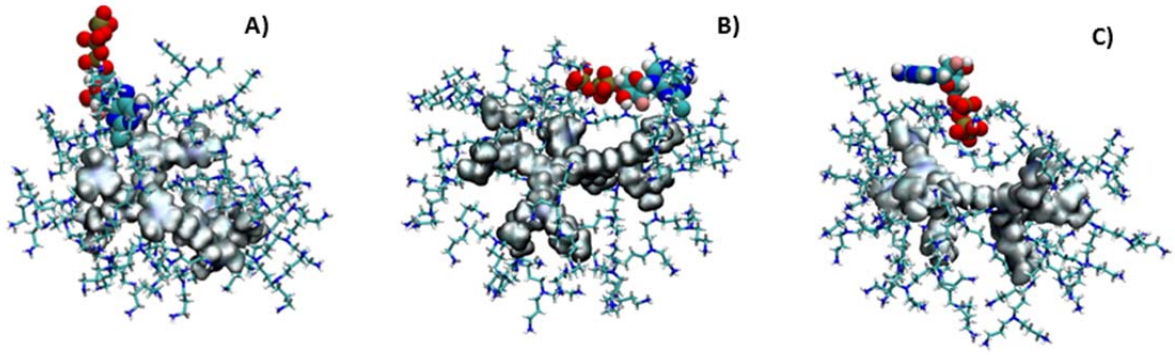

Figure 32. Compound orientation over dendrimer surface. This case shows the clofarabine triphosphate orientation over the PPI G4 p dendrimer. A) The compound oriented with the head toward the dendrimer center. B) The compound lies flat over the dendrimer surface. C) The compound oriented with the tail toward the dendrimer center.

The probability of each of three compound orientations was calculated throughout the ensemble trajectory considering only frames with complexed compound-dendrimer. For the sake of simplification, angle values were discretized in 3 outcomes: 0°-75° (head oriented toward the dendrimer center), 75°-105° (flat), 105°-180° (tail oriented toward the dendrimer center). The angle probability along the ensemble trajectory of the ligand triphosphate-dendrimer complex is shown in Figure 33.

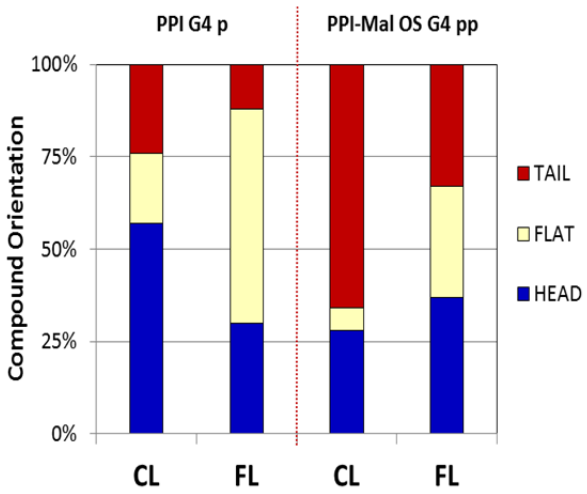

Figure 33. Probability of the triphosphate compound orientation when complexed with the protonated dendrimers. The blue histograms represent the probability of the compound oriented with the head turned to the center of the dendrimer (angle in a range 0°-75°). The yellow histograms show the probability of the ligand to have a flat placement over the dendrimer surface (angle in a range 75°-105°). The red histograms represent the probability of the ligand placed with the tail turned to the center of the dendrimer (angle in a range 105°-180°).

It is interesting to notice the different compound interaction modes over the dendrimer surfaces, in term of orientation. Notable was the fludarabine nucleotide placement over PPI G4 p dendrimer surface, which had mainly a flat orientation. Furthermore, the probability of finding the compound oriented with the tail toward the dendrimer center increases in PPI-Mal OS G4 pp dendrimer. This is an expected effect due to the negative charge of the compound (-4) and the positive charge of protonated dendrimers. In particular, it is evident that the double protonation causes orientation changes of the compound over the dendrimer surface. Indeed the clofarabine triphosphate had the 66 % of probability to have the tail oriented toward the dendrimer center.

The calculation of the compound penetration into the dendrimer layers was conducted by analyzing the variation of the distance between the compound and the dendrimer and by comparing it with the dendrimer radius of gyration layer by layer (Figure 34). The histograms show the radius of gyration of the dendrimer layers, starting from the inner branches (grey histogram), the outer amine layer (blue) and the maltose layer (orange). The black dot with error bars represents the mean value of the distance between the compound and the dendrimer center of mass. The plot highlights when the compound lies inside a specific layer of the dendrimer as for the case of CL-PPI G4 p, in which the compound penetrate until the dendrimer inner layers.

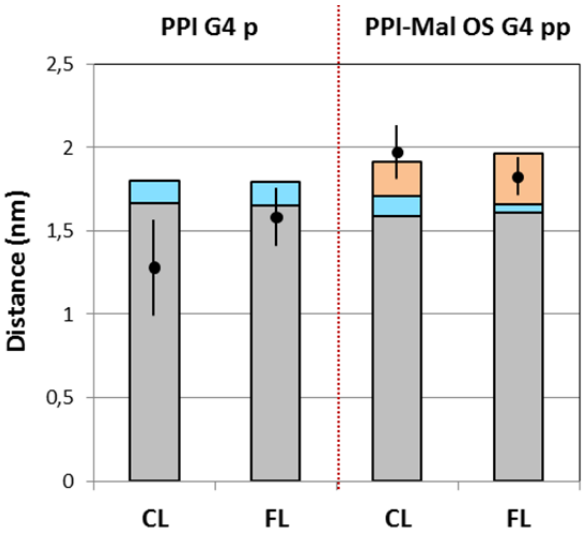

Figure 34. Graphics of the penetration data of the triphosphate compound-dendrimer systems. The histograms show the radius of gyration of the dendrimer layers, starting from the inner branches (grey), the outer amine layer (blue) and the maltose layer (orange). The black point represents the mean value and the standard deviation of the distance between the compound and the dendrimer.

The nucleotide compound-dendrimer system showed different behavior (Figure 34). Both clofarabine and fludarabine triphosphate compounds were completely embedded in PPI G4 p dendrimer, in line with binding enthalpy data (Figure 30). On the other hand, analyzing active compound forms interacting with the PPI-Mal OS G4 pp dendrimer, it was evident that the compounds were less able to penetrate inside the dendrimer. Interestingly, in case of clofarabine triphosphate interacting with PPI-Mal OS G4 pp dendrimer, its distance from the dendrimer center of mass was greater than the fludarabine one. This is the consequence of the different orientation of the compounds over the dendrimer surface. Besides, it is necessary to underline that the thickness of PPI-Mal OS G4 layers is different in case of interaction with the compounds. The differences were always in the same order of the standard deviation of the layer size (around 0.05 nm), therefore they could be considered negligible and mostly correlated with structure fluctuations and dendrimer orientation in the sampled ensemble.

5.4.3 Interaction Mode: Associated Molecular Interactions

The Radial Distribution Function (RDF) was calculated to get a precise information on the molecular phenomena driving the compound-dendrimer system complexation, as function of the compound-dendrimer distance. RDFs were calculated for two well defined atom groups (Figure 35) of the compound (Head and Tail) with respect to the outer dendrimer layer. The Head group (blue atoms presented in Figure 35) was composed by the nitrogen atoms and by the chlorine and fluorine atoms for the clofarabine compound. Instead, the Head group was composed by the nitrogen atoms and by the fluorine and the oxygen of the 2' end of the ribose for the fludarabine compound. Instead, the Tail (red atoms present in Figure 35) was composed by the seven oxygen atoms which are connected to the triphosphate group, in the triphosphate compounds.

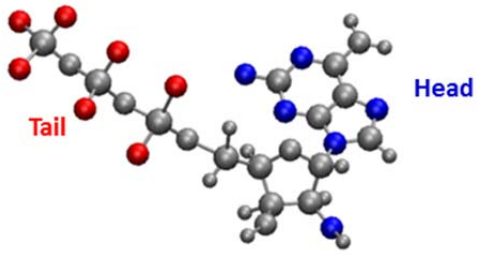

Figure 35. The Head group is composed by the blue atoms, and the tail group is composed by the red atoms. The Head group was composed by the nitrogen atoms and by the chlorine and fluorine atoms for the clofarabine compound. Instead, the Head group was composed by the nitrogen atoms and by the fluorine and the oxygen of the 2' end of the ribose for the fludarabine compound. The Tail was composed by the seven oxygen atoms which are connected to the triphosphate group, in the triphosphate compounds.

Figure 36 shows the radial distribution function of the Head group (on left side) and of the Tail group (on right side). The black line shows the RDF of the clofarabine nucleotide and the red line shows the fludarabine nucleotide. Both compounds had primary interaction with the outer dendrimer layer. Interestingly both the Tail groups, of the clofarabine and fludarabine triphosphates, had the main peak one order of magnitude higher than the Head group. Analyzing clofarabine interaction with PPI G4 p and PPI-Mal OS G4 pp (Figure 36) is possible to note that its Head did not have significant primary interactions. In case of PPI G4 p, nucleotide Head group was either positioned in the inner layer. On the other hand in case of PPI-Mal OS G4 pp dendrimer, clofarabine Head group was exposed to the solvent. Notable was that the main interaction was leaded by the clofarabine Tail group, which was stabilized by primary interaction with amino groups of the dendrimer surface. Contrariwise, the fludarabine triphosphate complexed with PPI G4 protonated and PPI-Mal OS G4 double

protonated dendrimers, had similar primary interaction with both Head and Tail groups. Plots are in agreement with orientation (Figure 33) and penetration data (Figure 34) shown above.

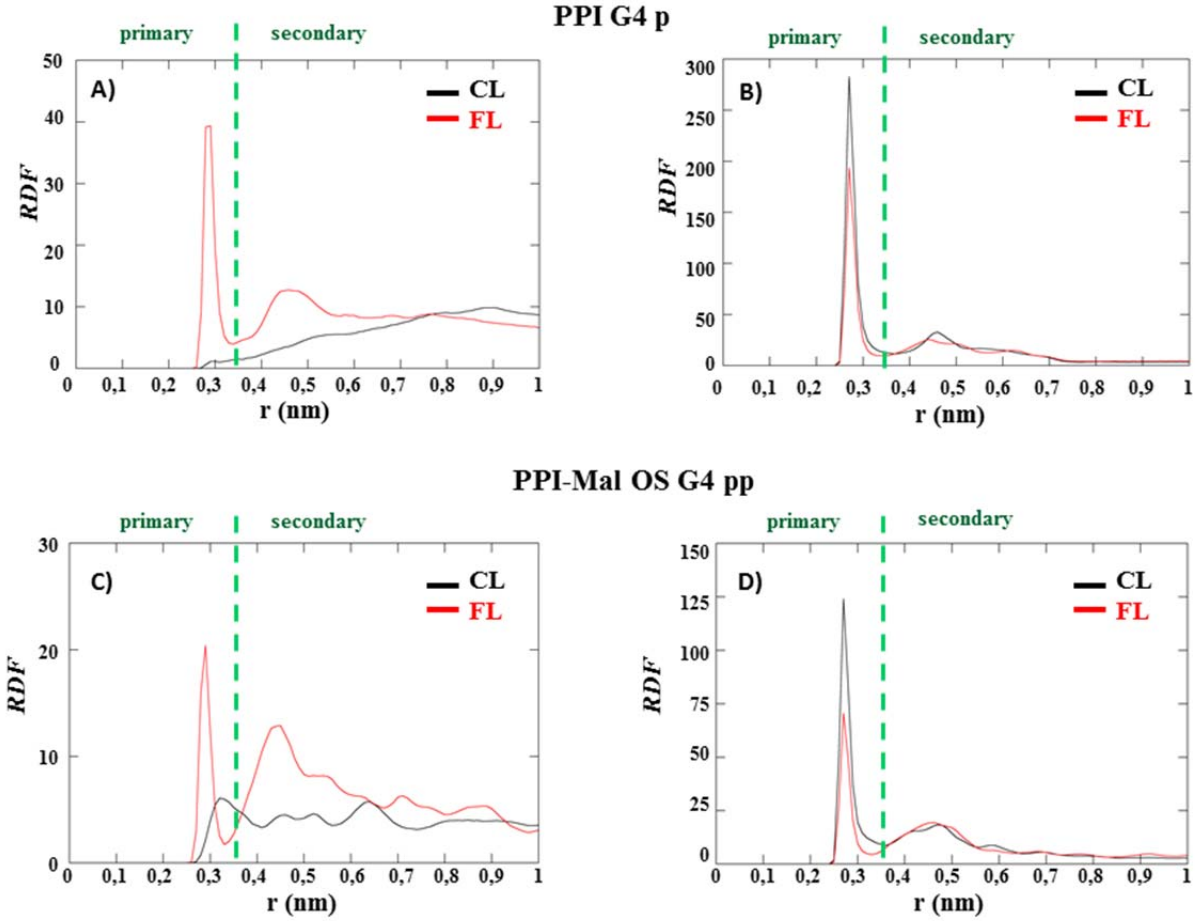

Figure 36. Radial Distribution Functions of the triphosphate compounds respect to the PPI G4 p, PPI-Mal OS G4 p and PPI-Mal OS G4 pp dendrimers. Figures A), C) and E) represent the Head group RDFs for respectively the clofarabine triphosphate-dendrimer complex (black curve) and the fludarabine triphosphate-dendrimer complex (red curve). Figures B), D) and F) represent the Tail group RDFs for respectively the clofarabine triphosphate-dendrimer complex (black curve) and the fludarabine-triphosphate dendrimer complex (red curve).

Data from orientation, penetration and RDF analysis highlighted the interaction mode of both compounds when they bound to PPI G4 p and PPI-Mal OS G4 pp dendrimers. Figure 37 shows representative trajectory snapshots providing a clear picture of the interaction mode. As previously said, the clofarabine triphosphate was characterized by the nucleotide head oriented toward the dendrimer center and interacting with the deeper layers in case of interaction with PPI G4 p dendrimer. Notable was clofarabine nucleotide displacement that change when it interacted with PPI-Mal OS G4 double protonated dendrimer. As shown in Figure 37-D, clofarabine tail was completely embedded into maltose groups, and its head was exposed to the solvent. On the other hand, fludarabine triphosphate interaction mode with the PPI G4 dendrimer was similar to the clofarabine ones. Contrariwise, fludarabine triphosphate favored a flat orientation over the PPI-Mal OS G4 pp dendrimer surface.

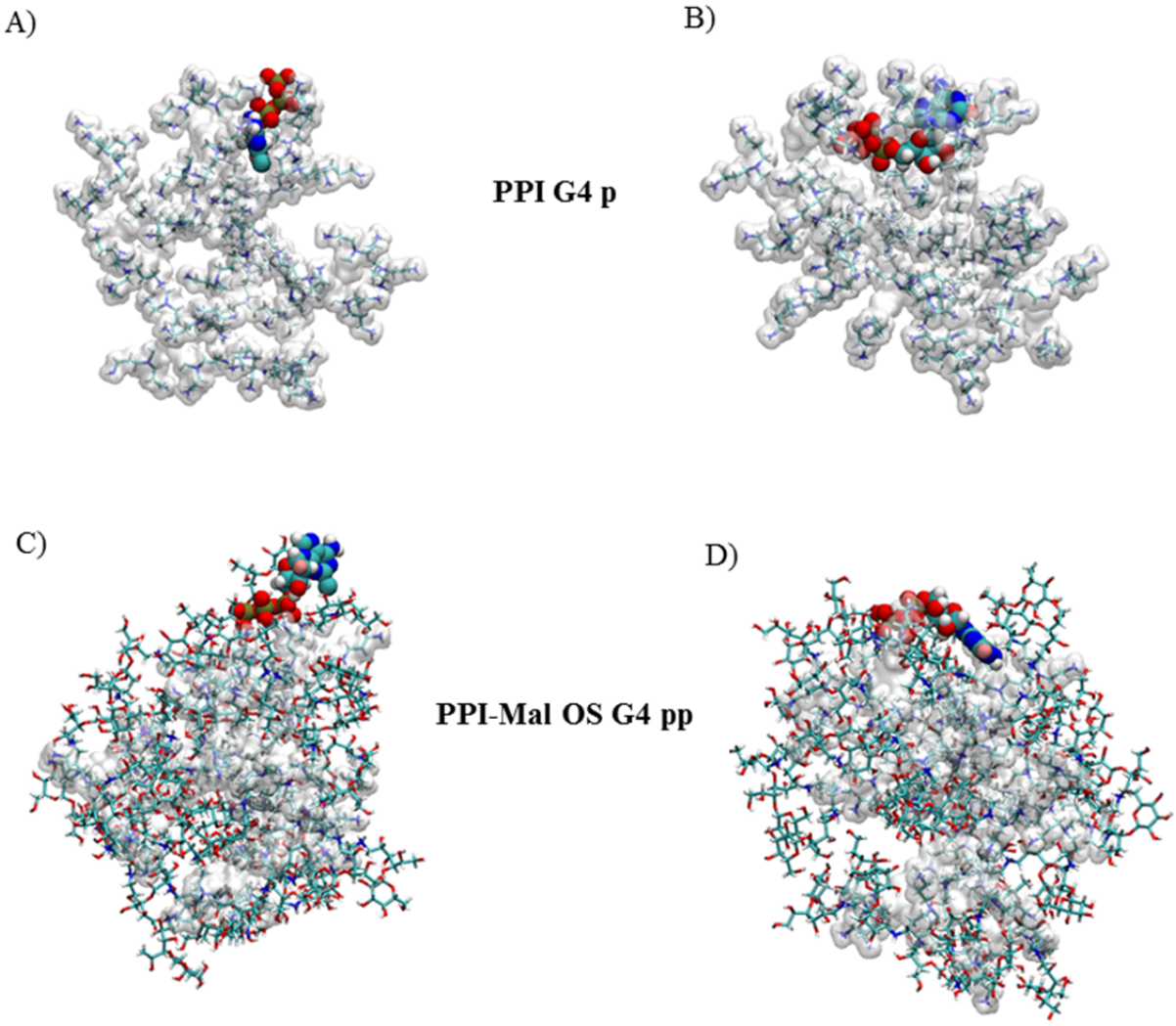

Figure 37. Representative snapshots of the nucleotide-dendrimer configuration for each investigated system. Figures A) and C) show the clofarabine triphosphate and the figures B) and D) show the fludarabine triphosphate.

5.5 Results (Compound-Dendrimer ratio 10:1)

Overall nanoparticle surface properties can be determined by the compound interaction mode. To further investigate this aspect, a set of simulations based on the 10:1 drug-dendrimer ratio was performed. In the following section, results of the simulations of ten triphosphate compounds in contact with the most relevant dendrimers (PPI G4 protonated and PPI-Mal OS G4 double protonated) are described. In fact, dendrimers are expected to be fully protonated at pH 5.0. Notable is that in all considered trajectories the ten nucleotide molecules never detached throughout the simulation but they stayed bound to the dendrimer. Figure 38 shows a representative snapshot of a single dendrimer PPI G4 p (on the first line) and PPI-Mal OS G4 pp (on the second line) interacting with 10 compounds.

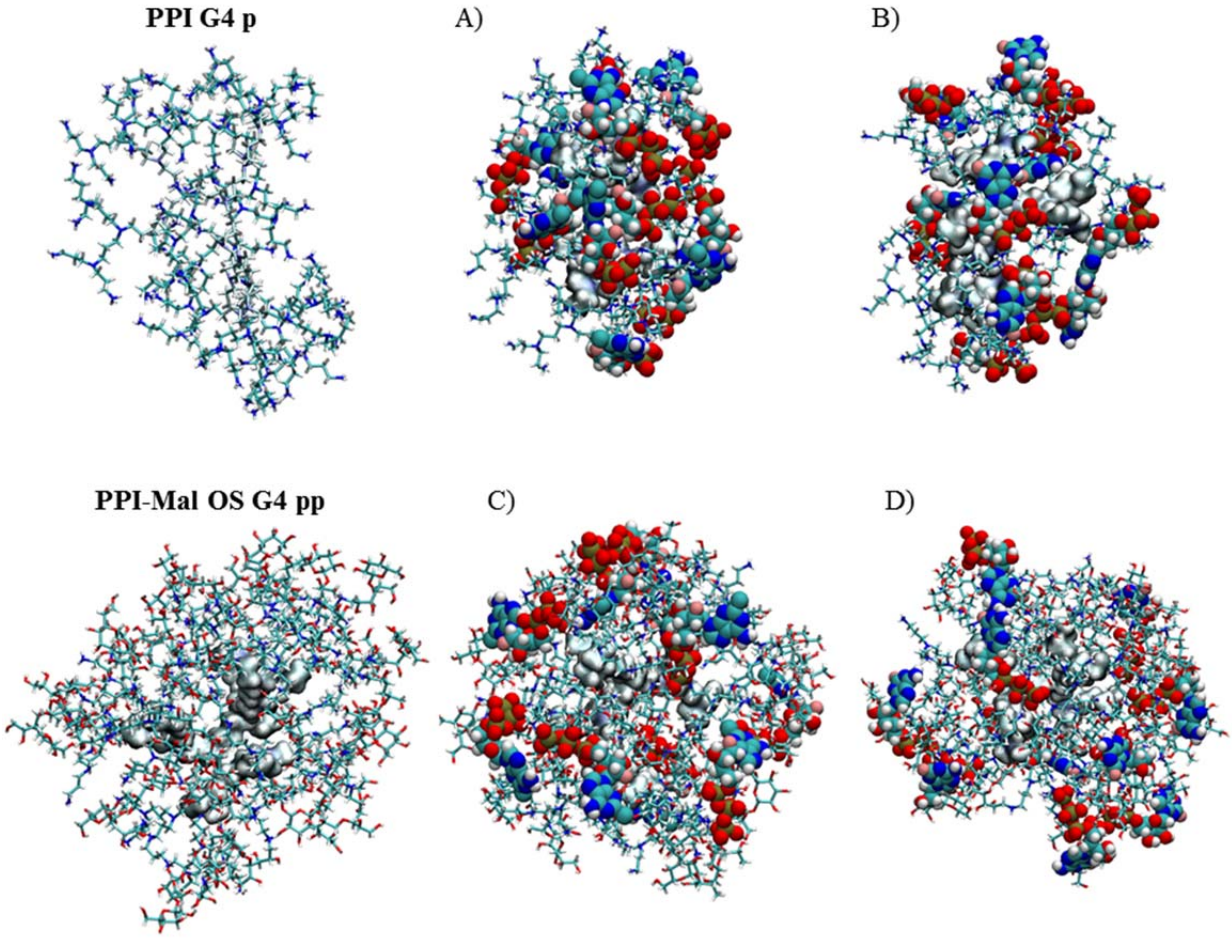

Figure 38. Representative snapshots of single dendrimer macromolecules and nucleotide dendrimer 10:1 ratio configurations for each investigated system. Figures A) and C) show the clofarabine triphosphate and the figures B) and D) show the fludarabine triphosphate.

5.5.1 Interaction Energy

The result of complexation analysis reflects on binding enthalpy (Figure 39). To calculate the binding enthalpy the well-known "Molecular Mechanics / Generalized Born model augmented with the solvent accessible surface area term (GBSA)" approach was considered, as employed in earlier literature to estimate and compare binding energies calculated from MD simulations [126–132]. It is worth mentioning that the calculated binding enthalpy cannot provide any indication on the absolute value of affinity given that the binding entropy has not been calculated. Nevertheless, the data can be used to rank similar systems. As an example, the plot may provide an indication of affinity rank for different compounds bound to the same dendrimer.

In line with what we have seen for ratio 1:1 clofarabine and fludarabine, these values showed very similar binding energies for same dendrimers. In other words, both compounds bind the dendrimer with similar affinity in both non functionalized and functionalized dendrimers.

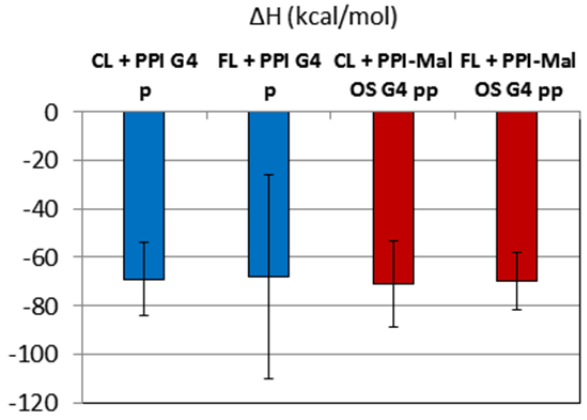

Figure 39. Binding enthalpy calculated by sampling all frames in which the compound and dendrimer are complexed. Maltose modified dendrimers are shown with red bar, whereas non-modified dendrimers are shown in blue. Standard errors are reported for each value.

5.5.2 Interaction Modes: Binding Orientation

The interaction mode has been investigated by determining compound orientation and distance with respect to the dendrimer, over all conformational states of the complex system. The calculation of the orientation of the compound over the surface of the dendrimer, was conducted as explained in the previous chapter. It was analyzed the variation of the amplitude of a specific angle (ϑ) during the simulation (see 5.4.2 Interaction Modes: Binding Orientation and Distance).

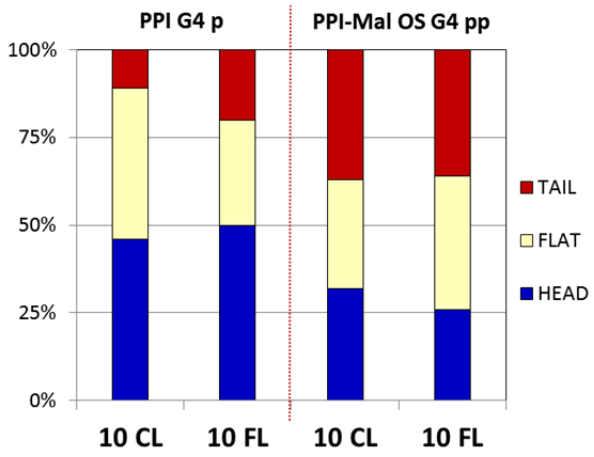

Figure 40. Probability of the ten triphosphate compounds orientation when complexed with the protonated dendrimer. The blue histograms represent the probability of the compounds oriented with the head turned to the center of the dendrimer (angle in a range 0°-75°). The yellow histograms show the probability of the ligands to have a flat placement over the dendrimer surface (angle in a range 75°-105°). The red histograms represent the probability of the ligands placed with the tail turned to the center of the dendrimer (angle in a range 105°-180°).

Analyzing Figure 40 is possible to note that the 10 clofarabine and the 10 fludarabine had a comparable behavior when they interacted with the studied protonated dendrimers. Interestingly both the triphosphate compounds had the head turned to the center of the dendrimer, when they interacted with the PPI G4 protonated dendrimer. Instead when these compounds interacted with the PPI-Mal OS G4 dendrimer, data indicated no preferential orientation of compound.

5.5.3 Effect of the binding on dendrimer electrostatic profile

For the calculation of the electrostatic potential simulation frames were extracted from the ensemble trajectory of complexed dendrimer-compound systems. The electrostatic potentials were computed by the APBS package.[143] In detail, the non-linear Poisson-Boltzmann equation was applied using single Debye-Huckel sphere boundary conditions on a 200x200x200 grid with a spacing of 1Å centered at the COM of the molecular system. The relative dielectric constants of the solute and the solvent were set to 4 and 78.4[144,145], respectively. The ionic strength was set to 150 mM and the temperature was fixed at 300K.[144,145]

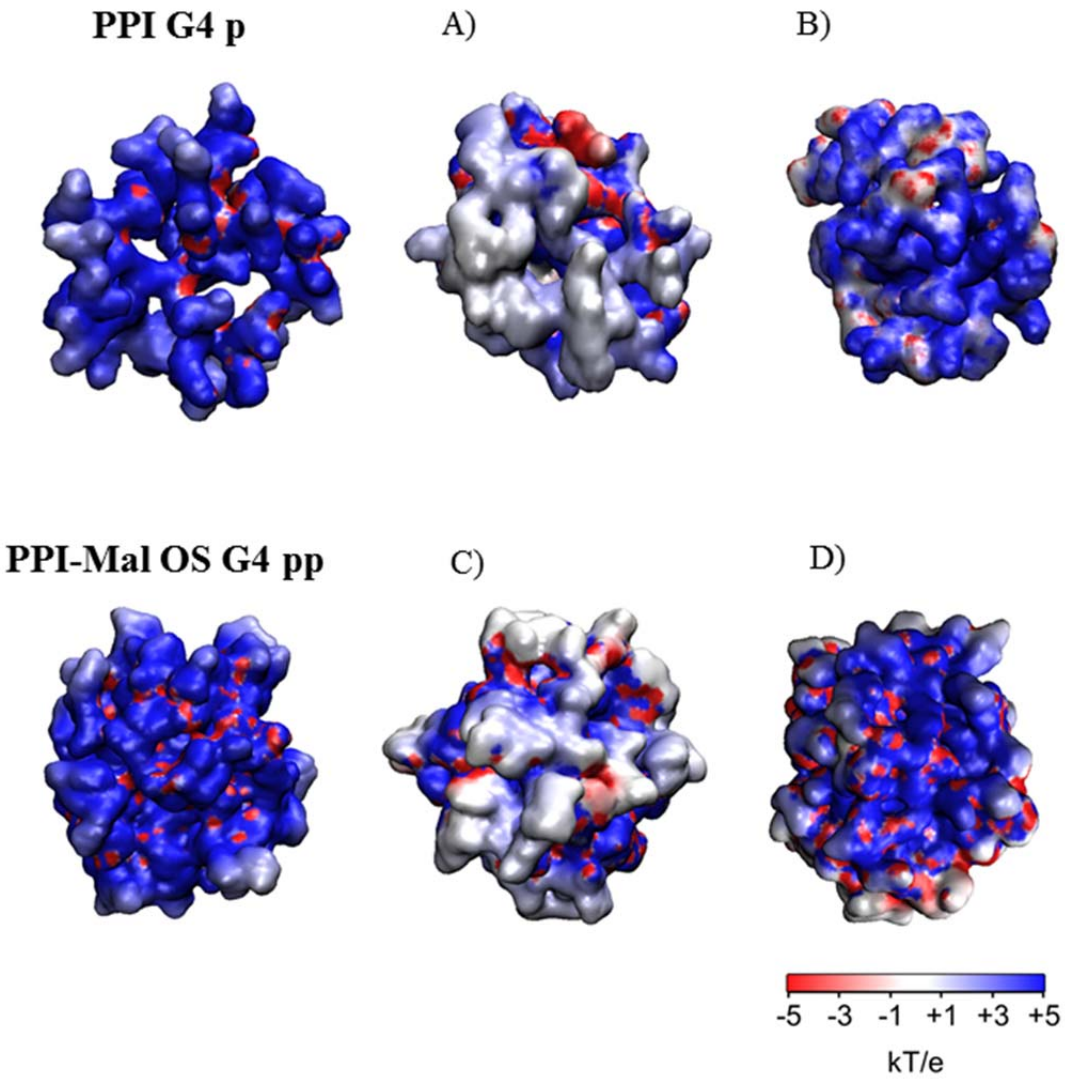

Figure 41. The electrostatic map presented for single dendrimer macromolecule and nucleotide-dendrimer complexes 10:1 ratio. Figures A) and C) show the clofarabine triphosphate and the figures B) and D) show the fludarabine triphosphate. Potential isocontours are shown in the range from +5 kT/e (blue) to -5 kT/e (red) and obtained by solution of the NLPBE at 150 mM ionic strength with a solute dielectric of 4 and a solvent dielectric of 78.4.

Figure 41 shows the electrostatic potential calculated for the single dendrimer macromolecule in water (PPI G4 p on the first line and PPI-Mal OS G4 on the second one) and its change when it interacted with the 10 compounds. Figure 41-A) and C) show the 10 clofarabine triphosphate compounds and Figure 41-B) and D) show the 10 fludarabine triphosphate ones. Notable was the overall positive electrostatic potential of the single dendrimer, as expected. Moreover, a quantitative examination of the electrostatic data showed interesting differences in the compound binding regions. Clofarabine showed a better efficacy to neutralize the dendrimer electrostatic potential in the binding region with respect to fludarabine, in particular for maltose decorated dendrimers. This clofarabine feature might differently affect the complex ability to cross the cell membrane.

5.6 Discussion

Nucleoside analogues were one of the first chemotherapeutic agents introduced for the medical treatment of cancer. These compounds are commonly used against hematological malignancies, including leukemia and lymphoma, as well as against solid tumors.[9] NAs includes a variety of purine and pyrimidine nucleoside derivatives with numerous cytotoxic activities. Indeed, NAs are antimetabolites and their toxic mechanisms are various. Their strength is based on their ability to be directly incorporated into newly synthesized nucleic acid chains and causing DNA and RNA synthesis inhibition. Moreover, NAs can decrease the activity of the enzymes involved in metabolism of natural nucleosides and nucleotides. The main NAs goal is to induce cell apoptosis, and this is achieved through different modes of action which depend on NAs structure, specificity and stability.[133] Noteworthy, all NAs share common intracellular transport and metabolic pathways. As hydrophilic molecules, these compounds cannot penetrate the cell membrane by passive diffusion and they need specialized nucleoside transporters. NTs mediate the cellular entry and enable active transfer through the cell membrane. Nevertheless the use of NTs is limited, indeed NTs are able to delivery only dephosphorylated forms, therefore NA entries inside the cell only in a deactivated form. Once inside, it needs to be progressively phosphorylated to its triphosphate form, which is critical for its cytotoxic activity.[134] The use of NT leads to delayed NA therapeutic effects and emergence of drug resistance due to downregulation of transporter expression or decreased activity of intracellular kinases.[98] Furthermore, the clinical effectiveness of these anticancer drugs is limited by various undesirable factors such as fast metabolism, unfavorable bio-distribution, low specificity of interaction and nonspecific toxicity.[68] The main crucial point is the cancer not specificity of the NAs that can endanger all the types of cells, and it can determine the emergence of various side effects.[28,98] A promising approach to overcome all the mentioned resistance mechanisms may involve the application of drug carrier systems, which provide enhanced cellular uptake of active triphosphate forms independently of NTs. Numerous studies were conducted on the use of dendrimers as DDS and it was highlighted that poly(propylene imine) dendrimers, with their surface partially modified with maltose moieties, can be a very promising vehicle for nucleotides.[68] Indeed, thanks to their high loading capacity, dendrimers improved bio-distribution and solubility of the drug. Cellular entry and blood circulation are facilitated by their nanometric size and globular shape. Furthermore, the presence of sugar moieties on the dendrimer surface, improves its biocompatibility and bioavailability. The use of glycosylate dendrimers helps also to overcome the not cancer specificity of the drug, due to the fact that leukemic cells usually overexpress lectin receptors which bind carbohydrate ligands with high affinity.[135,59]

Sugar modified PPI dendrimers have the potential of active interaction with cancer cells and they allow to decrease the detrimental effects on healthy tissues. Moreover, drug-dendrimer complexation is based on non-covalent physical incorporation of drug molecules into PPI dendrimer structure, and this conjugation enhances relative easy preparation of carrier system and lead the possibility to not modify the pharmacological activity of the therapeutic. Using these non-covalent complexes, it is possible to transport active triphosphate compound forms directly inside the cells, potentially overcoming the limits of standard chemotherapy.[136] Our studies were concentrated on the use on PPI G4 and PPI-Mal OS G4 dendrimers for the delivery of clofarabine and fludarabine, in their nucleoside and activate triphosphate forms. Firstly, the drug-dendrimer compounds were investigated at different protonation states, aimed at emulating neutral (pH 7.0) and acid (pH 5.0) conditions. At neutral pH, both dendrimers remain neutrals, whereas under acid environment the amines are protonated. In this case of study we focused our interest on the full protonated dendrimers. Based on the theory that the presence of cancer cells causes acidification of the environment, we would further analyze the dendrimer full protonated interactions when 64 hydrogens were added on its surface. Analyzing the results of nucleoside-dendrimer compounds ensemble trajectory frames, it was evident that both the nucleoside compounds (CL0 and FL0) show a very low complexation probability value with the dendrimers, with a cluster percentage value below 70%. This low value indicated, that during the simulation the compound was able to attach and to detach from the not modified dendrimer several times, suggesting a low binding energy (i.e. close to the thermal energy, kT). Supporting these results, also the enthalpy analysis highlighted that CL and FL had a very low value of affinity. Therefore our investigation was mainly directed to the interaction with nucleotide drug forms. For both drugs, as shown, the nucleotide phosphate parts (previously referred as “Tail”) were responsible for primary interactions with surface amino groups of PPI G4 p dendrimer. Noteworthy was the different orientation of the two compounds over the dendrimer surface. Indeed, the fludarabine nucleoside part (referred as "Head") also interacted with amino surface layer, although much less than phosphate moieties. Mainly, the fludarabine did not penetrate into PPI G interior and remained on its surface. This compound orientation/behavior may contribute to easier release of nucleotide from the complex. Contrariwise, the clofarabine nucleoside part had a tendency to penetrate into deeper layers of PPI G4, which might further stabilize the interaction by trapping the nucleotide inside the dendrimer structure. In this case, two types of interactions were probable nonionic (between the “Head” and internal tertiary amino groups) and ionic (between the “Tail” and surface primary amino groups). This drug behavior significantly hinder the release of clofarabine triphosphate from PPI G4 dendrimer. The same analysis

were conducted on the compound-dendrimer complexes in presence of maltose modified PPI G4 dendrimer. In this case, the fludarabine had a comparable behavior to the case of PPI G4 not modified dendrimer. Noteworthy, was the change of orientation and interaction of the other studied compound. Indeed, the nucleoside part of clofarabine triphosphate did not penetrate inside PPI-Mal OS G4 dendrimer; its "Tail" part interacting mainly with surface primary amino groups and its nucleotide "Head" was exposed to the solvent. This displacement was most probably because of the steric hindrance posed by maltose units and lead the possibility to release the clofarabine easier than in case of PPI G4. Additionally, the different compounds interaction may be partially due to the fact that the fludarabine is more polar (its polar surface area is 140 A^2, whereas it is only 119 A^2 for clofarabine) and exhibits higher hydrophilicity.[146] Therefore fludarabine polarity can cause its interaction with the charged surface of the dendrimer, while clofarabine may enter more easily inside dendrimer layers. Moreover, the fludarabine has more flexible structure which hampers the incorporation of its nucleoside part into dendrimer's interior. On the other hand, the clofarabine structure, which presents a fluorine atom into the sugar ring, may additionally stiffen structure of its triphosphate, preventing the simultaneous interaction of the "Tail" and the "Head" with the surface of the dendrimer.[7]

Further analysis were conducted on the compounds-dendrimer complexes with ratio 10:1. Interestingly, the investigation of electrostatic potential of complex formulations showed that the clofarabine was able to neutralize the dendrimer surface charge. Instead the fludarabine-PPI dendrimer complexes remain positively charged. Noteworthy, PPI dendrimers were introduced as efficient nanocarriers due to their positive charged surface which have much greater tendency to penetrate cell membranes than neutral or negatively charged ones.[147,148] This unexpected clofarabine feature may limit the ability of compound-dendrimer complex to enter the cell and the drug delivery potential of PPI macromolecules may be significantly decreased. Therefore, we postulate that the observed *in vivo* differences in the interactions between the two drugs and PPI dendrimers are primarily associated with the ability of the complex to cross the cell membrane. Most likely, the dendrimer can deliver fludarabine triphosphate to the cytoplasm, whereas the clofarabine-dendrimer complex remains outside the cell. Furthermore, the different rate of inhibition of clofarabine cytotoxicity by PPI G4 and PPI-Mal OS G4 may be associated with the mode of interactions (*in situ* studies) and their strength (SPR analysis), indicating that clofarabine triphosphate binds stronger to the unmodified dendrimer. Contrariwise, we can postulate that PPI-Mal OS G4 dendrimer significantly enhances cellular uptake of fludarabine triphosphate without causing any change to its pharmacological activity. [67,53]

5.7 Conclusions

In this chapter, eight different compound-dendrimer complexes ratio 1:1 and four drugs-dendrimer complexes ratio 10:1 were analyzed. The aims of this study were to fully investigate compound- PPI G4 and PPI-Mal OS G4 full protonated complexes, to compare different dynamic behaviors and to understand more stable and effective structures. *In vivo* studies were conducted to investigate the actual differences of these drugs and drug-dendrimer complexes in U937 cancer cells. Our intent was to further verify *in vivo* experiments, using MD simulations by showing conformational changes of compound-dendrimer complexes. We have simulated full protonated dendrimers assuming that under carcinogen acid environment (pH 5.0) the amine are protonated. Analyzing the chemical differences between the two studied drugs, it was evident that the presence of a clorine and a fluorine atoms on the clofarabine nucleoside part strongly determines a different behavior of the drug. This atomic difference determined that the clofarabine carried a more rigid structure and, in ratio studies 10:1, was highlighted that this drug was also able to neutralize the positive charged dendrimer surface. On the other hand, fludarabine showed a more flexible structure and preserved the positive charged dendrimer surface, which enable cellular entry.

6. Conclusions

This chapter is devoted to general conclusion of this master thesis work.

Nowadays the development of new types of nanotechnology has became a very interesting and promising approach to overcome biological and medical limitations. Indeed the use of nanometric scale disposals leads a more targeted and effective therapy, giving significant benefits to cancer patients. The efficient use of drug delivery systems, such as the glycodendrimers analyzed in this study, as nanocarriers for nucleoside analogues drugs gives the possibility to overcome many of the problems connected with the direct use of this chemotherapeutics. The vast majority of current experimental approaches, such as X-ray crystallography, NMR spectroscopy, SPR analysis, resazurin assay or infrared spectroscopy investigate drug-dendrimer complex aggregation based on traditional ensemble techniques. On the other hand, computational approaches (MD) allow the investigation of structural and dynamical characterization of compound-dendrimer systems with an atomic resolution. Moreover the use of simulations have often demonstrated to be a helpful and crucial method, enable to add valuable quantitative information to experimental data.

The results presented in this master thesis work provide insight into the fludarabine and clofarabine behavior in presence of a poly(propileneimine) dendrimers with significant implications in several aspects. In detail, the use of MD allows the identification of the NAs orientation and displacement over the dendrimer surface. Our findings, in line with the *in vivo* collected data, showed that both the nucleoside forms of this drugs did not interact with the dendrimers, suggesting that with these drugs the use of a PPI dendrimer was unhelpful. Contrariwise, the clofarabine and fludarabine nucleotides were able to interact with the PPI dendrimer and its glycosylate form PPI-Mal OS G4 dendrimer. Our work provide that the fludarabine-PPI-Mal OS G4 complex can be an effective nanocarrier, enabling the direct delivery of the active triphosphate drug, across the cell membrane. On the other hand, the clofarabine displacement do not permit an easy detachment of the compound from the dendrimer surface, and it caused the neutralization of the dendrimer surface charge. In particular, our computational results highlight how small changes in drug structure may significantly impact its bindings with the dendrimer, influencing surface properties as well as mode and strength of interaction. This work does not pretend to be an exhaustive overview about fludarabine and clofarabine complex with the PPI and PPI-Mal OS G4 dendrimers. Further investigations are needed in order to better describe compound-dendrimer models. For this purpose, molecular modelling is very powerful tools in order to shed light on the

possibility to use these dendrimers as a powerful drug delivery system for NAs. An interesting avenue for future computational studies could be the investigation of these PPI dendrimers, recently glycosylate with other types of sugar moieties, as drug delivery system for other approved and used NAs.

ACKNOWLEDGEMENTS

After thirteen long and intense months, finally has arrived the time to put an end to my master thesis work. It was a period of profound learning, strong research and long waiting, without lose the hope to find the right results. These months had a strong impact on my life, on my thoughts and on my personality, not only at scientific level but also at personal one. Now I would like to spend two words of thanks to all the people who crossed my way during these months.

The first thanks goes to my advisor Professor Marco Agostino Deriu. I would like to express all my sincere gratitude and regard for his assiduous dedication, valuable guidance and continuous motivation during the thesis work. Without his help and his different way to see the problem I would never arrive at this point. I am very thankful for helping me to improve my background in Molecular Modeling research field and for giving me the special opportunity to work in the Computational Science Research Group of the Dalle Molle Institute for Artificial Intelligence.

I would also like to thank my co-supervisor Professor Umberto Morbiducci from Polytechnic University of Turin for his evaluation and review of my research.

I am grateful to Ing. Gianvito Grasso for having always answered to all my question with a smile on his face, and for sharing his advices and knowledge of molecular modeling skills with me.

I wish also to acknowledge Professor Andrea Danani and all the people working in the Computational Science Research Group of the Dalle Molle Institute for Artificial Intelligence in Switzerland.

A special thanks goes to Filip, who pushed me to face this experience in Switzerland with him and had always help and supported me during all these years of Poli. My fixed point in the middle of a vortex of changes.

Sincere thanks goes to Martina and Stefano for having sharing their knowledge and tips with me, as well as pizza on Thursday nights.

I wish also to thank Maryem and Khalid to have help me to find the right words to complete this work.

I am grateful to Antonella, a friend which has hosted me during all these months and that made me fells at home.

I would like to thank Claudia for being close to me, making me see things differently with few words, and always having me smile again.

A grateful thanks to my sister Valeria and Andrea that have always encourage and supported me during these years of Poli. Their evening calls have always made me return in a good mood.

The last but not the least thanks is for my parents. My mother Rosalina and my father Riccardo that have taught to me how to build my own future, never stopping at the first problem, but always struggling to achieve my goals.

Alessia

References

1. Oliveira, P. D. Leukaemia prevalence worldwide: raising aetiology questions. *Lancet. Haematol.* **5,** e2–e3 (2018).

2. Rodriguez-Abreu, D., Bordoni, A. & Zucca, E. Epidemiology of hematological malignancies. *Ann. Oncol.* **18,** i3–i8 (2007).

3. Jurlander, J. in *Encyclopedia of Cancer* 1640–1644 (Springer Berlin Heidelberg, 2011). doi:10.1007/978-3-642-16483-5_2615

4. Greaves, M. Leukaemia 'firsts' in cancer research and treatment. *Nat. Rev. Cancer* **16,** 163–172 (2016).

5. Galmarini, C. M., Mackey, J. R. & Dumontet, C. Nucleoside analogues and nucleobases in cancer treatment. *Lancet Oncology* **3,** 415–424 (2002).

6. Galmarini, C., Mackey, J. & Dumontet, C. Nucleoside analogues: mechanisms of drug resistance and reversal strategies. *Leukemia* **15,** 875–890 (2001).

7. Gorzkiewicz, M. *et al.* Fludarabine-specific molecular interactions with maltose-modified poly(propyleneimine) dendrimer enable effective cell entry of active drug form: comparison with clofarabine. *Biomacromolecules* (2019). doi:10.1021/ACS.BIOMAC.9B00010

8. Ziemba, B. *et al.* Toxicity and proapoptotic activity of poly(propylene imine) glycodendrimers in vitro: Considering their contrary potential as biocompatible entity and drug molecule in cancer. *Int. J. Pharm.* **461,** 391–402 (2014).

9. Gorzkiewicz, M. & Klajnert-Maculewicz, B. Dendrimers as nanocarriers for nucleoside analogues. *European Journal of Pharmaceutics and Biopharmaceutics* **114,** 43–56 (2017).

10. Gorzkiewicz, M. *et al.* Poly(propyleneimine) glycodendrimers non-covalently bind ATP in a pH- and salt-dependent manner – model studies for adenosine analogue drug delivery. *Int. J. Pharm.* **544,** 83–90 (2018).

11. Kojima, C., Kono, K., Maruyama, K. & Takagishi, T. Synthesis of polyamidoamine dendrimers having poly(ethylene glycol) grafts and their ability to encapsulate anticancer drugs. *Bioconjug. Chem.* **11,** 910–917 (2000).

12. Gorzkiewicz, M. *et al.* Terminal Sugar Moiety Determines Immunomodulatory Properties of Poly(propyleneimine) Glycodendrimers. doi:10.1021/acs.biomac.8b00168

13. Ribeiro, R. *et al.* Philadelphia chromosome-positive acute lymphoblastic leukemia in children: durable responses to chemotherapy associated with low initial white blood cell counts. *Leukemia* **11,** 1493–1496 (1997).

14. Rhoades, K. L. *et al.* Analysis of the role of AML1-ETO in leukemogenesis, using an inducible transgenic mouse model. *Blood* **96,** 2108–15 (2000).

15. Grigoropoulos, N. F., Petter, R., Van 't Veer, M. B., Scott, M. A. & Follows, G. A. Leukaemia update. Part 1: diagnosis and management. *Bmj* **346,** f1660–f1660 (2013).

16. Harris, N. L. *et al.* World Health Organization Classification of Neoplastic Diseases of the Hematopoietic and Lymphoid Tissues: Report of the Clinical Advisory Committee Meeting—Airlie House, Virginia, November 1997. *J. Clin. Oncol.* **17,** 3835–3849 (1999).

17. National Cancer Institute. Leukemia - Cancer Stat Facts. (2012). Available at: https://seer.cancer.gov/statfacts/html/leuks.html. (Accessed: 16th October 2018)

18. De Kouchkovsky, I. & Abdul-Hay, M. 'Acute myeloid leukemia: A comprehensive review and 2016 update'. *Blood Cancer J.* **6,** (2016).

19. Miranda-Filho, A. *et al.* Epidemiological patterns of leukaemia in 184 countries: a population-based study. *Lancet Haematol.* **5,** e14–e24 (2018).

20. Foà, R., Del Giudice, I., Guarini, A., Rossi, D. & Gaidano, G. Clinical implications of the molecular genetics of chronic lymphocytic leukemia. *Haematologica* **98,** 675–685 (2013).

21. CollaborativeGroup, C. L. L. T. Chemotherapeutic Options in Chronic Lymphocytic Leukemia: a Meta-analysis of the Randomized Trials. *J. Natl. Cancer Inst.* **91,** 861–868 (1999).

22. Freres, P., Jerusalem, G. & Moonen, M. *Categories of Anticancer Treatments*. *Anticancer Treatments and Cardiotoxicity: Mechanisms, Diagnostic and Therapeutic Interventions* (Elsevier Inc., 2016). doi:10.1016/B978-0-12-802509-3.00002-9

23. Capizzi, R. L., Courtland White, J. & Fernandes, D. J. *Antimetabolites*. *Bailliere's Clinical Haematology* **4,** (1991).

24. Pharmacokinetics, H. Antimetabolites. (2007).

25. Tsesmetzis, N., Paulin, C., Rudd, S. & Herold, N. Nucleobase and Nucleoside Analogues: Resistance and Re-Sensitisation at the Level of Pharmacokinetics, Pharmacodynamics and Metabolism. *Cancers (Basel).* **10,** 240 (2018).

26. Cheson, B. D. New antimetabolites in the treatment of human malignancies. *Semin. Oncol.* **19,** 695–706 (1992).

27. Lapponi, M. J., Rivero, C. W., Zinni, M. A., Britos, C. N. & Trelles, J. A. New developments in nucleoside analogues biosynthesis: A review. *J. Mol. Catal. B Enzym.* **133,** 218–233 (2016).

28. Galmarini, C. M., Mackey, J. R. & Dumontet, C. Nucleoside analogues: Mechanisms of drug resistance and reversal strategies. *Leukemia* **15,** 875–890 (2001).

29. Baldwin, S. A., Mackey, J. R., Cass, C. E. & Young, J. D. Nucleoside transporters: Molecular biology and implications for therapeutic development. *Molecular Medicine Today* **5,** 216–224 (1999).

30. Young, J. D., Yao, S. Y. M., Baldwin, J. M., Cass, C. E. & Baldwin, S. A. The human concentrative and equilibrative nucleoside transporter families, SLC28 and SLC29. *Mol. Aspects Med.* **34,** 529–47 (2013).

31. Jordheim, L. P. & Dumontet, C. Review of recent studies on resistance to cytotoxic deoxynucleoside analogues. *Biochim. Biophys. Acta - Rev. Cancer* **1776,** 138–159 (2007).

32. Braess, J. *et al.* Proliferative activity of leukaemic blasts and cytosine arabinoside pharmacodynamics are associated with cytogenetically defined prognostic subgroups in acute myeloid leukaemia. *Br. J. Haematol.* **113,** 975–82 (2001).

33. Yamauchi, T., Kawai, Y. & Ueda, T. Inhibition of Nucleotide Excision Repair by Fludarabine in Normal Lymphocytes *in vitro* , Measured by the Alkaline Single Cell Gel Electrophoresis (Comet) Assay. *Japanese J. Cancer Res.* **93,** 567–573 (2002).

34. Parker, W. B. *et al.* Effects of 2-chloro-9-(2-deoxy-2-fluoro-beta-D-arabinofuranosyl)adenine on K562 cellular metabolism and the inhibition of human ribonucleotide reductase and DNA polymerases by its 5'-triphosphate. *Cancer Res.* **51,** 2386–94 (1991).

35. Schwab, M. (Manfred). *Encyclopedia of cancer*. (Springer, 2009).

36. Montgomery, J. & Hewson, K. Nucleosides of 2-Fluoroadenine. *J. Med. Chem.* **12,** 498–504 (1969).

37. Ricci, F., Tedeschi, A., Morra, E., Montillo, M. & Marco, M. Fludarabine in the treatment of chronic lymphocytic leukemia: a review. *Ther. Clin. Risk Manag.* **5,** 187–207 (2009).

38. Fludarabine, O. & Fda, N. Oforta. 18–19 (2018).

39. Food and Drug Administration. FLUDARA (fludarabine phosphate), NDA 020038. 1–13 (2010).

40. Bonate, P. L. *et al.* Discovery and development of clofarabine: a nucleoside analogue for treating cancer. *Nat. Rev. Drug Discov.* **5,** 855–863 (2006).

41. Fozza, C. The role of Clofarabine in the treatment of adults with acute myeloid leukemia. *Crit. Rev. Oncol. Hematol.* **93,** 237–245 (2015).

42. Larson, M. L. & Venugopal, P. Clofarabine: a new treatment option for patients with acute myeloid leukemia. *Expert Opin. Pharmacother.* **10,** 1353–1357 (2009).

43. Kohrs, N. J., Liyanage, T., Venkatesan, N., Najarzadeh, A. & Puleo, D. A. *Drug Delivery Systems and Controlled Release*. *Reference Module in Biomedical Sciences* (Elsevier Inc., 2018). doi:10.1016/B978-0-12-801238-3.11037-2

44. Kakde, D., Jain, D., Shrivastava, V., Kakde, R. & Patil, A. T. Cancer therapeutics-opportunities, challenges and advances in drug delivery. *J. Appl. Pharm. Sci.* **1,** 1–10 (2011).

45. Newkome, G. R., Yao, Z., Baker, G. R. & Gupta, V. K. Micelles. Part 1. Cascade molecules: a new approach to micelles. A [27]-arborol. *J. Org. Chem.* **50,** 2003–2004 (1985).

46. Buhleier, E., Wehner, W., Chemischer, F. V.- & 1978, undefined. ′ CASCADE′-AND′ NONSKID-CHAIN-LIKE′ SYNTHESES OF MOLECULAR CAVITY TOPOLOGIES. *Wiley Online Libr.*

47. Tomalia, D. A. *et al.* A New Class of Polymers: Starburst-Dendritic Macromolecules. *Polym. J.* **17,** 117–132 (1985).

48. Nanjwade, B. K., Bechra, H. M., Derkar, G. K., Manvi, F. V. & Nanjwade, V. K. Dendrimers: Emerging polymers for drug-delivery systems. *Eur. J. Pharm. Sci.* **38,** 185–196 (2009).

49. Nanjwade, B. K., Bechra, H. M., Derkar, G. K., Manvi, F. V & Nanjwade, V. K. Dendrimers: Emerging polymers for drug-delivery systems. *Eur. J. Pharm. Sci.* **38,** 185–196 (2009).

50. Kalomiraki, M., Thermos, K. & Chaniotakis, N. A. Dendrimers as tunable vectors of drug delivery systems and biomedical and ocular applications. *International Journal of Nanomedicine* **11,** 1–12 (2015).

51. Cai, X., Hu, J., Xiao, J. & Cheng, Y. Dendrimer and cancer: a patent review (2006 – present). *Expert Opin. Ther. Pat.* **23,** 515–529 (2013).

52. Sherje, A. P., Jadhav, M., Dravyakar, B. R. & Kadam, D. Dendrimers: A versatile nanocarrier for drug delivery and targeting. *Int. J. Pharm.* **548,** 707–720 (2018).

53. Gorzkiewicz, M. *et al.* Glycodendrimer Nanocarriers for Direct Delivery of Fludarabine Triphosphate to Leukemic Cells: Improved Pharmacokinetics and Pharmacodynamics of Fludarabine. doi:10.1021/acs.biomac.7b01650

54. Weener, J.-W., Dongen, J. L. J. Van & Meijer, E. W. Electrospray Mass Spectrometry Studies of Poly (Propylene Imine) Dendrimers : Probing Reactivity in the Gas Phase Electrospray Mass Spectrometry Studies of Poly (Propylene Imine) Dendrimers : Probing Reactivity in the Gas Phase. *Science (80-.).* 10346–10355 (1999). doi:10.1021/ja984432

55. Szulc, A., Appelhans, D., Voit, B., Bryszewska, M. & Klajnert, B. Characteristics of complexes between poly(propylene imine) dendrimers and nucleotides. *New J. Chem.* **36,** 1610 (2012).

56. Drzewi Ska, J., Appelhans, D., Voit, B., Bryszewska, M. & Klajnert, B. Drzewińska-2012-Poly(propylene imine.pdf. *Biochemical and Biophysical Research Communications* **427,** 197–201 (2012).

57. Appelhans, D., Klajnert-Maculewicz, B., Janaszewska, A., Lazniewska, J. & Voit, B. Dendritic glycopolymers based on dendritic polyamine scaffolds: view on their synthetic approaches, characteristics and potential for biomedical applications. *Chem. Soc. Rev.* **44,** 3968–3996 (2015).

58. Franiak-Pietryga, I. *et al.* The influence of maltotriose-modified poly(propylene imine) dendrimers on the chronic lymphocytic leukemia cells in vitro: Dense shell G4 PPI. *Mol. Pharm.* **10,** 2490–2501 (2013).

59. Janaszewska, A. *et al.* Cytotoxicity of PAMAM, PPI and maltose modified PPIdendrimers in Chinese hamster ovary (CHO) and human ovarian carcinoma (SKOV3) cells. *New J. Chem.* **36,** 428–437 (2012).

60. Ciolkowski, M. *et al.* The influence of maltose modified poly(propylene imine) dendrimers on hen egg white lysozyme structure and thermal stability. *Colloids Surfaces B Biointerfaces* **95,** 103–108 (2012).

61. Bhadra, D., Yadav, A. K., Bhadra, S. & Jain, N. K. Glycodendrimeric nanoparticulate carriers of primaquine phosphate for liver targeting. *Int. J. Pharm.* **295,** 221–233 (2005).

62. Jain, K., Kesharwani, P., Gupta, U. & Jain, N. K. A review of glycosylated carriers for drug delivery. *Biomaterials* **33,** 4166–4186 (2012).

63. Gorzkiewicz, M. & Klajnert-Maculewicz, B. Dendrimers as nanocarriers for nucleoside analogues. *Eur. J. Pharm. Biopharm.* **114,** 43–56 (2017).

64. Filimon, A., Sima, L. E., Appelhans, D., Voit, B. & Negroiu, G. Internalization and intracellular trafficking of poly(propylene imine) glycodendrimers with maltose shell in melanoma cells. *Curr. Med. Chem.* **19,** 4955–68 (2012).

65. Szulc, A., Pulaski, L., Appelhans, D., Voit, B. & Klajnert-Maculewicz, B. Sugar-modified poly(propylene imine) dendrimers as drug delivery agents for cytarabine to overcome drug resistance. (2016). doi:10.1016/j.ijpharm.2016.09.063

66. Studzian, M. *et al.* Mechanisms of Internalization of Maltose-Modified Poly(propyleneimine) Glycodendrimers into Leukemic Cell Lines. *Biomacromolecules* **18,** 1509–1520 (2017).

67. Szulc, A., Appelhans, D., Voit, B., Bryszewska, M. & Klajnert, B. Characteristics of complexes between poly(propylene imine) dendrimers and nucleotides. *New J. Chem.* **36,** 1610 (2012).

68. Szulc, A. *et al.* Maltose modified poly(propylene imine) dendrimers as potential carriers of nucleoside analog 5′-triphosphates. *Int. J. Pharm.* **495,** 940–947 (2015).

69. Szulc, A., Appelhans, D., Voit, B., Bryszewska, M. & Klajnert, B. Studying complexes between PPI dendrimers and mant-ATP. *J. Fluoresc.* **23,** 349–356 (2013).

70. Boas, U., Christensen, J. B. & Heegaard, P. M. H. Dendrimers: design, synthesis and chemical properties. *J. Mater. Chem.* **16,** 3785 (2006).

71. Maiti, P. K., Çağin, T., Lin, S. T. & Goddard, W. A. Effect of solvent and pH on the structure of PAMAM dendrimers. *Macromolecules* **38,** 979–991 (2005).

72. Khanna, V., Ranganathan, S. & Petrovsky, N. *Rational Structure-Based Drug Design*. *Reference Module in Life Sciences* (Elsevier Ltd., 2018). doi:10.1016/B978-0-12-809633-8.20275-6

73. Vanommeslaeghe, K., Guvench, O. & MacKerell, A. D. Molecular mechanics. *Curr. Pharm. Des.* **20,** 3281–92 (2014).

74. Monkhorst, H. J. Chemical physics without the Born-Oppenheimer approximation: The molecular coupled-cluster method. *Phys. Rev. A* **36,** 1544–1561 (1987).

75. Kettering, C. F., Shutts, L. W. & Andrews, D. H. A Representation of the Dynamic Properties of Molecules by Mechanical Models. *Phys. Rev.* **36,** 531–543 (1930).

76. Leach, A. *Molecular modelling: principles and applications*. (2001).

77. Dezfoli, A. A., Mehrabian, M. A. & Hashemipour, H. Molecular Dynamics Simulation of Heavy Metal Ions in Aqueous Solution Using Lennard-Jones 12-6 Potential. *Chem. Eng. Commun.* **202,** 1685–1692 (2015).

78. Notman, R. & Anwar, J. Breaching the skin barrier — Insights from molecular simulation of model membranes. *Adv. Drug Deliv. Rev.* **65,** 237–250 (2013).

79. Deserno, M. & Holm, C. How to mesh up Ewald sums (I): A theoretical and numerical comparison of various particle mesh routines. (1998). doi:10.1063/1.477414

80. Lin, Y. *et al.* An image-based reaction field method for electrostatic interactions in molecular dynamics simulations of aqueous solutions. *J. Chem. Phys.* **131,** 154103 (2009).

81. Fletcher, R. & Powell, M. J. D. A Rapidly Convergent Descent Method for Minimization. *Comput. J.* **6,** 163–168 (1963).

82. Powell, M. J. D. Restart procedures for the conjugate gradient method. *Math. Program.* **12,** 241–254 (1977).

83. Fincham, D. Leapfrog Rotational Algorithms. *Mol. Simul.* **8,** 165–178 (1992).

84. Case, D. A. *et al.* The Amber biomolecular simulation programs. *J. Comput. Chem.* **26,** 1668–1688 (2005).

85. Brooks, B. R. *et al.* CHARMM: A Program for Macromolecular Energy, Minimization, and Dynamics Calculations. **4,** 187–217 (1983).

86. Pronk, S. *et al.* GROMACS 4.5: a high-throughput and highly parallel open source molecular simulation toolkit. *Bioinformatics* **29,** 845–854 (2013).

87. Phillips, J. C. *et al.* Scalable molecular dynamics with NAMD. *J. Comput. Chem.* **26,** 1781–1802 (2005).

88. Abraham, M. J. *et al.* Gromacs: High performance molecular simulations through multi-level parallelism from laptops to supercomputers. *SoftwareX* **1–2,** 19–25 (2015).

89. Apol, E. *et al.* GROMACS 2016 Reference Manual Contributions from. (1991).

90. Kindt, J. T. Accounting for Finite-Number Effects on Cluster Size Distributions in Simulations of Equilibrium Aggregation. *J. Chem. Theory Comput.* **9,** 147–152 (2013).

91. Kindt, J. T. Determining bulk equilibrium constants for cluster formation from constant NVT ensemble simulations at small N. *Phys. Procedia* **53,** 63–70 (2014).

92. Genheden, S. & Ryde, U. The MM/PBSA and MM/GBSA methods to estimate ligand-binding affinities. *Expert Opin. Drug Discov.* **10,** 449–461 (2015).

93. Homeyer, N. & Gohlke, H. Free Energy Calculations by the Molecular Mechanics Poisson−Boltzmann Surface Area Method. *Mol. Inform.* **31,** 114–122 (2012).

94. Kumari, R., Kumar, R. & Lynn, A. G-mmpbsa -A GROMACS tool for high-throughput MM-PBSA calculations. *J. Chem. Inf. Model.* **54,** 1951–1962 (2014).

95. Paissoni, C., Spiliotopoulos, D., Musco, G. & Spitaleri, A. GMXPBSA 2.0: A GROMACS tool to perform MM/PBSA and computational alanine scanning. *Comput. Phys. Commun.* **185,** 2920–2929 (2014).

96. Honig, B. & Nicholls, A. Classical electrostatics in biology and chemistry. *Science* **268,** 1144–9 (1995).

97. Seley-Radtke, K. L. & Yates, M. K. The evolution of nucleoside analogue antivirals: A review for chemists and non-chemists. Part 1: Early structural modifications to the nucleoside scaffold. *Antiviral Res.* **154,** 66–86 (2018).

98. Jordheim, L. P. & Dumontet, C. Review of recent studies on resistance to cytotoxic deoxynucleoside analogues. *Biochimica et Biophysica Acta - Reviews on Cancer* **1776,** 138–159 (2007).

99. Jordheim, L. P., Durantel, D., Zoulim, F. & Dumontet, C. Advances in the development of nucleoside and nucleotide analogues for cancer and viral diseases. *Nat. Rev. Drug Discov.* **12,** 447–464 (2013).

100. Zhang, J. *et al.* The role of nucleoside transporters in cancer chemotherapy with nucleoside drugs. *Cancer and Metastasis Reviews* **26,** 85–110 (2007).

101. Kakde, D., Jain, D., Shrivastava, V., Kakde, R. & Patil, A. T. Cancer therapeutics-opportunities, challenges and advances in drug delivery. *J. Appl. Pharm. Sci.* **1,** 1–10 (2011).

102. Granja, S., Tavares-Valente, D., Queirós, O. & Baltazar, F. Value of pH regulators in the diagnosis, prognosis and treatment of cancer. *Semin. Cancer Biol.* **43,** 17–34 (2017).

103. Gatenby, R. A. & Gillies, R. J. Why do cancers have high aerobic glycolysis? *Nat. Rev. Cancer* **4,** 891–899 (2004).

104. Parks, S. K. & Pouysségur, J. Targeting pH regulating proteins for cancer therapy–Progress and limitations. *Semin. Cancer Biol.* **43,** 66–73 (2017).

105. Barraza, L. F., Zuñiga, M., Alderete, J. B., Arbeloa, E. M. & Jiménez, V. A. Effect of pH on Eosin Y/PAMAM interactions studied from absorption spectroscopy and molecular dynamics simulations. *J. Lumin.* **199,** 258–265 (2018).

106. Maingi, V., Kumar, M. V. S. & Maiti, P. K. PAMAM dendrimer-drug interactions: Effect of pH on the binding and release pattern. *J. Phys. Chem. B* **116,** 4370–4376 (2012).

107. Hanwell, M. D. *et al.* Avogadro: an advanced semantic chemical editor, visualization, and analysis platform. *J. Cheminform.* **4,** 17 (2012).

108. Wang, J., Wolf, R. M., Caldwell, J. W., Kollman, P. A. & Case, D. A. Development and testing of a general Amber force field. *J. Comput. Chem.* **25,** 1157–1174 (2004).

109. Caminade, A.-M. *et al.* The key role of the scaffold on the efficiency of dendrimer nanodrugs. *Nat. Commun.* **6,** 7722 (2015).

110. Jensen, L. B. *et al.* Elucidating the molecular mechanism of PAMAM-siRNA dendriplex self-assembly: effect of dendrimer charge density. *Int. J. Pharm.* **416,** 410–8 (2011).

111. Lim, J., Pavan, G. M., Annunziata, O. & Simanek, E. E. Experimental and computational evidence for an inversion in guest capacity in high-generation triazine dendrimer hosts. *J. Am. Chem. Soc.* **134,** 1942–5 (2012).

112. Pavan, G. M., Danani, A., Pricl, S. & Smith, D. K. Modeling the Multivalent Recognition between Dendritic Molecules and DNA: Understanding How Ligand " Sacrifice " and Screening Can Enhance Binding. doi:10.1021/ja901174k

113. M. Pavan, G. & Danani, A. Supporting the Design of Efficient Dendritic DNA and siRNA Nano-Carriers with Molecular Modeling. *Curr. Drug Discov. Technol.* **8,** 314–328 (2011).

114. Deriu, M. A. *et al.* Elucidating the role of surface chemistry on cationic phosphorus dendrimer–siRNA complexation. *Nanoscale* **10,** 10952–10962 (2018).

115. Abraham, M. J. *et al.* GROMACS: High performance molecular simulations through multi-level parallelism from laptops to supercomputers. *SoftwareX* **1–2,** 19–25 (2015).

116. Wang, J., Wang, W., Kollman, P. A. & Case, D. A. Antechamber, An Accessory Software PackageFor Molecular Mechanical Calculation. *J. Comput. Chem.* **25,** 1157–1174 (2005).

117. Wang, J., Wang, W., Kollman, P. A. & Case, D. A. Automatic atom type and bond type perception in molecular mechanical calculations. *J. Mol. Graph. Model.* **25,** 247–260 (2006).

118. Sousa da Silva, A. W. & Vranken, W. F. ACPYPE - AnteChamber PYthon Parser interfacE. *BMC Res. Notes* **5,** 367 (2012).

119. Hess, B., Kutzner, C., Van Der Spoel, D. & Lindahl, E. GRGMACS 4: Algorithms for highly efficient, load-balanced, and scalable molecular simulation. *J. Chem. Theory Comput.* (2008). doi:10.1021/ct700301q

120. Jorgensen, W. L., Chandrasekhar, J., Madura, J. D., Impey, R. W. & Klein, M. L. Comparison of simple potential functions for simulating liquid water. *J. Chem. Phys.* **79,** 926–935 (1983).

121. Bussi, G., Donadio, D. & Parrinello, M. Canonical sampling through velocity rescaling. *J. Chem. Phys.* **126,** 014101 (2007).

122. Berendsen, H. J. C., Postma, J. P. M., van Gunsteren, W. F., DiNola, A. & Haak, J. R. Molecular dynamics with coupling to an external bath. *J. Chem. Phys.* **81,** 3684–3690 (1984).

123. Hess, B., Bekker, H., Berendsen, H. J. C. & Fraaije, J. G. E. M. LINCS: A linear constraint solver for molecular simulations. *J. Comput. Chem.* **18,** 1463–1472 (1997).

124. Humphrey, W., Dalke, A. & Schulten, K. VMD: visual molecular dynamics. *J. Mol. Graph.* **14,** 33–8, 27–8 (1996).

125. Torda, A. E. & Wilfred, F. Dynamics Configurations. *J. Comput. Chem.* **15,** 1331–1340 (1994).

126. Hou, T., Wang, J., Li, Y. & Wang, W. Assessing the Performance of the MM/PBSA and MM/GBSA Methods. 1. The Accuracy of Binding Free Energy Calculations Based on Molecular Dynamics Simulations. *J. Chem. Inf. Model.* **51,** 69–82 (2011).

127. Genheden, S. & Ryde, U. The MM/PBSA and MM/GBSA methods to estimate ligand-binding affinities. *Expert Opin. Drug Discov.* **10,** 449–461 (2015).

128. Martínez-Muñoz, A. *et al.* Binding free energy calculations using MMPB/GBSA approaches for PAMAM-G4-drug complexes at neutral, basic and acid pH conditions. *J. Mol. Graph. Model.* **76,** 330–341 (2017).

129. Hou, T., Wang, J., Li, Y. & Wang, W. Assessing the performance of the molecular mechanics/Poisson Boltzmann surface area and molecular mechanics/generalized Born surface area methods. II. The accuracy of ranking poses generated from docking. *J. Comput. Chem.* **32,** 866–77 (2011).

130. Ayoub, A. T., Klobukowski, M. & Tuszynski, J. A. Detailed Per-residue Energetic Analysis Explains the Driving Force for Microtubule Disassembly. *PLoS Comput. Biol.* **11,** e1004313 (2015).

131. Wu, C., Wang, Z., Lei, H., Zhang, W. & Duan, Y. Dual binding modes of Congo red to amyloid protofibril surface observed in molecular dynamics simulations. *J. Am. Chem. Soc.* **129,** 1225–32 (2007).

132. Deriu, M. A., Popescu, L. M., Ottaviani, M. F., Danani, A. & Piticescu, R. M. Iron oxide/PAMAM nanostructured hybrids: combined computational and experimental studies. *J. Mater. Sci.* **51,** 1996–2007 (2016).

133. Wang, D. *et al.* Nucleoside Analogue-Based Supramolecular Nanodrugs Driven by Molecular Recognition for Synergistic Cancer Therapy. *J. Am. Chem. Soc.* **140,** 8797–8806 (2018).

134. Blanco, E., Shen, H. & Ferrari, M. Principles of nanoparticle design for overcoming biological barriers to drug delivery. *Nat. Biotechnol.* **33,** 941–951 (2015).

135. Klajnert, B. *et al.* The Influence of Densely Organized Maltose Shells on the Biological Properties of Poly(propylene imine) Dendrimers: New Effects Dependent on Hydrogen Bonding. *Chem. - A Eur. J.* **14,** 7030–7041 (2008).

136. Ahmed, M. How can nanoparticles be used in sentinel node detection ? **12,** 1525–1527 (2017).

137. Ananda Mohan, A., Veera Raghava Sharma, G. & Vidavalur, S. Synthesis, characterization and biological evaluation of C5′-N-cyclopropylcarboxamido-C6-amino-C2-alkynylated purine nucleoside analogues. *Nucleosides, Nucleotides and Nucleic Acids* **58,** 1–15 (2017).

138. Kampen, K. R. The discovery and early understanding of leukemia. *Leuk. Res.* **36,** 6–13 (2012).

139. Filimon, A., Sima, L. E., Appelhans, D., Voit, B. & Negroiu, G. Internalization and Intracellular Trafficking of Poly(propylene imine) Glycodendrimers with Maltose Shell in Melanoma Cells. *Curr. Med. Chem.* **19,** 4955–4968 (2012).

140. Freire, J. J., Ahmadi, A. & McBride, C. Molecular dynamics simulations of the protonated G4 PAMAM dendrimer in an ionic liquid system. *J. Phys. Chem. B* **117,** 15157–15164 (2013).

141. Merwe, P. A. Van Der. Surface Plasmon Resonance. *Physics (College. Park. Md).* **627,** 1–50 (2010).

142. O'Brien, J., Wilson, I., Orton, T. & Pognan, F. Investigation of the Alamar Blue (resazurin) fluorescent dye for the assessment of mammalian cell cytotoxicity. *Eur. J. Biochem.* **267,** 5421–6 (2000).

143. Baker, N. A. in 94–118 (2004). doi:10.1016/S0076-6879(04)83005-2

144. Chen, C. & Pettitt, B. M. The Binding Process of a Nonspecific Enzyme with DNA. *Biophys. J.* **101,** 1139–1147 (2011).

145. Baker, N. A., Sept, D., Joseph, S., Holst, M. J. & McCammon, J. A. Electrostatics of nanosystems: Application to microtubules and the ribosome. *Proc. Natl. Acad. Sci.* **98,** 10037–10041 (2001).

146. Rahman, A.- & Choudhary, M. I. *Frontiers in anti-cancer drug discovery. [Volume 1]*. (Bentham Science Publishers, 2010).

147. Hong, S. *et al.* Interaction of Polycationic Polymers with Supported Lipid Bilayers and Cells: Nanoscale Hole Formation and Enhanced Membrane Permeability. *Bioconjug. Chem.* **17,** 728–734 (2006).

148. Honary, S. & Zahir, F. Effect of Zeta Potential on the Properties of Nano-Drug Delivery Systems - A Review (Part 1). *Trop. J. Pharm. Res.* **12,** 255–264 (2013).

149. King, K. *et al.* A comparison of the transportability, and its role in cytotoxicity, of clofarabine, cladribine and fludarabine by recombinant human nucleoside transporters produced in three model expression systems. *Mol. Pharmacol.* **69,** 346–53 (2005).

Supporting Information

The following chapter shows the experiments conducted in vivo on the fludarabine and clofarabine complexes with the PPI G4 dendrimers, aim of this thesis work. Our MD simulations were conducted to further analyze and conduct mechanical analysis on the drug-dendrimer interactions.

Fludarabine and Clofarabine uptake into U937 cells

The first *in vivo* experiments were performed on U937 cells line (histiocytic lymphoma cells) to comprehensively illustrate cellular uptake in presence of nucleoside or nucleotide drugs, and in presence of drug-dendrimer complexes. Notable was that fludarabine triphosphate had limited toxicity compared to the nucleoside form, nevertheless nucleotide toxicity increases when it was complexed with the PPI-Mal OS dendrimer. This is highlighted in Figure 42, that shows the results of DNA synthesis inhibition treatments conducted with fludarabine nucleotide alone or complexed with the maltose modified PPI dendrimer.[53]

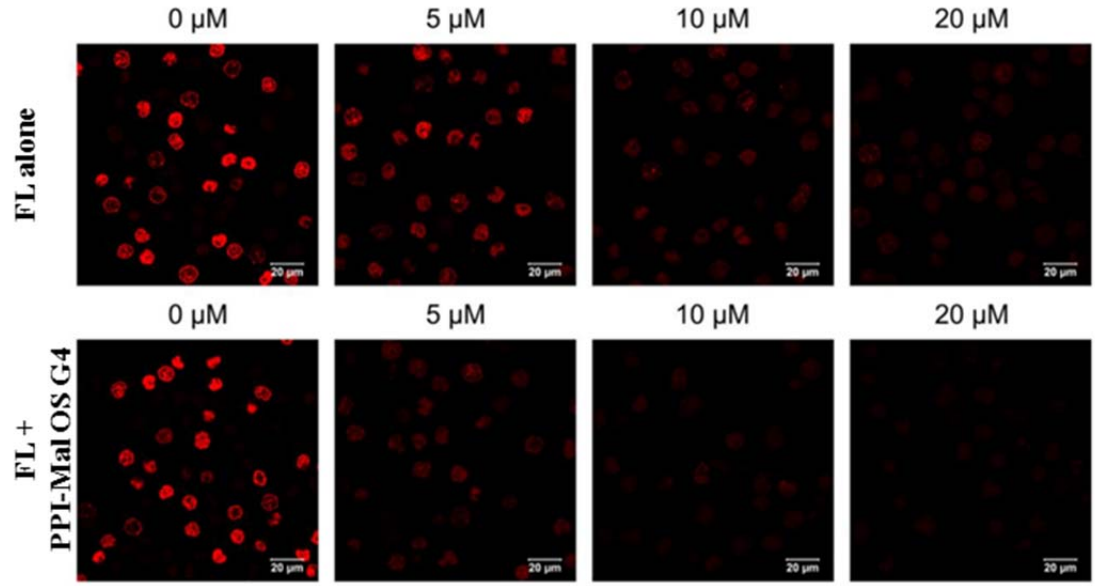

Figure 42. Representative confocal images for each DNA synthesis inhibition treatment with fludarabine triphosphate and the compound-dendrimer complex, made by fludarabine triphosphate and PPI-Mal OS G4 dendrimer.[53]

Likewise, it was verified whether application of dendrimer carrier would improve the cellular pharmacokinetics of clofarabine triphosphate. Taking into account that clofarabine is known to be more toxic than fludarabine. In line with the expectations, clofarabine nucleoside was found to be more toxic than its triphosphate derivative. Surprisingly, after it complexation with PPI-Mal OS G4 dendrimer, the activity of the clofarabine nucleotide was decreased compared to the free nucleotide. As well as its compound-PPI G4 dendrimer complex showed even more inhibited activity compared to the maltose modified complex. Moreover, clofarabine showed no altered cytotoxic activity in complexation with both the dendrimers.[7]

To validate the hypothesis that the majority of fludarabine enters cells via nucleotide-dendrimer complex, the cellular uptake of drug was tested in presence of nitrobenzylmercaptopurine (NBMPR), which is a well know inhibitor of hENT1. These tests provide the previously formulated hypothesis, and it was demonstrated that the drug triphosphate-dendrimer complex enables cellular entry, regardless of hENT1. It was highlighted that nucleoside form of both the drugs does not show complex formation, as well as nucleoside-dendrimer complexes showed no detectable bindings. Contrariwise triphosphate forms of fludarabine and clofarabine showed to bind PPI-Mal OS G4 dendrimer with quantifiable affinities.

Confirmation of drug-dendrimer complexation by SPR

Moreover, to characterize the properties of these bindings, it has been used the label-free biophysical methods of surface plasmon resonance (SPR). The SPR is an affinity-based technique which enable the evaluation of interactions among macromolecules and the determination of kinetics parameters, such as the dissociation constant (K_D). Lower K_D values were directly correlated with greater nucleotide-dendrimer affinity (see Table 7).

Table 7. Dissociation constant (K_D) values determined by Surface Plasmon Resonance (SPR), which is an affinity analysis. Lower K_D value corresponds to greater affinity between the nucleotide and the dendrimer. Furthermore, the micromolar range of K_D value indicates weak nucleotide-dendrimer interactions.

Compounds	**K_D ± SEM (μM)**
CL + PPI G4	54.95 ± 4.37
CL + PPI- Mal OS G4	87.60 ± 1.74
FL + PPI G4	100.20 ± 0.21
FL + PPI- Mal OS G4	157.65 ± 5.85

Furthermore, the K_D range values indicated weak nucleotide-dendrimer interactions. Analyzing the SPR data collected in Table 7, it was evident that clofarabine triphosphate had higher affinity with both the dendrimers. Moreover, for both the drugs, the nucleotide-dendrimer interactions were stronger in presence of unmodified PPI G4 dendrimer. Therefore, the presence of the amino groups on the PPI G4 dendrimer surface could determinate or alter the compound-dendrimer strength of interaction.

Viability assays showed that the clofarabine nucleoside cytotoxicy was higher compared to its triphosphate form. Notable was that clofarabine toxicity (IC50=31.05 ± 2.66 nM) remarkably exceeded that observed for fludarabine (IC50= 1.11 ± 0.06 μM).[53] Finally, it was important to note that despite the different intracellular accumulation of both drugs, the transmembrane transports had the same speed, and in both cases the maximum concentration is reached after 5 minutes.[149]